

## THE EVOLUTION OF CATAclySMIC AND LOW-MASS X-RAY BINARIES

JOSEPH PATTERSON

Harvard-Smithsonian Center for Astrophysics, and Department of Astronomy, Columbia University

Received 1982 December 22; accepted 1983 August 26

## CONTENTS

I. Introduction	444	8-A9	iii) A $\dot{J}(v)$ Relation for G Stars	474	8-C13
II. The Observational Data	446	8-A11	iv) Wanted: A $\dot{J}(M)$ Relation	476	8-D1
III. The Secondaries: Main-Sequence Stars?	452	8-B3	v) Found: A $\dot{J}(M)$ Relation at $v = 130$ Kilometers per Second	476	8-D1
IV. The Search for the Mass Transfer Rate	458	8-B9	vi) Overall Results	477	8-D2
a) $M_v$ of the Disk	459	8-B10	c) Producing $\dot{M}$ from $\dot{J}$	478	8-D3
b) Distance-independent Indicators	460	8-B11	d) Confrontation with Data	478	8-D3
c) Cookbook for $\dot{M}$	461	8-B12	i) Mass Transfer Rates	478	8-D3
i) Systems with Disks	461	8-B12	ii) Perturbing Effects	479	8-D4
ii) Systems without Disks (AM Herculis Stars)	462	8-B13	e) Time Scale for Synchronization	481	8-D6
iii) X-Ray Binaries	462	8-B13	f) Summary	482	8-D7
d) $\dot{M}$ versus Orbital Period, and Uncertainties	462	8-B13	VII. The Period Gap	482	8-D7
V. Cataclysmic Variable Demography	465	8-C4	a) Previous Attempts	482	8-D7
a) Scale Height in the Galactic Disk	465	8-C4	i) Webbink's Hypothesis	482	8-D7
b) Space Densities of Known Systems	466	8-C5	ii) The Onset of Complete Convection	482	8-D7
i) AM Herculis Stars	466	8-C5	iii) Cessation of Mass Transfer	483	8-D8
ii) Other Low- $\dot{M}$ Systems	466	8-C5	b) Interpretation of the Gap	484	8-D9
iii) High- $\dot{M}$ Dwarf Novae	466	8-C5	i) Constant $\dot{J}$	484	8-D9
iv) Low-Mass X-Ray Binaries	466	8-C5	ii) Smoothly Decreasing $\dot{J}$	484	8-D9
v) Classical Novae	466	8-C5	iii) Turning off the Wind	484	8-D9
c) Space Densities from Unbiased Surveys at High Galactic Latitude	467	8-C6	c) Hiding the Dead Novae	484	8-D9
d) Space Densities of Classical Novae: Surveys at Low Galactic Latitude	468	8-C7	d) Summary	485	8-D10
e) Dependence of Space Density on Orbital Period	469	8-C8	VIII. The Big Picture	485	8-D10
f) Absolute Magnitudes, Mass Transfer Rates, Lifetimes, and Space Densities	470	8-C9	a) The Formation of a Close Binary	485	8-D10
g) Which Stars Make Novae?	470	8-C9	b) The V471 Tauri Stars: Precataclysmic Variables	485	8-D10
h) Whither Cataclysmic Variables?	471	8-C10	c) Where Are the Early-Type Secondaries?	486	8-D11
VI. The Origin of the Mass Transfer	471	8-C10	d) Magnetic Braking in Cool Stars	486	8-D11
a) Possible Mechanisms	471	8-C10	e) Birthrate and Death Rate of Cataclysmic Variables	488	8-D13
b) Estimating $\dot{J}$	472	8-C11	i) Birthrate	488	8-D13
i) Single Stars	472	8-C11	ii) Death Rate	489	8-D14
ii) Eclipsing Binaries	473	8-C12	f) Cookbook for Evolution	489	8-D14
			IX. Summary and Conclusions	490	8-E1

## LIST OF TABLES

Table 1 The Observational Data ( $P < 1$ Day)	447	8-A12	Table 4 Space Density Constraints from High Latitude Surveys	468	8-C7
Table 2 "Low-Mass" Systems with $P > 1$ Day	453	8-B4	Table 5 Cataclysmic Variable Demography	470	8-C9
Table 3 Other Constraints on Nova Space Density	467	8-C6			

## LIST OF ILLUSTRATIONS

Fig. 1 Orbital Period Distributions	454	8-B5	Fig. 12 Distribution of $M_v$ for Old Novae	471	8-C10
Fig. 2 Secondaries in the Mass-Radius Plane	455	8-B6	Fig. 13 Rotational Velocity versus Time	473	8-C12
Fig. 3 Secondaries in the Mass- $M_v$ Plane	457	8-B8	Fig. 14 Acceptable Fits to $v = ft^{-n}$	473	8-C12
Fig. 4 Secondaries in the $P-T_e$ and $P-M_v$ Planes	458	8-B9	Fig. 15 $O - C$ Diagrams for "Classical" Main- Sequence Binaries	474	8-C13
Fig. 5 $\dot{M}$ versus Period (distance known)	460	8-B11	Fig. 16 $\dot{P}/P$ versus $M_2$ for All Systems	475	8-C14
Fig. 6 Equivalent Width ( $H\beta$ ) versus $M_v$ (distance known)	462	8-B13	Fig. 17 $\dot{J}$ versus $v$ in G Stars	476	8-D1
Fig. 7 $\dot{M}$ versus Period for All Systems	463	8-C1	Fig. 18 Acceptable $\dot{J}(v)$ Laws	476	8-D1
Fig. 8 The Two Regimes: High and Low $\dot{M}$	464	8-C3	Fig. 19 $\dot{J}(M)$ for Cataclysmic Variable Secondaries	477	8-D2
Fig. 9 Distances above Galactic Disk	466	8-C5	Fig. 20 Constraints on Acceptable $\dot{J}(M)$ Laws	477	8-D2
Fig. 10 Constraints on $D$ (Period)	469	8-C8	Fig. 21 Theoretical $\dot{M}$ versus $P$ , with Favored Braking Law	479	8-D4
Fig. 11 Admissible $D$ (Period) Relations	470	8-C9			

Fig. 22 Theoretical $\dot{M}$ versus $P$ , with a Different Braking Law	479	8-D4	Fig. 26 Spectral Types of Secondaries	487	8-D12
Fig. 23 $\dot{M}$ Time Scale versus Thermal Time Scale	480	8-D5	Fig. 27 Distribution of Main-Sequence Spectroscopic Binaries with Orbital Period	488	8-D13
Fig. 24 White Dwarf Mass versus Orbital Period	482	8-D7	Fig. 28 Distribution of Main-Sequence Eclipsing Binaries with Orbital Period	488	8-D13
Fig. 25 Orbital Periods of "Low- $\dot{M}$ " Systems	483	8-D8			

## ABSTRACT

We present an observational study of the structure and evolution of cataclysmic and low-mass X-ray binaries, concentrating on the 124 systems for which orbital periods are known. The eruptive properties and mass transfer rates of these stars are found to be highly correlated with their orbital periods, suggesting that both the eruptive activity and the long-term evolution are determined by the properties of the lobe-filling secondaries. The secondaries do not satisfy the commonly used theoretical models of low-mass zero-age main-sequence (ZAMS) stars, but are, in general, consistent with the empirically derived properties of the lower main sequence. We show that  $R/R_{\odot} = (M/M_{\odot})^{0.88}$  for low-mass ZAMS stars in the field, in wide binaries, and in cataclysmic binaries. For masses above  $0.8 M_{\odot}$ , the empirical ZAMS is in reasonable agreement with the models. But in this regime (corresponding to orbital periods  $\geq 9$  hr), the secondaries in cataclysmic binaries are found to be slightly evolved from the ZAMS.

Distance and absolute magnitude estimates are made for 83 systems, using a variety of techniques: expansion parallax, interstellar absorption, photometric parallax of the secondary, and an empirical absolute magnitude–equivalent width relation. These distances, coupled with an analysis of sky surveys at high and low galactic latitude, lead to estimates of the local space density of each kind of eruptive variable:  $8 \times 10^{-7} \text{ pc}^{-3}$  for high- $\dot{M}$  dwarf novae,  $4 \times 10^{-6} \text{ pc}^{-3}$  for low- $\dot{M}$  dwarf novae,  $4 \times 10^{-7} \text{ pc}^{-3}$  for classical novae,  $5 \times 10^{-7} \text{ pc}^{-3}$  for AM Her stars, and  $5 \times 10^{-10} \text{ pc}^{-3}$  for low-mass X-ray binaries.

Various methods for deducing the mass transfer rate  $\dot{M}$  are reviewed; the most generally useful method yields  $\dot{M}$  by comparing the observed magnitudes to models of accretion disks. There is a good correlation with orbital period ( $\dot{M} \propto P_{\text{orb}}^{3.2}$ ). The observed values of  $\dot{M}$  suggest that there are two important regimes of evolution: (1)  $0.7 \text{ hr} < P_{\text{orb}} \leq 3.3 \text{ hr}$ , in which  $\dot{M}$  is always low ( $10^{-11}$ – $10^{-10} M_{\odot} \text{ yr}^{-1}$ ) and the evolution is driven by gravitational radiation; (2)  $3.3 \text{ hr} < P_{\text{orb}} \leq 1 \text{ day}$ , in which  $\dot{M}$  is, in general, high ( $10^{-9}$ – $10^{-8} M_{\odot} \text{ yr}^{-1}$ ) and the evolution is driven by some mechanism which removes angular momentum from the binary with far greater efficiency.

We believe that this mechanism can be identified as *magnetic braking in a stellar wind emanating from the secondary*. Observed orbital period changes and observed correlations of rotational velocity with age and spectral type indicate that this mechanism appears to operate efficiently wherever rapidly rotating stars with convective envelopes are found: in solitary dwarfs, in solitary giants, and in every type of binary (detached, semidetached, and contact). We show in detail that the rate of angular momentum loss inferred from these observations suffices to drive the observed rates of mass transfer in cataclysmic binaries. Surprisingly, the theoretical time scale for mass transfer through magnetic braking is found to be always very near the thermal time scale of the lobe-filling secondary, independent of the secondary's mass.

An evolutionary model is constructed which is capable of reproducing most of the characteristics of observed systems: the  $\dot{M}(P_{\text{orb}})$  relation; the period distribution and the period "gap"; the restriction of secondaries to spectral types later than G0; and most of the observed lifetimes and space densities. But we are still unable to identify the descendants of classical novae, which are produced in enormous numbers since novae are fairly common and have short lifetimes. The most likely explanation is that some unknown mechanism manages to destroy many systems in a time short compared to the age of the Galaxy. In order to produce a period gap, the secondaries probably turn off the magnetic braking rather suddenly at an orbital period of  $\sim 3$ – $4$  hr. This could arise from the inability of completely convective, low-mass secondaries ( $\leq 0.3 M_{\odot}$ ) to drive significant magnetic winds.

Finally, we note that magnetic braking should shorten the lifetimes of *all* close binaries with cool main-sequence components, whether or not an accreting compact star is present. Available data on the frequency of spectroscopic and eclipsing binaries are consistent with this possibility. It seems likely that magnetic braking controls the evolution of all low-mass binaries with orbital periods  $\leq 10$  days.

*Subject headings:* stars: binaries — stars: dwarf novae — stars: evolution — stars: mass loss — stars: winds

## I. INTRODUCTION

Cataclysmic variables are binary stars of very short orbital period, in which a low-mass, late-type star ("the secondary") fills its critical Roche surface and transfers matter to its companion star ("the primary"), which is a white dwarf. Because the transferred material carries substantial angular

momentum, it does not settle immediately onto the white dwarf but forms an encircling ring, which viscosity broadens into a disk. As accreting material spirals through the disk, it releases its gravitational energy and heats the disk to temperatures of  $\sim 3000$ – $100,000$  K, conferring a luminosity of  $0.001$ – $10 L_{\odot}$  on the disk. In most cases, this exceeds the visible luminosity of the two component stars, and hence the

visible spectrum is dominated by the featureless blue continuum of the accretion disk.

Various kinds of eruptive behavior may occur. Dwarf novae, recurrent novae, and classical novae are in systems of this type, as well as stars showing rapid, irregular light variations that do not fit easily into these categories ("nova-like variables"). These eruptions have been variously attributed to runaway mass transfer in the secondary, unstable flow in the accretion disk, and runaway thermonuclear reactions on the white dwarf (for general reviews, see Robinson 1976; Warner 1976; Cordova and Mason 1983).

A few binary systems of this kind are found to be powerful sources of hard X-rays ( $L_x \approx 10^{35} - 10^{38}$  ergs s<sup>-1</sup>), indicating that the accreting star is more compact than a white dwarf. These are the "low-mass X-ray binaries" or the "Sco-like sources," named for their prototype Sco X-1 (for reviews see van Paradijs 1981, Bradt and McClintock 1983). These systems resemble cataclysmic variables (hereafter CVs) in their binary properties, but are thought to contain neutron stars or black holes as their accreting components. From the standpoint of present-day evolution, the low-mass X-ray binaries present problems similar to those posed by CVs; in particular, the mechanism driving the mass transfer is still unknown. Therefore, in this paper we will usually include this class under the term "CV," with a few departures from this practice where the nature of the compact star makes a critical difference.

The evolution of CVs, and of binary stars in general, is not well-understood, but theories continue to pour out of the journals at an impressive rate. The first calculations of binary star evolution (see Kruszewski 1966; Plavec 1968; Paczyński 1971 for reviews) invoked the conservation of total mass and angular momentum in the binary ("conservative mass transfer"). Now, under such an assumption, mass transfer from a low-mass star to a high-mass star increases the binary separation, while the low-mass star itself should contract to adjust to its lower mass. With the Roche lobe growing and the secondary shrinking, the star must certainly detach itself from its critical Roche surface and cease transferring mass. Thus, mass transfer must shut off as soon as it begins. Since we observe stars in a vigorous and sustained state of mass transfer, it is obvious that *conservative mass transfer cannot even approximately describe the present state of CVs, much less their evolution.*

There are only two possible solutions: the star must expand as it transfers matter, or the Roche lobe must shrink. Single stars do expand when hydrogen is exhausted in their cores (Schwarzschild 1958), and in principle it is possible to power the mass transfer in CVs in this way. But if this were the normal mechanism, we would expect that the secondaries should be substantially larger and more luminous than single main-sequence stars of the same mass, whereas the observational data indicate that the secondaries are approximately on the main sequence.<sup>1</sup> In addition, it is difficult to understand

<sup>1</sup>This point has been vigorously disputed many times in the literature (e.g., Warner 1978; Wade 1979, 1981; Stover 1981*a, b*; Rappaport, Joss, and Webbink 1982), but the disputes usually center on departures from the main sequence that are smaller than the accuracy with which the main

why such low-mass stars (say, 0.2–0.6  $M_\odot$ ) should have exhausted hydrogen, when their nuclear burning lifetimes ( $10^{11-12}$  yr) are many times longer than the age of the Galaxy. Other, less obvious schemes for forcing expansion of the star have been proposed (e.g., Faulkner 1976; Whyte and Eggleton 1980). Some of these may well work for certain brief periods of evolution, but insofar as they require departures from the main sequence, they conflict with the observational data and therefore cannot be the principal driving mechanism for the mass transfer.

A more promising approach is to make the Roche lobe shrink. This is most easily done by shrinking the dimensions of the binary, which is in turn most easily done by the removal of angular momentum. Gravitational radiation (GR) will inexorably remove angular momentum from a close binary, and many studies (e.g., Paczyński 1967; Faulkner 1971; Tutukov and Yungelson 1979) have proposed that mass transfer is driven by GR in at least some of the CVs. More recently, three papers have appeared (Paczyński 1981; Paczyński and Sienkewicz 1981; Rappaport, Joss, and Webbink 1982) which calculate the effects of GR in greater detail, in particular including the response of the secondary to the thermal imbalance created in its atmosphere by mass loss. These studies, in substantial agreement with each other, have succeeded in reproducing some of the observed features, in particular: (1) the "minimum orbital period" of CVs with hydrogen-rich secondaries, at  $\sim 70$ –80 minutes; and (2) the existence of a "standard" mass transfer rate of  $\sim 3 \times 10^{-11} M_\odot \text{ yr}^{-1}$ . However, many other observed properties remain unexplained: the existence of much higher mass transfer rates ( $\sim 10^{-8} M_\odot \text{ yr}^{-1}$ ) in some systems, the orbital period gap between 2.2 and 2.8 hr, the existence of "double degenerates" at very short orbital periods (down to 18 minutes), and, perhaps most importantly, the fact that real CVs manage to reach the GR regime at all (they must lose more than 90% of their original angular momentum by some *other* process to reach periods as short as  $\sim 4$  hr, where GR can become effective). None of these authors attempted any detailed comparison of theory and observation.

In response to these inspiring successes and heroic failures, we attempt here to assemble in a systematic way the existing empirical data, in order to compare with predictions of theories. We present the relevant data on CVs of known orbital period in § II. We will find that the eruption properties are very well correlated with the orbital periods, in a manner that suggests that the mass transfer rate  $\dot{M}$  is the all-important determinant of evolution and of the eruptive behavior. This will lead us to examine the properties of the mass-losing secondary in § III, and then to consider the checkered history of  $\dot{M}$  in § IV. We will find transfer rates in the range  $10^{-11} - 10^{-7} M_\odot \text{ yr}^{-1}$ , well correlated with orbital period. In § V we digress, using the transfer rates and distances to deduce approximate space densities and lifetimes for each kind of eruptive variable. The higher mass transfer rates cannot be explained by GR, and it seems inevitable that these

sequence is known. We will show below that essentially all the observational data on CVs of periods  $\leq 0.4$  require the presence of a star which satisfies the main-sequence mass-radius relation.

systems are being driven by a mechanism which removes angular momentum much more efficiently. This mechanism need not be special to binary stars, since single stars in the field also need such a mechanism. In § VI, we consider what that mechanism might be, and conclude that it is *the magnetic braking of the secondary's rotation by its own stellar wind*, coupled with the enforcement of synchronous rotation by tidal friction. This allows CVs to lose sufficient angular momentum to begin mass transfer in a reasonable time (less than the age of the Galaxy), and drives the mass transfer at a high rate ( $10^{-10}$ – $10^{-7} M_{\odot} \text{ yr}^{-1}$ ) once it begins. This magnetic braking appears to operate efficiently wherever cool stars are found: in solitary dwarfs, in solitary giants, in detached binaries (e.g., RS CVn stars), in semidetached binaries (e.g., CVs), and in contact binaries (e.g., W UMa stars). In §§ VII and VIII, we gather these ideas together for a nearly complete account of the long-lived phases of CV evolution: we find that most of the observed properties of CVs can be understood, as well as the absence of CVs with A and F star secondaries. We also consider how to turn off the magnetic braking and allow the existence—reasonably certified by observation—of short-period binaries evolving under the control of GR.

## II. THE OBSERVATIONAL DATA

The most important single parameter for each star is the orbital period of the binary system. The orbital period enables estimates of the dimensions and evolutionary state of the binary, and uniquely determines the mean density of the secondary star (and therefore its mass, if a particular mass-radius relation is adopted; see § III below). Very little can be known about any individual system until the orbital period is found. We have therefore collected in Table 1 the basic observational data for all CVs with known orbital periods, including all data judged to be relevant for evolutionary questions. We include all interacting binaries with accreting compact stars and orbital periods less than 1 day. There are a few stars (e.g., HZ Her, T CrB, Cyg X-2) excluded by this period limit, but the lobe-filling stars in these systems are probably all considerably evolved from the main sequence. Mass transfer in such stars may easily be driven by nuclear evolution, which places them in a different category. Accordingly, we list these stars in Table 2. We also include the “V471 Tauri” stars, which resemble CVs except that the secondary star does not fill its Roche lobe, therefore does not transfer mass, and therefore does not produce an accretion disk. These stars are important in a discussion of evolution since they appear to be the progenitors of ordinary CVs.

Most of the data in Table 1 come directly from observation, but many columns deserve more comment. Column (3) gives the period in days. Parentheses indicate that the exact value is uncertain, and double parentheses indicate that even the approximate value may be in error (usually due to uncertainty in cycle count). Column (4) gives the total range of variability in the visual magnitude  $m_v$  (with the effects of eclipses and classical nova outbursts omitted), the mean  $m_v$  in the normal luminosity state (generally quiescence), and the correction factor by which the normal visual flux should be multiplied to obtain the time-averaged visual flux. This correction factor was derived by measurement of the available long-term visual

light curves, principally those of the AAVSO. Column (5) gives the best estimate of the distance, usually obtained from the expansion parallax (for the classical novae) or the photometric parallax of the secondary; these methods give essentially sound results. Distance estimates in parentheses are more uncertain; these are based on methods discussed below, and identified in column (5) by a code explained in the notes to Table 1. Column (6) gives the equivalent width of the H $\beta$  emission line, measured in the normal luminosity state unless otherwise stated. Because the H $\beta$  equivalent widths of all dwarf novae in eruption become very small or zero, we do not list them individually. The data were obtained from the following sources: the tabulations of Oke and Wade (1982), Williams (1983), and Williams and Ferguson (1982); unpublished spectra taken by the author; and the cited literature references. Column (7) gives the observed spectral type of the secondary and the best available estimate for the masses of the component stars. Some editorial judgment has been exercised here, based on the quality of the measurement; low-weight estimates are given in parentheses, and many published estimates (especially for noneclipsing systems) are omitted altogether. While the individual mass determinations are often open to criticism, the tabulated values may very well be adequate for our statistical purposes. For systems of known distance, the nondetection of the secondary's spectrum yields a limit on its effective temperature (the exact constraint differs for various systems, but is typically  $M_v(\text{sec}) \geq M_v + 2.0$ ). The corresponding limits on spectral type (“>” meaning “later than”) are included in column (7); no assumption of a main-sequence structure is needed, since the secondary's radius is approximately given by the orbital period. Finally, we give literature references in column (8); in cases where there are many to choose from, we have tended to cite recent papers containing the spectroscopic results. Other large compilations of CV data and references are given by Warner (1976), Cordova and Mason (1983), Ritter (1982, private circulation), and Webbink (1982, private circulation).

In Figure 1 we have plotted the distribution of orbital periods in several ways. The dashed line at the top of the figure indicates the distribution for all stars; the dearth of stars near  $\log P = -1.0$  represents the famous “period gap” between 2 and 3 hr, extensively discussed by many authors (e.g., Whyte and Eggleton 1980).

It is instructive to segregate CVs by the nature of their favorite cataclysm. Lest we run quickly afoul of small-number statistics, we shall keep the segregation minimal, lumping together (a) AM Her and U Gem stars, often considered to have relatively low mass transfer rates, and (b) old novae and Z Cam stars, in which the mass transfer rates are thought to be higher ( $\geq 10^{-9} M_{\odot} \text{ yr}^{-1}$ ). Twenty-four stars exhibit cataclysmic activity not readily associated with any of these classes; these we gather into the class (c) “other CVs.” Finally, we present in the remaining class (d) the rather sparse data on orbital periods of low-mass X-ray binaries.

Figure 1 shows that the orbital periods of CVs are highly correlated with their eruption characteristics. The old novae and Z Cam stars are all long-period systems ( $P > 3.3$  hr), while the AM Her and U Gem stars prefer much shorter periods ( $P < 2$  hr) but contain a few members all the way out to the longest periods observed. On the basis of Figure 1, it

TABLE 1  
THE OBSERVATIONAL DATA ( $P < 1$  day)

Star (Alternate Name) (1)	Type (2)	$P_{\text{orb}}$ (3)	$m_v$ Range Typical $m_v$ Correction (4)	Distance (pc) Clues (5)	E.W.(H $\beta$ ) ( $\text{\AA}$ ) (6)	Sp. Secondary $M_2/M_\odot$ $M_1/M_\odot$ (7)	References (8)
AM CVn ..... (HZ 29)	NL(He) DD	0 <sup>d</sup> 0122	13.9–14.1 14.0 1.0		no H!		1,2
E2259+586.....	XR	((0.0266))	$\geq 22$	3600			3,4
KZ TrA ..... (4U 1626–67)	XR	0.0288	18.5 1.0		no H?		5
GP Com ..... (G61–29)	NL(He) DD	0.0323	15–16 15.7 1.0	(< 90) 3,4,7,8	no H!		6
2S 1916–053 .....	XR	((0.0345))	> 17				7,8
EF Eri..... (2A 0311–227)	AM	0.0563	13.5– > 17 14.6 0.8	(200) 7,9	44	> M5	9,10
WZ Sge ..... UG (SU)	UG (SU)	0.0567	7.7–15.5 15.3 2.0	< 110 3,4,5,6	47	> M5 (0.04) (0.70)	11,12
SW UMa..... UG (SU?)	UG (SU?)	0.0568	11–16 15.7 2.0	(140) 4	68	> M2	13,14
T Leo..... UG	UG	0.0588	10–15.5 15.4	(70) 3,4,6	121	> M4	15,16
GD 552 ..... NL	NL	0.062	$\sim 15$		60		17
E1114+18..... AM	AM	0.0624	$\sim 18$				18
V2051 Oph..... NL (UG?)	NL (UG?)	0.0624	14–16 15.7 1.3	(140) 4,8	75	> M4	19,20
V436 Cen ..... UG (SU)	UG (SU)	0.0625	11.5–15.8 15.3 2.0	(76) 4,8	140	> M4 (0.17) (0.70)	21
OY Car ..... UG (SU)	UG (SU)	0.0631	12–16.5 16 1.8	120 1,4,8	47	> M4 0.14 0.95	21,22
EK TrA ..... UG (SU)	UG (SU)	0.0649 (SH)	12–17				23
EX Hya ..... UG	UG	0.0682	11.5–14.0 13.7 1.0	(125) 3,4,7,8	63	> M2 0.19 1.4	24,25, 26,27
VV Pup ..... AM	AM	0.0697	14–18 16 1.0	115 1,3,6	82	late M	28,29,30
RZ Sge ..... UG (SU)	UG (SU)	0.0701 (SH)	12.2–17.5 17.4 3.0		70		31
E1405–451..... AM	AM	0.0706	$\sim 15.5$		50		32,33
IR Gem ..... UG (SU)	UG (SU)	0.0708 (SH)	11.5–17.5 17.0		90		34
E1013–477..... AM? NL?	AM? NL?	0.0718	$\sim 17$		118		35
HT Cas ..... UG	UG	0.0736	12.2–17.0 16.8 1.7	(190) 4,8	88	> M4 0.19 0.70	36,37

TABLE 1—Continued

Star (Alternate Name) (1)	Type (2)	$P_{\text{orb}}$ (3)	$m_r$ Range Typical $m_r$ Correction (4)	Distance (pc) Clues (5)	E.W.(H $\beta$ ) ( $\text{\AA}$ ) (6)	Sp. Secondary $M_2/M_{\odot}$ $M_1/M_{\odot}$ (7)	References (8)
VW Hyi .....	UG (SU)	0.0743	8.5–13.4 13.4	(150) 4, 6, 8, 9	25	0.11 0.63 late M	25, 38
Z Cha .....	UG (SU)	0.0745	12–16 15.5 2.1	134 1, 3, 4, 7, 8	27	0.17 0.85	39, 40
WX Hyi .....	UG (SU)	0.0748	11–14.8 14.4 2.8	(100) 4, 8	45		38, 41
AY Lyr .....	UG (SU)	0.0755 (SH)	11.8–18.3 18.2 4.0	(400) 3, 4, 9	29	> M4	42
SU UMa .....	UG (SU)	(0.0763)	10.8–15.0 14.6 4.0				43
H0139–68 .....	AM	0.0764	~15	(180) 9		> M3	44, 45
PG 1550+191 .....	AM	0.0789	15.4	(200) 1, 9	50	> M2	46, 47
CW 1103+254 .....	AM	0.0791	~16	(180) 7, 9	90	> M1	48, 49
CU Vel .....	UG (SU)	0.0799 (SH)	11–15.5 15.4 1.8				50
AN UMa .....	AM	0.0798	14.7–19 17.0 1.0	(400) 7, 9	22	> M4	51
TY Psc .....	UG (SU)	0.080 (SH)	12.5–16				52
PS 74 .....	UG (SU)	0.0841 (SH)	12–16.5				53
YZ Cnc .....	UG (SU)	0.0903 (SH)	10.2–14.8 14.5 4.0	(130) 4, 8	80		42, 54
Abell 41 .....	V471 (PN)	0.1132	15				55
TU Men .....	UG (SU)	0.1176	11.4– >16				56
AM Her .....	AM	0.1289	12.5–15.3 12.7 0.7	75 1, 3, 6	56(12.8) 14(15.2)	M4.5 0.26 0.39 M5	57, 58, 59, 60, 61
MV Lyr .....	NL	0.1336	12.5–17.8 12.7 0.7	320 1, 4, 8	30(16.5) 4(13.0)		62, 63
PG 1012–03 .....	NL	0.1347	14.5	(250) 4, 8	21	> M0 0.35 0.60	64
3A 0729+103 .....	NL	(0.1349)	15.5		15		65
TT Ari.....	NL (ZC?)	0.1375 (0.1326?)	9.7–16.3 10.6 0.7	(135) 4, 8, 9	30(14.1) 2(10.2)		66, 67, 68
V1500 Cyg .....	CN (1975)	0.1396	20	1400 2, 5, 9			69

TABLE 1—Continued

Star (Alternate Name) (1)	Type (2)	$P_{\text{orb}}$ (3)	$m_e$ Range Typical $m_e$ Correction (4)	Distance (pc) Clues (5)	E.W. (H $\beta$ ) ( $\text{\AA}$ ) (6)	Sp. Secondary $M_2/M_\odot$ $M_1/M_\odot$ (7)	References (8)
V442 Oph .....	NL	(0.1406)	12.6– >14.5 13.7		10		15,70
V1223 Sgr .....	NL	(0.1408)	13.3– >16 13.4 0.9		9		71
0623+71 .....	NL	(0.144)	13				72
VZ Scl .....	NL	0.1446	15.6–20 15.6 0.9	(250) 4,7	33	> M3	73
V603 Aql .....	CN (1918)	0.1449 (0.138?)	11.3–11.8 11.6 1.0	376 2,8,9	7	> G8	74,54
RR Pic .....	CN (1925)	0.1450	12.0	480 2,4,8	8	> G8	75,76
V801 Ara .....	XR	(0.148)	16				77
AO Psc .....	NL	0.1496	13.3–14.3 13.4 1.0	(250) 4,7,8	8	> M0	78,79
V425 Cas .....	NL	(0.1496)	14.5–19 14.5 0.7				15
WY Sge .....	CN? (1783)	(0.1536)	18.0–19.5 19.5		20		80
E2003+225 .....	AM	0.1544	15.0				81
LX Ser .....	NL	0.1584	14.5–17.0 14.5 1.0	(210) 4,8	25	> M2 0.35 0.40	82,83
V380 Oph .....	NL	(0.16)					84
CM Del .....	NL	(0.16)					84
KR Aur .....	NL(ZC?)	0.1628	13–17 14.0 0.8	(180) 4,8	50(15.5) 4(13.8)	> M3	85
YY Dra .....	NL(UG?)	0.163	12–17 16.9 1.8	100 1,4,7,8	110	M5	86
CN Ori .....	ZC	0.1631	15.5 5.0	(400) 3,4,8	20	> M0	87
H2215–086 .....	NL	0.1680	13.5	(200) 4,7,8	22	> M0	88
WW Cet .....	NL(ZC?)	(0.17)	9.3–16.3 13.9 1.3	(130) 3,4,7,8	60(14.2) 23(12.8)	> M3	89,13
U Gem .....	UG	0.1769	8.8–14.5 14.3 2.7	78 1,3,4,6,8	37	M4.5 0.50 1.1	90,91
BD Pav .....	UG(SU?)	0.1793	12.4–17 16.6 2.0				92
V926 Sco .....	XR	(0.18)	17.5	7000 5,7			93
SS Aur .....	UG	0.1806	10.5–14.8 14.4 3.1	(190) 3,4,6,8	78	> M2	89,13

TABLE 1—Continued

Star (Alternate Name) (1)	Type (2)	$P_{\text{orb}}$ (3)	$m_v$ Range Typical $m_v$ Correction (4)	Distance (pc) Clues (5)	E.W.(H $\beta$ ) ( $\text{\AA}$ ) (6)	Sp. Secondary $M_2/M_\odot$ $M_1/M_\odot$ (7)	References (8)
4U 1755–33 .....	XR	(0.182)	19				94
TW Vir .....	UG	0.1826	11.5–15.8 15.5 3.5				84,13
DQ Her .....	CN(1934)	0.1936	14.2–15.0 14.7 1.0	420 1,2,3	16	M3 0.32 0.45	95,96, 97
UX UMa .....	NL(ZC?)	0.1967	12.8	340 3,4,7,9	5	78	98,99
V1521 Cyg .....	XR	0.1997	$\geq 21$	10000			100,101
(Cyg X-3)				5,7,9			
T Aur .....	CN(1891)	0.2044	15.2–15.8 15.4 1.0	830 2,4,8,9	6	> K4 (0.63) (0.68) > G7	102,103
V3885 Sgr .....	ZC	0.2057	10.4	(130) 4,8,9	2		104
RX And .....	ZC	0.2115	10.3–13.6 13.5 5.0	(200) 3,4,8	58	> K9	105,106
HR Del .....	CN(1967)	(0.2142) 0.1775	12.4	810 2,4,8	6	> G6	107,108
HL CMa .....	UG	(0.217)	10–15 13.2 4,8	(80) 4,8	65(15.0) 50(13.8) 5(12.2)	> M0	109,110
V1727 Cyg .....	XR	0.2183	17.5	1400 1		K 0.65 1.3	111,112, 113,114
(4U 2129+47)							
TV Col .....	NL	0.2286	13.8	(160) 4,7,8	16		115,116, 117
(2A 0526–328)							
RW Tri .....	NL	0.2319	12–14 13.5 1.0	(250) 4,8,9	18(13.7) 3(12.6)	> K8 0.5 0.5	118,119, 120
V691 CrA .....	XR	0.2321	15.7	(500)			114,121, 122
(2A 1822–37)							
BD+50°2869 .....	V471(PN)	0.2377	10.6			Of	123
(NGC 6826)							
RW Sex .....	NL(ZC?)	(0.247)	10.6	(150) 4,8,9	2	> K0	124
(BD – 7°3007)							
V751 Cyg .....	NL(ZC?)	((0.25))	14–16 14.2 1.0		3		84
V426 Oph .....	NL	(0.25)	12.6		15(13.0)		125
V794 Aql .....	NL	(0.25)	15				125,84
AH Her .....	ZC	0.2581	11–15 13.8 2.0	(250) 1,8	26(14.8)	K	126,127
AA Dor .....	V471? DD?	0.2615	11.4			0.04 0.24	128
(LB 3459)							



TABLE 1—Continued

Star (Alternate Name) (1)	Type (2)	$P_{\text{orb}}$ (3)	$m_i$ Range Typical $m_i$ Correction (4)	Distance (pc) Clues (5)	E. W. (H $\beta$ ) ( $\text{\AA}$ ) (6)	Sp. Secondary $M_2/M_{\odot}$ $M_1/M_{\odot}$ (7)	References (8)
SS Cyg.....	UG	0.2751	8.2–12.2 12.1 5.0 14–16	95 1, 3, 4, 6, 8	44	K5 0.8 1, 3 > G9	129, 130
V533 Her.....	CN(1963)	(0.28)	15.7 1.6 10.2–14.5	1200 2, 4, 7, 8	3(14.4) 17(15.7)	K	54
Z Cam.....	ZC	0.2898	11.5 1.0 11.9–14.4	350 1, 3, 4, 7, 8	5(11.5) 20(12.5)	0.9 1.2 K5	131, 132
EM Cyg.....	ZC	0.2909	13.9 2.3	350 1, 4, 8	2(12.2) 15(13.9)	0.75 0.55	133, 134
MXB 1659–29.....	XR	0.296	18.3	10000?			135
AC Cnc..... (H0850+13)	NL	0.3005	14–16 14.7 1.0	400 1, 4, 8	7	K4 > G6	136, 54
Lanning 10.....	NL	0.3213	14.8	(1000) 4, 5, 8	7		137, 138
V616 Mon..... (A0620–00)	XR	(0.322)	11–19 19	1100 1		K6	139
BT Mon.....	CN (1939)	0.3338	15–16 15.4 1.0 13–18	1400 2, 5, 7	22	> K0 (0.8) (1.0) K3	140, 141, 142
V822 Cen..... (Cen X-4)	XR	0.342 0.314?	18	1700 1, 5	37		143, 144
GK Vir..... (PG 1413+01)	V471	0.3443	17.3			late M	145
RU Peg.....	UG	0.3746	0.9–13.1 13.1 2.4	250 1, 3, 4	5(11, 8) 20(13.1)	G9	146
SY Cnc.....	ZC	0.38 0.32?	10.8–14.5 14.2 5.5	300 1, 3, 4	14(13.0)	G9	36, 84
AE Aqr.....	NL	0.4117	9–12.5 12.4 1.3	84 1, 3, 4, 6	22(11.5) 30(12.4)	K5 0.74 0.94	147, 148
V1668 Cyg.....	CN(1978)	0.4392	18.5	3600 5			149
QU Car..... (HDE 310376)	NL	0.454	11.2		3		150
UU Sge.....	V471(PN)	0.4651	14.7				151
V477 Lyr..... (Abell 46)	V471(PN)	0.4717	15	6000			19
V Sge.....	NL?	0.5142	9–13.9 11.5 1.0	2700 5		WN5??	152
V471 Tau..... (BD +16°516)	V471	0.5212	9.7	42 1, 3, 6		K2, DA 0.80 0.79 M5e, DA	153, 154
HZ 9.....	V471	0.5643	13.9	42 1, 3, 6			155
UX CVn..... (HZ 22)	V471??	0.5737	13.1			(sdB) (0.4) (0.4)	156, 157

TABLE 1—Continued

Star (Alternate Name) (1)	Type (2)	$P_{\text{orb}}$ (3)	$m_v$ Range Typical $m_v$ Correction (4)	Distance (pc) Clues (5)	E.W.(H $\beta$ ) ( $\text{\AA}$ ) (6)	Sp. Secondary $M_2/M_\odot$ $M_1/M_\odot$ (7)	References (8)
BV Cen .....	UG	0.6101	10.5–14.2 13.9 2.0	450 1,3,4	5	G5–8 0.90 0.83 M2e,DA	158,159
Case 1 .....	V471	0.6676	13.3	(120) 1			155,160
VW Pyx .....	V471(PN) (K 1-2)	0.6707	16.5				161
V818 Sco .....	XR (Sco X-1)	0.7873	11–14 13.2 1.5	500 7,8,9		> G5	162,163, 67

NOTES.—Code: UG = U Gem star; AM = AM Her star; ZC = Z Cam star; NL = nova-like; CN = classical nova; XR = X-ray binary (with neutron star); DD = double degenerate (degenerate secondary); SU = SU UMa star (subclass of UG); V471 = V471 Tau star (short-period *detached* binary consisting of white dwarf and red dwarf); SH = superhump period, *probably* 1%–5% longer than orbital period; PN = planetary nebula nucleus. Single parentheses denote that exact value is uncertain, double parentheses that period is uncertain, alias period is possible; single and double question marks denote peculiar values.

CODE FOR DISTANCE CLUES.—(1) detection of secondary; (2) nova shell; (3) proper motion; (4)  $M_v$ –E.W.(H $\beta$ ) relation; (5) interstellar absorption; (6) parallax; (7) position in the Galaxy; (8) continuum shape; (9) “standard candle” arguments.

REFERENCES.—(1) Smak 1975; (2) Robinson and Faulkner 1975; (3) Middleditch and Fahlman 1982; (4) Gregory and Fahlman 1981; (5) Middleditch *et al.* 1981; (6) Nather, Robinson, and Stover 1981; (7) Walter *et al.* 1982; (8) White and Swank 1982; (9) Hutchings *et al.* 1982; (10) Young *et al.* 1982; (11) Krzeminski and Smak 1971; (12) Brunt 1982; (13) Williams 1983; (14) Shafter 1983*b*; (15) Shafter and Ulrich 1982; (16) Shafter and Szkody 1984; (17) Stover 1984; (18) Biermann *et al.* 1982; (19) Grauer and Bond 1981; (20) Warner and Cropper 1983; (21) Gilliland 1982*a*; (22) Vogt *et al.* 1981; (23) Vogt and Semeniuk 1980; (24) Bath, Pringle, and Whelan 1980; (25) Sherrington *et al.* 1980; (26) Cowley, Hutchings, and Crampton 1981; (27) Gilliland 1982*b*; (28) Liebert *et al.* 1978; (29) Visvanathan and Wickramasinghe 1981; (30) Cowley *et al.* 1982*a*; (31) Bond, Kemper, and Mattei 1982; (32) Mason *et al.* 1983*a*; (33) Bailey *et al.* 1983; (34) Szkody, Shafter, and Cowley 1984; (35) Mason *et al.* 1983*b*; (36) Patterson 1981; (37) Young, Schneider, and Schectman 1981*a*; (38) Schoembs and Vogt 1981; (39) Vogt 1982; (40) Rayne and Whelan 1981; (41) Bailey 1979; (42) Patterson 1979*b*; (43) Wade and Oke 1982; (44) Visvanathan, Hillier, and Pickles 1982; (45) Agrawal, Riegler, and Rao 1983; (46) Liebert *et al.* 1982*a*; (47) Echevarria, Jones, and Costero 1983; (48) Stockman *et al.* 1982; (49) Schmidt, Stockman, and Grandi 1983; (50) Vogt 1983; (51) Liebert *et al.* 1982*b*; (52) Kemper 1982; (53) Barwig *et al.* 1982; (54) Patterson 1982; (55) Grauer and Bond 1982; (56) Stolz 1981; (57) Young and Schneider 1979; (58) Young, Schneider, and Schectman 1981*b*; (59) Latham, Liebert, and Steiner 1981; (60) Hutchings, Crampton, and Cowley 1981; (61) Schmidt, Stockman, and Margon 1981; (62) Schneider, Young, and Schectman 1981; (63) Robinson *et al.* 1981; (64) Williams and Ferguson 1982; (65) McHardy *et al.* 1982; (66) Cowley *et al.* 1975; (67) Thorstensen 1983; (68) Mardrossian *et al.* 1980; (69) Patterson 1979*a*; (70) Szkody and Shafter 1983; (71) Steiner *et al.* 1981; (72) Bond 1981; (73) Warner and Thackeray 1975; (74) Haefner 1981; (75) Vogt 1975; (76) Schoembs and Stolz 1981; (77) Pederson, van Paradijs, and Lewin 1981; (78) Patterson and Price 1981; (79) Hassall *et al.* 1981; (80) Shara and Moffett 1983; (81) Nousek *et al.* 1982; (82) Young, Schneider, and Schectman 1981*c*; (83) Horne 1980; (84) Shafter 1983*c*; (85) Shafter 1983*a*; (86) Patterson *et al.* 1984; (87) Schoembs 1982; (88) Patterson and Steiner 1983; (89) Kraft and Luyten 1965; (90) Stover 1981*a*; (91) Wade 1981; (92) Barwig and Schoembs 1981; (93) Hammerschlag-Hensberge, McClintock, and van Paradijs 1982; (94) White, Parmar, and Mason 1983; (95) Hutchings, Crampton, and Cowley 1979; (96) Young and Schneider 1981; (97) Young and Schneider 1980; (98) Frank *et al.* 1981; (99) Berriman 1983; (100) Ghosh *et al.* 1981; (101) van der Klis and Bonnet-Bidaud 1982; (102) Bianchini 1980; (103) Walker 1963; (104) Cowley, Crampton, and Hesser 1977*a*; (105) Kraft 1963; (106) Hutchings and Thomas 1982; (107) Hutchings 1979; (108) Bruch 1982; (109) Hutchings *et al.* 1981*a*; (110) Chlebowski, Halpern, and Steiner 1981; (111) McClintock, Remillard, and Margon 1981; (112) Thorstensen and Charles 1982; (113) McClintock *et al.* 1982; (114) White and Holt 1982; (115) Charles *et al.* 1979; (116) Hutchings *et al.* 1981*b*; (117) Motch 1981; (118) Frank and King 1981; (119) Young and Schneider 1981; (120) Kaitchuck, Honeycutt, and Schlegel 1983; (121) Cowley, Crampton, and Hutchings 1982*b*; (122) Mason and Cordova 1982; (123) Noskova 1982; (124) Cowley, Crampton, and Hesser 1977*b*; (125) Szkody 1982; (126) Horne *et al.* 1983; (127) Shara 1983; (128) Kilkenny, Hill, and Penfold 1981; (129) Cowley, Crampton, and Hutchings 1980; (130) Stover *et al.* 1980; (131) Kraft, Krzeminski, and Mumford 1969; (132) Szkody and Wade 1981; (133) Stover, Robinson, and Nather 1981; (134) Jameson, King, and Sherrington 1981; (135) Cominsky and Wood 1983; (136) Kurochkin and Shugarov 1980; (137) Szkody and Crosa 1981; (138) Horne, Lanning, and Gomer 1982; (139) McClintock *et al.* 1983; (140) Robinson, Nather, and Kepler 1982; (141) Williams and Patterson 1984; (142) Marsh, Wade, and Oke 1983; (143) Kaluzienski, Holt, and Swank 1980; (144) Blair *et al.* 1983; (145) Green, Richstone, and Schmidt 1978; (146) Stover 1981*b*; (147) Patterson 1979*c*; (148) Chincarini and Walker 1981; (149) Campolongo *et al.* 1980; (150) Gilliland and Phillips 1982; (151) Bond, Liller, and Mannery 1978; (152) Herbig *et al.* 1965; (153) Nelson and Young 1970; (154) Young and Capps 1971; (155) Lanning and Pesch 1981; (156) Young, Nelson, and Mielbrecht 1972; (157) Young and Wentworth 1982; (158) Vogt and Breysacher 1980; (159) Gilliland 1982*c*; (160) Lanning 1982; (161) Bond 1981; (162) Cowley and Crampton 1975; (163) Gottlieb, Wright, and Liller 1975.

seems quite possible that the “period gap” has arisen simply as a result of superposing two quite different distributions (as suggested by Paczyński 1981). We shall explore this possibility in § VII.

We will return to analyze the tabulated data in detail in § IV. But first the source of the mass transfer requires more attention. Every gram of accreting matter must somehow be coaxed from the low-mass secondary, which, with its deep

gravitational well and low luminosity, is quite poorly equipped to lose matter. Thus, it is important to examine just what is known about the lobe-filling secondaries.

### III. THE SECONDARIES: MAIN-SEQUENCE STARS?

Faulkner, Flannery, and Warner (1972) showed that in a binary system of orbital period  $P$  and mass ratio  $q$  (=

TABLE 2  
 "LOW-MASS" SYSTEMS WITH  $P > 1$  DAY

Star (1)	Type (2)	$P_{\text{orb}}$ (3)	$m_v$ Range Typical $m_v$ Correction (4)	Distance (pc) Clues (5)	E.W.(H $\beta$ ) ( $\text{\AA}$ ) (6)	Sp. Secondary $M_2/M_\odot$ $M_1/M_\odot$ (7)	References (8)
V1333 Aql..... (Aql X-1)	XR	(1.3)	14.8–19.2 19.0	1700 1		K0	1
HZ Her .....	XR	1.7001	13.5–15.0	5000 1		F0 IV	2,3
GK Per .....	CN(1901)	((1.9))	10–13.7 13.5 1.5 14.1–15.6 14.1	470 1,2,8	4(10.6) 12(13.1)	K2 IV	4,5,6
BE UMa .....	V471	2.2911					7,8
Feige 24 .....	V471	4.2319	12.3	90 3,5,6		M2	9
V1055 Ori..... (2S 0614+09)	XR	(5.2)	18.8	6000	2		10
V616 Mon..... (A0620–00)	XR	((7.39)) 0.32?	11.2–19 19.0	1100? 1	1(12.0)	K6 III?	11,12
2S 0921–63 .....	XR	(9.0)	16.3–17.3 17.3	8000? 1	3	F–G III	13,14,15
FF Aqr .....	V471	9.2077	9.4	650 1		G8 III 2.5 0.6 F5 III	16
V1341 Cyg .....	XR	9.843	14.5–15.4	8000 1			17,18
T CrB.....	CN? (1866,1946)	227.5	9.9	1200 1	6	M3 III	4

NOTE.—Columns and codes have a meaning identical to that of Table 1.

REFERENCES.—(1) Thorstensen, Charles, and Bowyer 1978; (2) Middleditch and Nelson 1976; (3) Bahcall and Chester 1977; (4) Paczyński 1965; (5) Bianchini, Sabbadin, and Hamazoglu 1982; (6) Wade 1982; (7) Ferguson *et al.* 1981; (8) Ferguson 1983; (9) Thorstensen *et al.* 1978; (10) Marshall and Millit 1981; (11) Murdin *et al.* 1980; (12) McClintock *et al.* 1983; (13) Cowley, Crampton, and Hutchings 1982 *c*; (14) Chevalier and Ilovaisky 1982; (15) Branduardi-Raymont *et al.* 1983; (16) Etzel *et al.* 1977; (17) Cowley, Crampton, and Hutchings 1979; (18) Crampton and Cowley 1980.

$M_2/M_1$ ), the mean density  $\rho$  of the lobe-filling star is given by

$$\rho = \frac{6.905}{(P/4 \text{ hr})^2} F(q) \text{ g cm}^{-3}, \quad (1)$$

where

$$F(q) = \begin{cases} 1 & q < 0.5 \\ \frac{q}{(1+q)(0.38+0.2 \log q)^3}, & q > 0.5 \end{cases} \quad (2)$$

Now  $F(q)$  is very weakly dependent on  $q$ ; it declines to 0.89 at  $q=1$  and to 0.82 at  $q=1.5$ , which is probably the largest mass ratio likely to be present in real CVs (formally, systems with  $q > 1$  are unstable, but since  $q=1.36$  in EM Cyg, it seems that nature does not rigidly adhere to this limit). This weak dependence guarantees that the mean density is determined to an accuracy of  $\sim 5\%$  by the orbital period alone, which is

easily measured to any accuracy desired. Therefore, since  $M/R^3$  is known, we need only one additional constraint on any function of  $M$  and  $R$  to determine  $M$  and  $R$  absolutely. Because a mass-radius relation (approximately  $R/R_\odot = M/M_\odot$ ) holds for main-sequence stars, it has become a common practice to apply this constraint. The rewards are considerable; radial velocity observations usually constrain the mass ratio fairly well, so that both of the component masses are known if one is.

Recently, it has become an even more common practice to criticize this approach, on the following grounds: (1) theory provides no compelling reason why the secondaries should be main-sequence stars (Rappaport, Joss, and Webbink 1982, hereafter RJW; Warner 1978; Paczyński and Sienkiewicz 1983); and (2) deviations from the main sequence have actually been observed (e.g., Wade 1979, 1981; Stover 1981 *a, b*; Robinson, Nather, and Kepler 1982). But essentially all observers have compared their results with the *theoretical zero-age* main sequence, despite evidence that theoretical models of

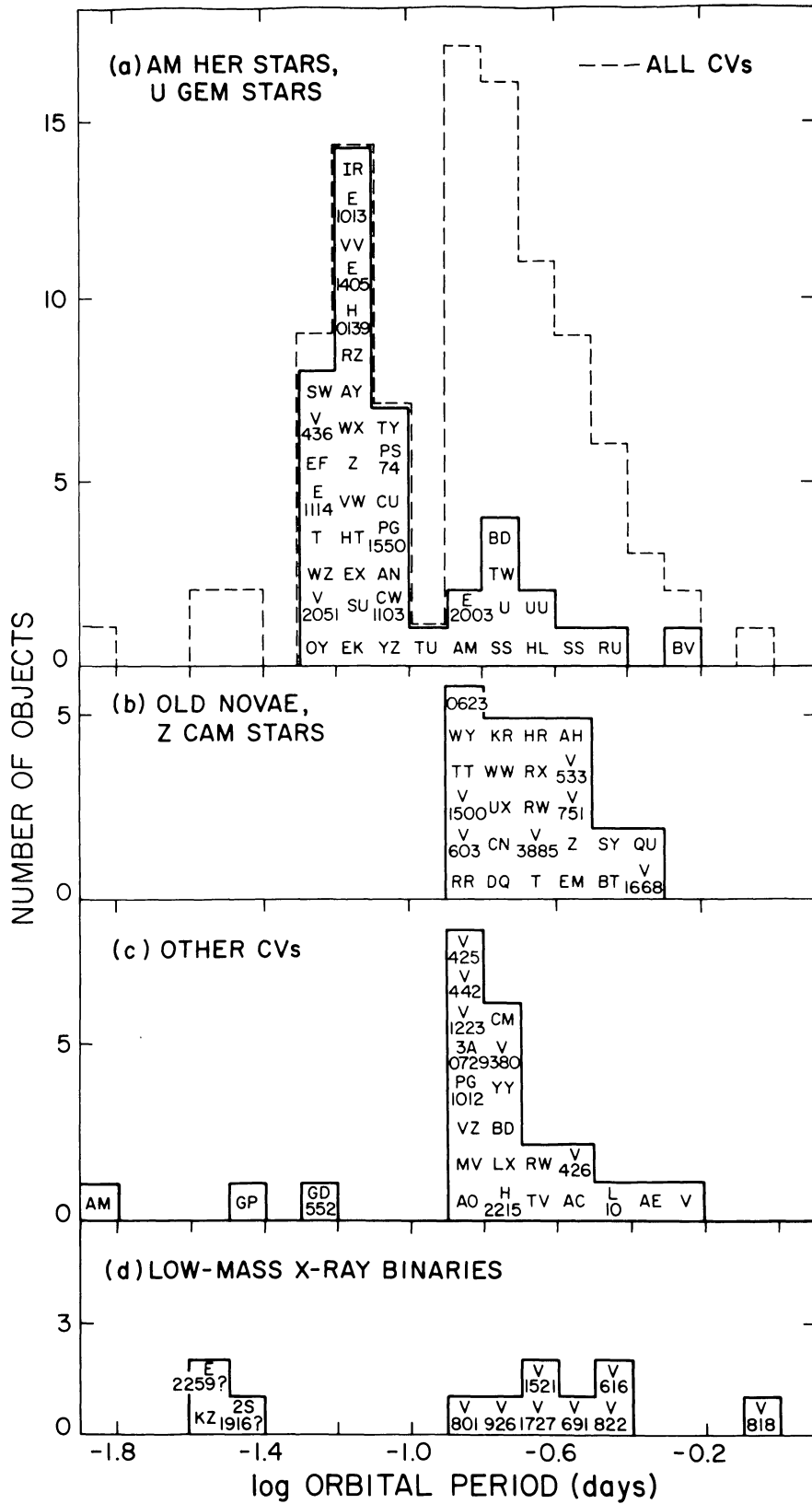


FIG. 1.—Distribution of orbital periods for cataclysmic variables and low-mass X-ray binaries. The sum of the four separate distributions is shown as the dashed line in (a).

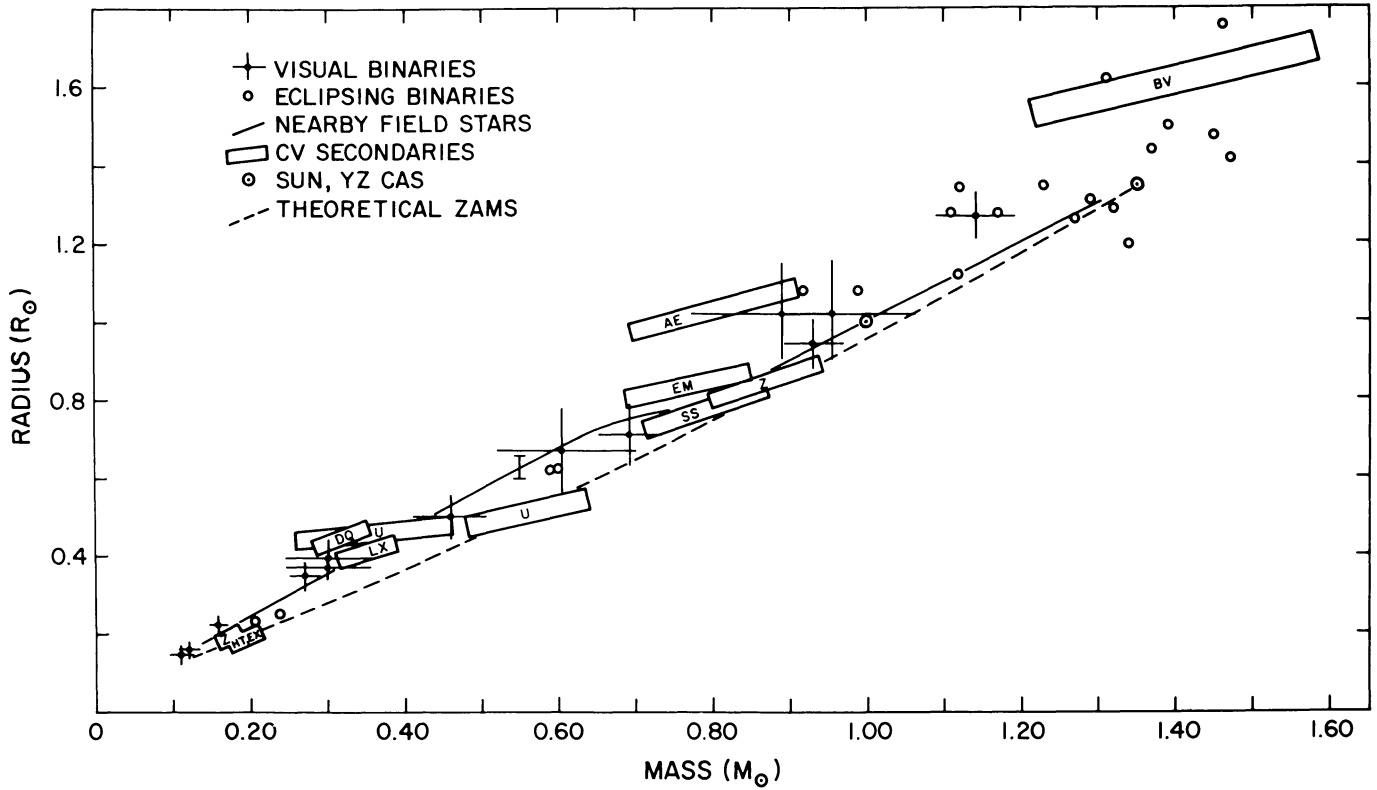


FIG. 2.—Mass-radius diagram for model ZAMS stars (*dashed curve*); stars in wide binaries (crosses, open circles); single stars (*solid curve*); and CVs (*rectangles*). The adopted empirical mass-radius relation (eq. [3]) is not shown, but is virtually indistinguishable from the solid curve.

low-mass stars are not very successful in accounting for the masses and radii of *any* stars (Hoxie 1973; Lacy 1977a).

We reexamine this question in the mass-radius diagram of Figure 2. The dashed curve is the theoretical ZAMS, namely, the mean of those computed by Grossman, Hays, and Graboske (1974) and by Copeland, Jensen, and Jorgensen (1970). The only empirical points accurate to  $\leq 1\%$  are the Sun and YZ Cas; the latter is especially useful because it is an F2 star in a binary whose age is much less than the main-sequence lifetime of an F2 star—therefore, it must reside strictly on the ZAMS (Lacy 1983). The data for eclipsing binaries, shown as open circles, are probably all accurate to  $\leq 5\%$ . The stars in visual binaries, shown as crosses, have larger uncertainties. Finally, we show as the solid curve the mean empirical relation found by Lacy (1977a) from applying the Barnes-Evans relation to 84 nearby field stars of known distance. To reduce clutter we do not show the individual points, but show a typical  $\pm 1 \sigma$  variance at  $(0.55 M_{\odot}, 0.60 R_{\odot})$ . Lacy's Figure 6 presents these data in the  $M_v$ - $R$  plane, and because masses are known for only a few of them, we require a mass- $M_v$  relation. *We have used the theoretical mass- $M_v$  relation for the ZAMS to convert the data to the mass-radius plane.* We adopt this assumption because: (1) these low-mass stars should not have evolved significantly, and should therefore reside on the ZAMS; and (2) the theoretical mass- $M_v$  relation fits the available observational data extremely well (see Lacy's Fig. 7).

Figure 2 shows that the empirical radii significantly exceed those of ZAMS models for  $M \leq 0.8 M_{\odot}$ , as already pointed out by Lacy and by Hoxie (1973). This is very strongly suggested by the binary star data alone, and is established beyond all doubt if the field star data are accepted. Can the latter be in error? It is difficult to see how. From Lacy's Figures 6 and 7 we see that (1) the Barnes-Evans relation yields consistent radii for both single stars and stars in wide binaries, and (2) the latter are known to satisfy the theoretical ZAMS mass- $M_v$  relation. Hence, we can see no way to justify ignoring the field star data.

Whether or not the field star data are accepted, it is clear that real stars are bigger than model stars in this regime, and we propose to replace the theoretical mass-radius relation with an empirical one. Taking all the data at face value and assigning weights  $\propto 1/\sigma^2$ , we find that a good empirical ZAMS mass-radius relation is

$$\frac{R}{R_{\odot}} = \begin{cases} \left(\frac{M}{M_{\odot}}\right)^{0.88 \pm 0.02} & 0.1 < \frac{M}{M_{\odot}} \leq 0.8 \\ 0.98 \left(\frac{M}{M_{\odot}}\right)^{1.00} & 0.8 < \frac{M}{M_{\odot}} < 1.4 \end{cases} \quad (3)$$

We will occasionally refer to this as "the" empirical mass-radius relation, but want to call attention to the fact that it is

quite poorly defined for  $M \leq 0.4 M_{\odot}$ , which turns out to be a very interesting regime. An improved relation for low-mass stars would be very desirable, and could have important consequences (see § VI).

Finally, we may ask where the lobe-filling stars in CVs live in the mass-radius plane. We have taken the published masses from Table 1, and derived radii through equations (1) and (2). Because the density is accurately known and  $R \propto (M/\rho)^{1/3}$ , the uncertainty in the radius is quite small. The results are the error boxes in Figure 2 (see also Ritter 1981).

It is evident that most of the CV secondaries are larger than ZAMS model stars of the same mass, but the deviations appear similar to those shown by the calibration stars. The only star certifiably above the empirical ZAMS is AE Aqr, which, as we shall see immediately below, shows other signs of being slightly evolved (but not beyond the TAMS). In general, the CV secondaries follow the mass-radius law for empirical ZAMS stars quite faithfully.

If the secondaries are on the ZAMS, their masses and radii are fairly well determined by the orbital period alone. Let us adopt the empirical mass-radius relation for the lower main sequence, and denote departures by the factor of  $\alpha$ :

$$\frac{R_2}{R_{\odot}} = \alpha \left( \frac{M_2}{M_{\odot}} \right)^{0.88} \quad (4)$$

Let us also adopt the standard spherical approximation to the Roche geometry for small  $q$  (Paczynski 1971) and denote departures by the factor  $\beta$ :

$$\frac{R_2}{a} = 0.462 \left( \frac{q}{1+q} \right)^{1/3} \beta \quad (5)$$

The value of  $\beta$  is always close to 1, and for the entire range of  $q$  is given to an accuracy of less than 1.5% by

$$\beta = \begin{cases} 1 & q < 0.52 \\ 1 + 0.066(q - 0.52) & 0.52 < q < 2 \end{cases} \quad (6)$$

It can then be easily shown that a lobe-filling secondary in a system must have

$$\frac{M_2}{M_{\odot}} = 0.380 \frac{\beta^{1.83}}{\alpha^{1.83}} P_4^{1.220}, \quad (7)$$

$$\frac{R_2}{R_{\odot}} = 0.427 \frac{\beta^{1.61}}{\alpha^{0.61}} P_4^{1.073}, \quad (8)$$

where  $P_4$  is  $P/(4 \text{ hr})$ .

These may be compared directly to the formulae derived by Warner (1976) from use of the theoretical ZAMS mass-radius relation:

$$\frac{M_2}{M_{\odot}} = 0.482 P_4^{1.00}, \quad (9)$$

$$\frac{R_2}{R_{\odot}} = 0.463 P_4^{1.00}. \quad (10)$$

One important result of replacing the theoretical with the empirical ZAMS is that significantly lower masses are predicted for stars of short orbital period ( $\leq 6 \text{ hr}$ ). We shall find below that the empirical ZAMS stars are also significantly cooler and fainter than model stars in binaries with the same orbital period.

Because effective temperatures are known from the spectral types and infrared colors of the secondary, we can also compare these stars with main-sequence stars in a mass- $M_v$  plane. Adopting the spectral type- $T_e$  relation of Popper (1980) and using the masses and radii found above, we show the location of CV secondaries relative to the main sequence in Figure 3. We have assumed an uncertainty in the spectral type of  $\pm 2$  subclasses, e.g., K5 $\pm 2$ . The stars congregate fairly closely along the main sequence, with the possible exceptions of Z Cam and U Gem. The spectral type of Z Cam has been taken as K7 from the energy distribution (Wade, private communication), but was reported as G1 from the absorption lines (Kraft, Krzemiński, and Mumford 1969). If we adopt a compromise value of K0, the star moves right up to the main sequence. U Gem is a more worrisome case; the Wade (1979) spectral type (M4.5) and the Stover *et al.* (1980) mass ( $0.56 M_{\odot}$ ) are not consistent with each other and with a ZAMS star (although with slightly larger errors, they might be). This star deserves further attention.

It is worth noting that no assumption about the distances has been made in preparing Figure 3. This exploits the fact that when the radius and the spectral type of the secondary are known, the absolute magnitude and the distance are determined. If the spectral type can be determined within  $\sim \pm 2$  subclasses, this is a useful distance indicator for any system of known orbital period. Adopting the notation used above, and dropping any assumption of a mass-radius relation, we have

$$\frac{R_2}{R_{\odot}} = 0.590 \beta \left( \frac{M_2}{M_{\odot}} \right)^{1/3} P_4^{2/3}. \quad (11)$$

Thus, if  $M_2$  can be estimated crudely, say within a factor of 3, then  $R_2$  is determined within a factor of 1.4. Knowledge of the spectral type within  $\sim 2$  subclasses fixes  $T_e$  within a factor of  $\sim 1.1$ , and hence the luminosity ( $\propto R^2 T_e^4$ ) is determined within a factor of 2. By measuring the magnitude of the secondary at some suitable wavelength (usually in the infrared), one can then determine the distance to within a factor of  $\sim 1.4$ . Of course, if the secondary is assumed to be a main-sequence star in the  $M$ - $R$  or  $M$ - $M_v$  plane, the uncertainty in the distance is reduced.

The importance of knowing the correct mass-radius law can be illustrated by deriving explicit  $P_{\text{orb}}-T_e$  and  $P_{\text{orb}}-M_v$  relations. These will be only weakly dependent on the white dwarf mass, so we have calculated them by assuming  $M_{\text{wd}} = 1.0 M_{\odot}$  in all cases, and using equations (4)–(8). The relations are shown in Figure 4 for both the empirical and the model ZAMS, with the observed spectral types also shown. For the “model ZAMS” we use equations (9) and (10) as a convenient approximation. The inset spectral type- $T_e$  relation is that of Popper (1980). From the figure it is obvious that real CV secondaries are too

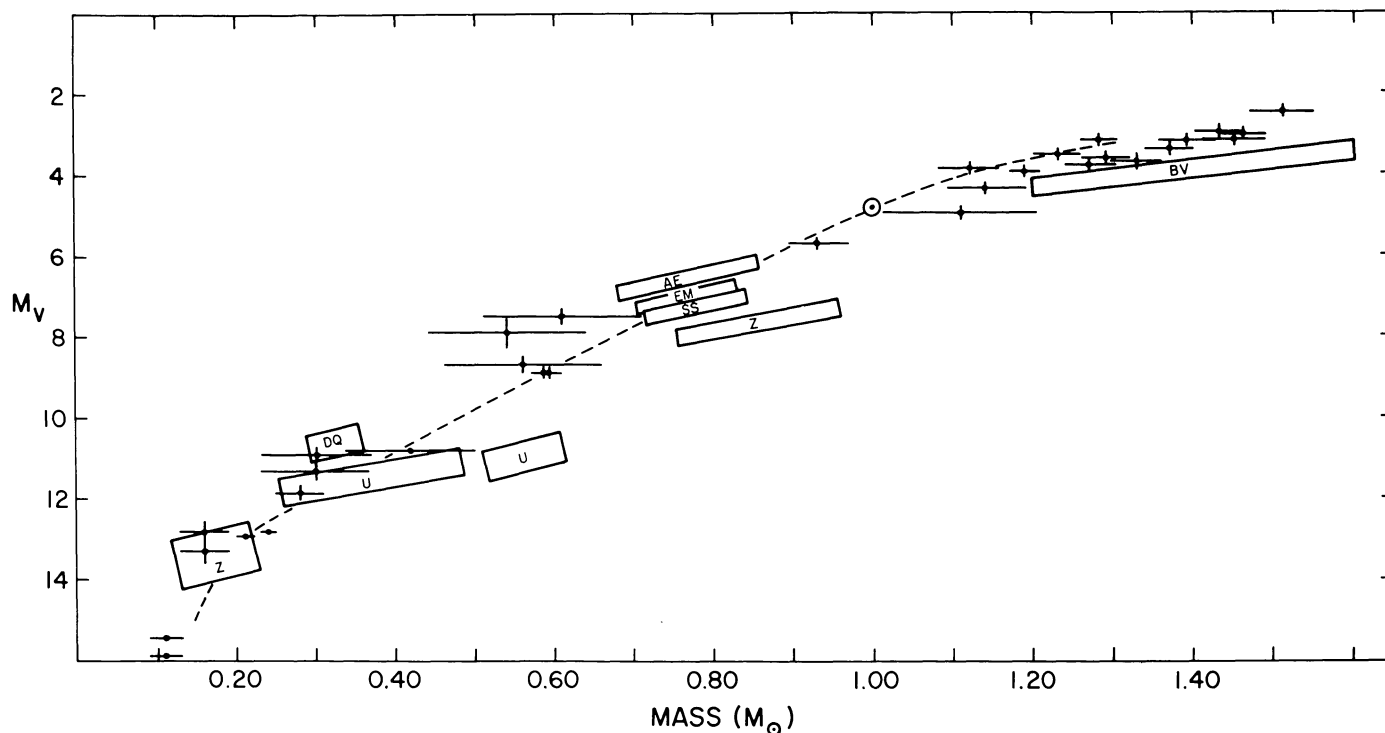


FIG. 3.—Mass- $M_v$  diagram for model ZAMS stars (dashed curve); stars in wide binaries (crosses); and CVs (rectangles). The CV data are derived from  $T_e$  and  $R$ , not from knowledge of the distances.

cool to be model ZAMS stars, but are in excellent agreement with the empirical ZAMS for  $P \leq 9$  hr. We do not show the 40 additional stars in Table 1 which have only *limits* on the spectral type available. But a check of Table 1 shows that these stars are in every case consistent with the empirical ZAMS, and frequently inconsistent with the model ZAMS.

The four stars with  $P > 9$  hr are too cool to be fitted by any kind of ZAMS star. We can determine the extent of their departure from the ZAMS by combining equations (4) and (11) and solving for  $\alpha$ :

$$\alpha = 0.590\beta (M_2/M_\odot)^{-0.55} P_4^{2/3}, \quad (12)$$

This yields  $\alpha = 1.05, 1.30,$  and  $1.19$  for RU Peg, AE Aqr, and BV Cen, respectively. According to the definition of Iben (1967) (see also Webbink 1979), the radii of low-mass stars grow  $\sim 70\%$  between the ZAMS and the terminal-age main sequence (TAMS). Thus, even these stars are “on the main sequence.”

Figure 4 shows that the departures of the empirical from the model ZAMS in  $T_e$  and  $M_v$  in the range  $3 < P_{\text{orb}} < 8$  hr are quite large. The reason for this is that the empirical masses are  $\sim 20\%$  smaller, and luminosity is a very sensitive function of mass ( $\propto M^4$ ). Thus, three important lessons emerge from Figure 4: (a) our empirical ZAMS is greatly superior to the model ZAMS; (b) the  $P_{\text{orb}}-T_e$  plane is usually a more sensitive test of the ZAMS identity of secondaries than the mass-radius plane; and (c) distance estimates based on the brightness of the secondary will be significantly too large if the model ZAMS is used.

Approximate linear fits to the empirical ZAMS curves in Figure 4 are given by:

$$M_v = \begin{cases} 17.7 - 11.00 \log P & 0.05 < \log P < 0.7 \\ 22.0 - 17.46 \log P & 0.7 < \log P < 1.1 \end{cases}, \quad (13)$$

$$T(K) = \begin{cases} 2630 + 1380 \log P & 0.05 < \log P < 0.7 \\ -1800 + 7800 \log P & 0.7 < \log P < 1.1 \end{cases}, \quad (14)$$

where the orbital period  $P$  is in units of hours.

We conclude this section by recapitulating what is known about CV secondaries:

1. Secondaries in all systems with  $P < 9$  hr are indistinguishable from zero-age main-sequence stars. Systems with  $P > 9$  hr contain secondaries that are probably somewhat evolved (but not beyond the terminal-age main sequence). Further efforts to calibrate the empirical ZAMS, especially for low-mass stars ( $< 0.4 M_\odot$ ), are warmly recommended.

2. The apparent main-sequence structure indicates that exotic assumptions about the internal density distribution (Warner 1978) and chemical composition (Williams and Ferguson 1982) are not warranted. The mass-radius and mass- $T_e$  relations are sensitive probes of the helium abundance, chiefly because luminosity depends so strongly on the mean molecular weight ( $\propto \mu^7$ ; Demarque 1972). The observations constrain the ratio of number densities  $N(\text{He})/N(\text{H})$  to be approximately in the range 0.09–0.14 (Popper *et al.* 1970), with 0.11 considered “normal.”

3. The fact that real stars are somewhat bigger than model ZAMS stars, but agree in  $M_v$ , suggests that the opacities are

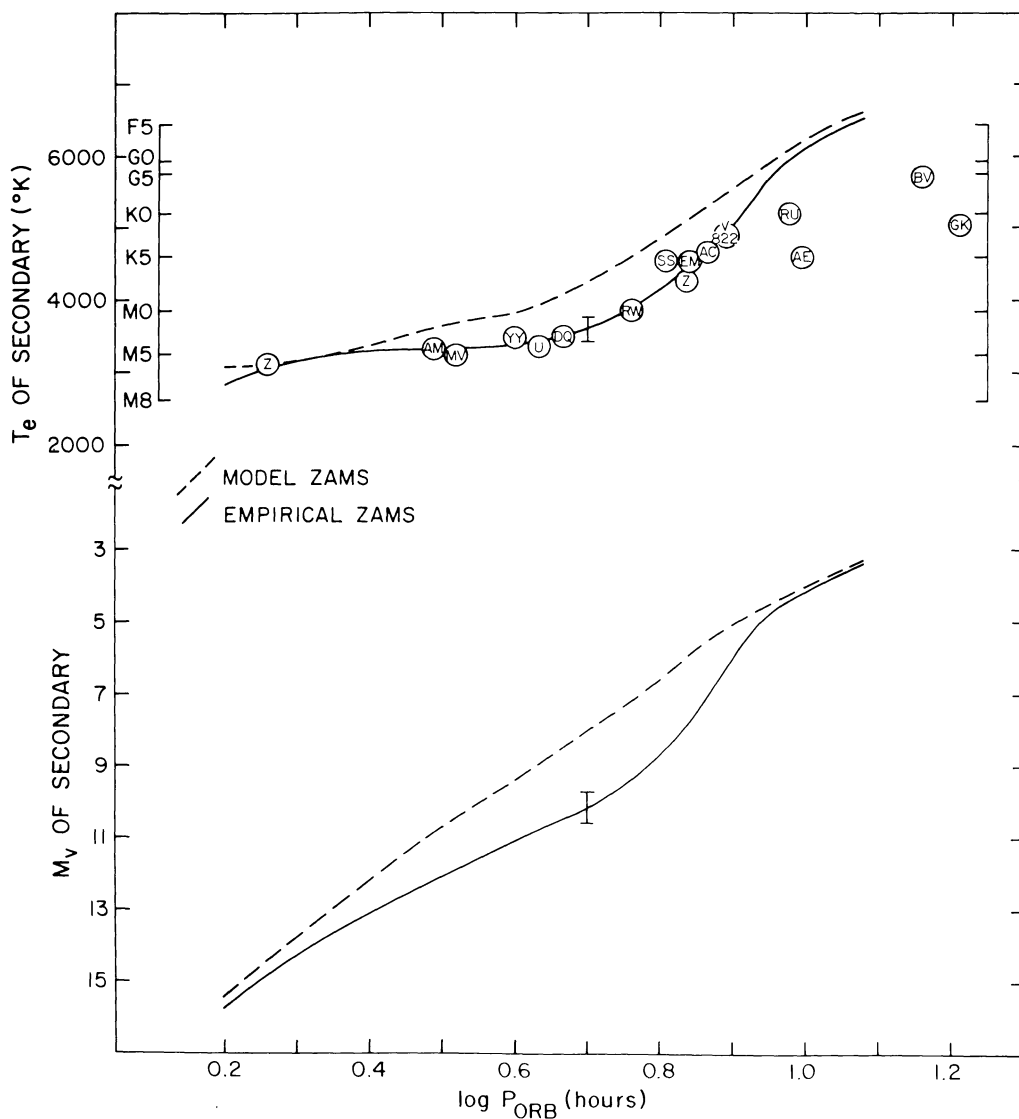


FIG. 4.—Dependence of the secondary's effective temperature  $T_e$  and absolute visual magnitude  $M_v$  on orbital period. Solid curves are the relations predicted from the empirical mass-radius relation (eq. [3]), while dashed curves assume a model ZAMS mass-radius relation.

larger than assumed by the models, as pointed out by Lacy (1977a). This is no great surprise, and should suggest caution in interpreting the minimum orbital period of CVs (see RJW; Paczyński 1981; Paczyński and Sienkiewicz 1983).

Of course, we are not arguing that the secondaries in CVs with  $P < 9$  hr *must* reside on the ZAMS, but only that no counterexample is known. As we shall see in §§ VI and VII, there are good theoretical reasons to believe that many secondaries are forced away from the ZAMS (viz., become too large for their mass) when thermal equilibrium is lost. Such a star will be more difficult to detect, since it will be less luminous than a ZAMS star in a binary with any given orbital period. This *may* explain why no such stars are known.

#### IV. THE SEARCH FOR THE MASS TRANSFER RATE

Knowledge of the mass transfer rate would be a tremendous aid both in interpreting the observational data and in under-

standing the evolutionary processes at work. The first modern attempts to derive  $\dot{M}$  (e.g., Smak 1971; Warner and Nather 1971) used the observed period changes from eclipse timings and the newly developed theory of binary star evolution, i.e., mass transfer with total mass and angular momentum conserved. (Although, as remarked earlier, this theory is flatly inconsistent with the mere *existence* of CVs!) Pringle (1975) strongly criticized this approach, pointing out that most of the claimed period changes were not statistically significant, and that the existence of period changes of alternating *sign* was sufficient warning that the observed changes do not arise from mass transfer. With a greater baseline of data now available, Patterson (1984) studied the subject of eclipse timings anew, and found that six CVs showed period changes significant at a confidence level of  $\geq 99\%$ . The magnitude and sign of the changes suggest that they are principally due to angular momentum loss, not mass transfer (see discussion below in



§ VI). In order to obtain  $\dot{M}$  from eclipse timings, it would be necessary to know the angular momentum loss rate, the mass-loss rate, and the component masses rather accurately. This is thoroughly unfeasible; eclipse timings just do not reveal  $\dot{M}$ , period.

A more promising method uses the bolometric luminosity of the “hot spot” (the shock front where the stream of transferred material strikes the disk) to find the transfer rate. This has been applied principally to WZ Sge (Krzeminski and Smak 1971) and U Gem (Paczynski and Schwarzenberg-Czerny 1980). Because the luminosity of the *spot* is used, this method yields the mass *transfer* rate, rather than the rate of accretion onto the white dwarf. The three principal drawbacks are as follows:

- 1) The distance of the star must be known;
- 2) The bolometric correction and radiation pattern of the spot are not known, so we do not know how to convert the observed flux into a luminosity;
- 3) There are only nine systems that show a clearly identified hot spot in their light curves.

A more generally applicable method is to obtain  $\dot{M}$  from the radiation emitted by the accretion disk, assuming it is entirely due to the release of gravitational energy:

$$L_{\text{bol}} = kGM_*\dot{M}/R_*, \quad (15)$$

where  $M_*$  and  $R_*$  are the mass and radius of the compact star, and  $k$  is 0.5 for the disk proper, 0.75 for the disk plus “boundary layer,” or 1 if the heating of the white dwarf surface is also counted. This argument has been invoked by many authors over the years to deduce  $\dot{M}$ , but three problems have seriously limited its precision: (1) uncertainty in the distance; (2) the large sensitivity to the unknown value of  $M_*$  — essentially  $M_*^{1.8}$ , since  $R \propto M^{-0.8}$  for white dwarfs of moderate mass; (3) the lack of sufficiently broad wavelength coverage, especially in the UV. These problems were in part overcome by fitting the spectrum in detail (rather than just the bolometric flux) to an optically thick disk model over a wide range of wavelengths, which now include the critical 1200–3000 Å region. This technique was pioneered by Kiplinger (1979, 1980), nobly carried forward by groups at Cambridge and Leicester (Bath, Pringle, and Whelan 1980; Frank and King 1981), and is now in very widespread use.

But the restriction to an optically *thick* disk is very serious, since the existence of bright emission lines testifies to the optically *thin* conditions that must prevail in at least the outer regions of many disks. Very recently, accretion disk models of arbitrary optical depth have been published (Williams 1980, Tylanda 1981; Williams and Ferguson 1982), and it seems likely that a “golden age” of fitting observed fluxes to disk models is imminent.

Of course, accurate determination of  $\dot{M}$  and other system parameters can only come from detailed fitting of each star’s flux distribution, with proper accounting of the red star, white dwarf, and hot spot, as well as the disk itself. This is an enormous undertaking, far beyond the scope of this paper. Pessimists might argue that it cannot be done at all until the EUV region (100–1200 Å), where many CVs could be bright, is explored. But for purposes of understanding the evolution-

ary processes at work, approximate estimates of  $\dot{M}$  may well suffice, and we now turn our attention to such estimates.

#### a) $M_v$ of the Disk

By far the greatest volume of data on CVs lies in the long-term light curves of amateur visual observers, as maintained, e.g., by the AAVSO. For the brighter stars, these light curves extend over ~50–100 yr and include over 10,000 individual observations. With the history of the visual magnitude so richly documented, it would be very desirable to use this quantity as the basic indicator of  $\dot{M}$ . The visual band is also a suitable choice because it is virtually free from any contribution by the red star (usually confined to the infrared), the white dwarf, or the boundary layer (both usually confined to the ultraviolet). In the few cases where the red star contributes significantly to the visual light, its contribution can be estimated from broad-band colors and therefore can be easily removed. The hot spot may produce up to ~20%–50% of the visual light, but this can be safely neglected at the level of accuracy we seek.

Figure 5 shows the dependence of  $\dot{M}$  on orbital period, for systems of known distance. We deduce the transfer rates from the data of Table 1 as follows:

1. Find the apparent visual magnitude of the accreting component of each system in its normal luminosity state. (Remove the contribution of the red star if necessary.)
2. Multiply the corresponding visual flux by the correction factor in column (4) to obtain the time-averaged visual flux.
3. For highly inclined systems, use the best estimate of binary inclination and interpolate in Table 2 of Mayo, Wickramasinghe, and Whelan (1980) to correct the flux to an inclination of 52°, which is the average over  $4\pi$  sr.
4. With the resultant  $m_v$ , the distance, and an estimate of interstellar absorption, compute  $M_v$  and interpolate in Tylanda’s (1981) models to find the corresponding  $\dot{M}$ .

Although this technique makes no assumptions about optical depth (which is determined, of course, by  $\dot{M}$  itself), it does assume that the energy source is steady-state accretion, which might be seriously in error for the following:

- 1) For the classical novae, because nuclear energy sources might be contributing a significant fraction of the light;
- 2) For the dwarf novae, because one of the presently viable models (the disk instability model; see Osaki 1974; Hoshi 1979) dumps matter into the inner disk only during eruption, wreaking havoc with our correction factor.

These problems are sufficiently serious, and Figure 5 sufficiently important, to consider in greater detail.

The reasons for attributing the light of classical novae to accretion rather than thermonuclear processes are as follows:

1. The pre-eruption and post-eruption magnitudes are essentially equal (Payne-Gaposchkin 1957; Robinson 1975), and the available data suggest that novae are fairly constant in light between eruptions. Since hydrogen shell burning in accreting white dwarfs is known to be unstable (e.g., Gallagher and Starrfield 1978, and references therein), it does not seem possible that steady nuclear burning can continue for the ~10<sup>4</sup> yr between eruptions.

2. The eclipse light curves of two classical novae, DQ Her and BT Mon, show no sudden jumps at the time of white

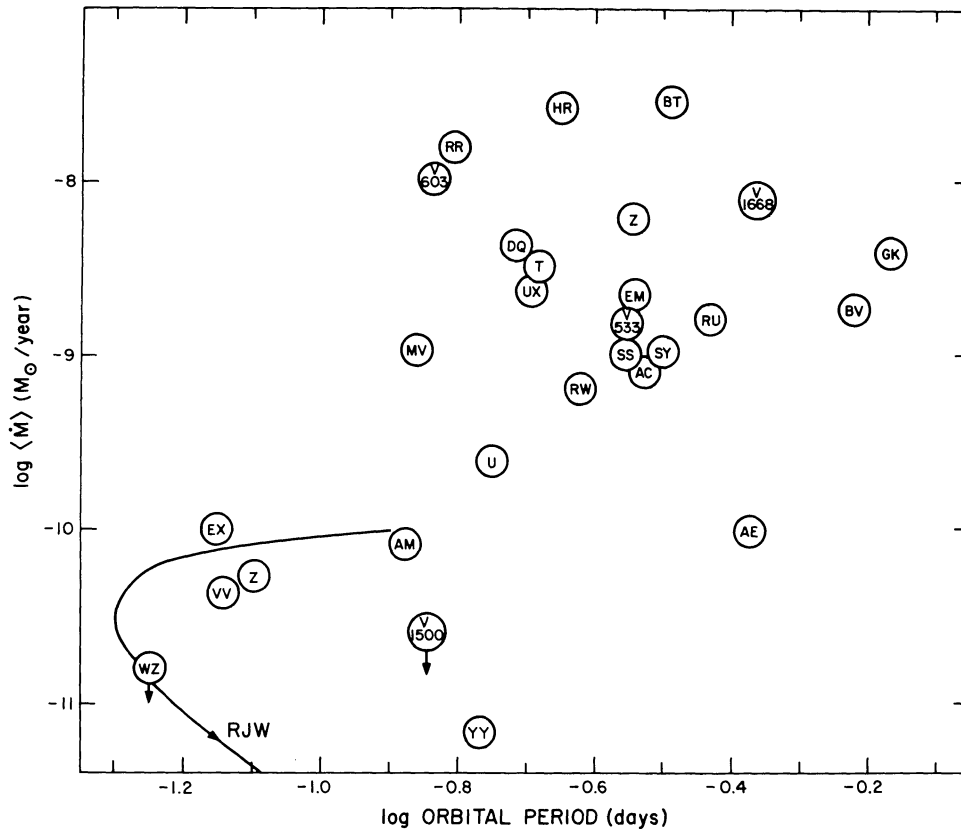


FIG. 5.—Dependence of mean mass transfer rate on orbital period for systems of known distance. The curve labeled RJW indicates the predicted location and evolution of systems evolving under the control of gravitational radiation (Rappaport, Joss, and Webbink 1982).

dwarf ingress and egress, suggesting that the white dwarf is a minor contributor to the light.

3. Nuclear burning tends to produce very high temperatures and UV luminosities, yielding an ultraviolet spectrum with a Rayleigh-Jeans flux distribution ( $F_{\nu} \propto \nu^2$ ), and creating a large reflection effect off the orbiting secondary (as seen in the central stars of planetary nebulae Bond 1983). In fact, *IUE* spectra generally show much flatter flux distributions ( $F_{\nu} \propto \nu^{-2-+0.3}$ ; Szkody 1982; Krautter *et al.* 1981), and reflections effects off the secondary have never been seen.

4. One old nova, DQ Her, possesses a magnetic white dwarf whose rotation is spinning up, presumably under the action of accretion torques (Lamb 1974). The  $\dot{M}$  deduced from the observed torque agrees with the  $\dot{M}$  deduced from the visual luminosity if the latter is due to accretion (Lamb and Patterson 1983).

The problem with dwarf novae is different. In principle, we should convert the time history of  $M_v$  to a time history of  $\dot{M}$  using disk models, and then integrate under the curve to find the time-averaged  $\langle \dot{M}(t) \rangle$ . However, the validity of the disk models may certainly be challenged if they are used to derive instantaneous values of  $\dot{M}(t)$ , since the viscous processes which allow the disk to radiate may vary strongly with time and radius in the disk. By averaging  $M_v$  over long periods of time (at least a few cycles of quiescence and eruption), we avoid this problem and enable use of steady disk models. In practice, almost any technique for calculating  $\langle \dot{M} \rangle$  from the

disk light will work reasonably well, because for the parameters typical of CVs ( $\dot{M} = 10^{-11} - 10^{-8} M_{\odot} \text{ yr}^{-1}$ ,  $M_{\text{wd}} \approx 1.0 M_{\odot}$ , viscosity parameter  $\alpha \sim 1$ ), the visual flux is approximately proportional to  $\dot{M}$  ( $\propto \dot{M}^{0.7}$  from Fig. 2 of Tylenda 1981). Hence, there is no great sensitivity to exactly how  $\langle \dot{M} \rangle$  is calculated.

We conclude that the observed “blue component” in CVs is powered by accretion energy released in a disk, that over a sufficiently long time it can be satisfactorily represented by a steady-state model, and that  $\langle M_v \rangle$  provides a reasonably good estimator of  $\langle \dot{M} \rangle$  for systems of known distance.

#### b) Distance-independent Indicators

Unfortunately, distances are known for only a few CVs, and prospects for dramatic improvement are not good. A few more secondaries will probably be found from spectroscopy in the infrared (0.7–1.1  $\mu\text{m}$ ; e.g., Oke and Wade 1982) and from broad-band infrared photometry (Bailey 1981; Berriman 1983), but data available at present suggest that the light of the secondary is frequently overpowered by the accretion disk even in the infrared.

It would be very desirable to have a technique for estimating  $\dot{M}$  from easily observable quantities. In principle, the broad-band colors of the disk could be used; disks with higher  $\dot{M}$  in general show higher temperatures and therefore bluer colors. But the models of Tylenda (1981) show the severe

problems with such a technique. For accretion rates in the range  $10^{-11}$ – $10^{-8} M_{\odot} \text{ yr}^{-1}$  and disk radii in the range  $2$ – $10 \times 10^{10}$  cm, the  $B-V$  and  $U-B$  colors vary by only 0.3 mag over the entire range. Therefore, even small contributions from other sources (white dwarf, secondary star, hot spot, emission-line source) can produce very large errors in  $\dot{M}$ . The ultraviolet colors, on the other hand, are *extremely* sensitive to  $\dot{M}$ , as shown by the theoretical disks of Tylenda (1981) and Williams and Ferguson (1982). The difficulty with the ultraviolet is that it is even more sensitive to the unknown mass of the white dwarf. In Tylenda's Figure 16, showing a model with  $\dot{M} = 1.5 \times 10^{-11} M_{\odot} \text{ yr}^{-1}$  and a range of white dwarf masses, the emergent flux at 1900 Å varies approximately as  $M_{\text{wd}}^{4.5}$ , and the emergent flux at 1300 Å varies approximately as  $M_{\text{wd}}^6$  (while the visual flux is varying only as  $M_{\text{wd}}^{1.2}$ ). This dependence will be less steep for higher accretion rates since the ultraviolet emission will then come from larger radii in the disk, where the mass of the central object is less important. By accounting for these effects in a detailed way, reasonable estimates of  $\dot{M}$  can probably be obtained, at least for rates  $\geq 10^{-10} M_{\odot} \text{ yr}^{-1}$ . But the demands on the data are severe: one requires accurate, reddening-corrected spectrophotometry over the entire interval 1200–10000 Å. Such data are available at present for only a few of the brightest systems. In addition, it will be necessary to improve the models, which still do not correctly account for the effects of Lyman absorption on the spectrum.

Perhaps the most readily obtainable quantity (not even requiring a clear night!) is the equivalent width of the emission lines. Because low- $\dot{M}$  systems produce disks of sufficiently low density that line emission plays a significant role in the cooling, the equivalent widths of the emission lines should, in general, increase as  $\dot{M}$  is decreased. We have therefore collected the available data on equivalent widths of the H $\beta$  emission line and present them in column (6) of Table 1. For the systems of known distance (and excluding the AM Her stars which presumably do not have disks), we show the relation between equivalent width and absolute visual magnitude in Figure 6. Where data are available for both the faint and bright states of a star (viz., TT Ari, MV Lyr, V533 Her, GK Per), we show two points, except for the dwarf novae, which are not individually shown during eruption because they all dive into the shaded region of Figure 6.

The equivalent widths predicted by the models of Tylenda for accretion disks<sup>2</sup> with  $M_{\text{wd}} = 1.0 M_{\odot}$ ,  $\alpha = 1.0$  are shown as a function of  $M_v$  and disk radius  $R_d$  by the three dashed lines at the lower right of Figure 6. Given the observed range of orbital periods and mass ratios, the  $R_d = 5 \times 10^{10}$  cm model is the most appropriate for real CVs. As Figure 6 illustrates, the observed emission lines are much stronger than those predicted by the model.

Yet the *shape* of the observed distribution certainly resembles the theoretical curves, and it seems possible that a minor

<sup>2</sup>Here we use the conventional representation of viscosity in the disk (Shakura and Sunyaev 1973; Tylenda 1981). We have previously used the symbol  $\alpha$  to characterize the secondary's departure from the lower main-sequence mass-radius relation (Eq. [4]). The latter is the consistent usage in this paper, except for this and the following paragraph.

modification of the models might bring the models up to fit the data. For example, Tylenda's models with  $\dot{M} = 10^{14} \text{ g s}^{-1}$  showed that the equivalent width increased by a factor of  $\sim 4$  when  $\alpha$  was changed from 1 to 10. This is principally because the higher viscosity decreases the density everywhere in the disk, which increases the size of the optically thin outer region responsible for the line emission. If this were true through the entire range of accretion rates shown in Figure 5, then the data could be fitted for  $M_v \geq 6.5$ , with an extra component of emission in the brighter systems remaining unexplained. Unfortunately, the case  $\alpha = 10$  requires supersonic turbulence in the disk; this is somewhat implausible, and only marginally consistent with light curves of dwarf novae in eruption (which favor  $\alpha = 1$ ; Bath and Pringle 1981). This surprising agreement of observation with implausible theory deserves a more thorough study.

For the present, we fit a function which has the same general shape as the models, and obtain an empirical equivalent width–absolute magnitude relation:

$$\text{E.W.}(H\beta) = 0.3 M_v^2 + e^{0.55(M_v - 4)}. \quad (16)$$

This empirical equation should certainly be abandoned if theoretical disk models can be brought into reasonable agreement with the data. In the meantime, the relation may be used for crude estimates of  $M_v$  ( $\pm \sim 1.5$  mag, from the scatter in Fig. 6) in systems with  $\text{E.W.}(H\beta) \geq 15$  Å. For systems with weaker lines, only an approximate constraint of  $M_v \leq +6$  can be derived.

### c) Cookbook for $\dot{M}$

We conclude this section with a summary of recommended methods of learning  $\dot{M}$ .

#### i) Systems with Disks

If both ultraviolet and optical photometry are available in eruption and quiescence, it may be feasible to find  $\dot{M}$  by summing the observed 1100–10000 Å flux, converting to " $L_{\odot}$ ," and using equation (15) with  $k = 0.5$ . For optically thick disks, this is likely to work fairly well, because for temperatures less than or approximately equal to  $10^5$  K, absorption in the disk atmosphere should remove most of the flux shortward of the Lyman limit at 912 Å. Lacking the required photometry, it is better to find  $M_v(\text{disk})$ , and fit it to disk models to obtain  $\dot{M}$ . In either case, we require a distance estimate.

1. *If the secondary is visible in the spectrum.*—Use the spectral type, radius, and brightness (in a band where the disk contribution can be easily removed) to determine the distance. Bailey (1981) has shown that the  $K$  magnitude is especially useful for this purpose. This determines  $M_v(\text{disk})$  to within  $\sim 1$  mag, or even better if the secondary is assumed to be a main-sequence star.

2. *In all cases.*—(i) Use the equivalent width– $M_v$  relation to find  $M_v(\text{disk})$ . (ii) Assuming the secondary to be on the main sequence, use equation (7) and Figure 3 to find its mass and  $M_v$ . Use the available limits on its presence in the spectrum (typically  $m_v(\text{sec}) \geq m_v(\text{system}) + 2.0$ ) to deduce a maximum  $M_v(\text{disk})$  (i.e., a minimum brightness). (iii) Use any

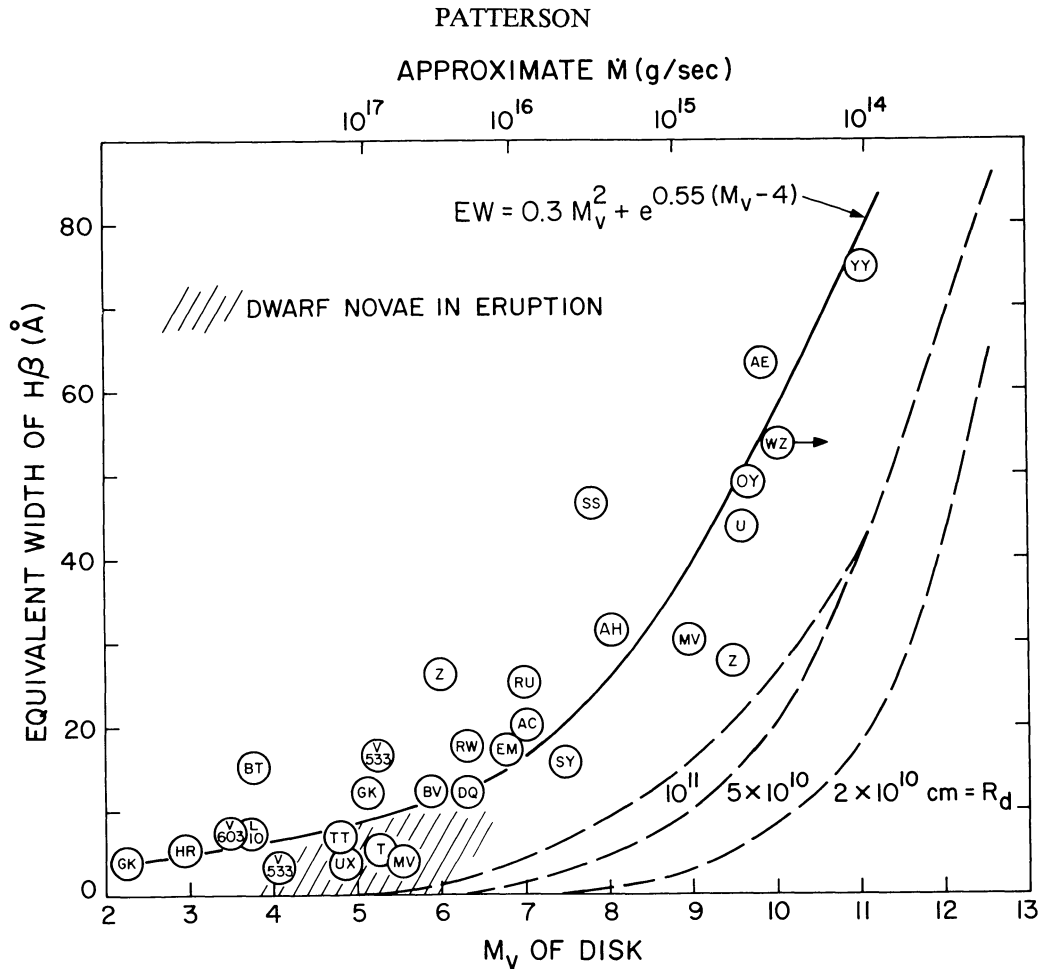


FIG. 6.—Equivalent width—absolute magnitude relation, for systems of known distance. Dwarf novae in eruption populate the shaded region. Dashed curves are the predictions of Tytenda's (1981) models (with  $M_{\text{wd}} = 1.0 M_{\odot}$ ,  $\alpha = 1$ ), for several choices of the outer disk radius. The solid curve is the empirical relation, eq. (16).

other distance information (e.g., interstellar lines, proper motion, parallax, common proper motion companions, location in the Galaxy, interstellar reddening [especially through the 2200 Å dip]) to obtain limits on  $M_v(\text{disk})$ . (iv) Use the UV colors, or the UV-to-optical ratio. We have discussed this technique only in passing, but it may be the most useful technique of all once it is calibrated. The obstacles to its general use are (1) the severe dependence on white dwarf mass, (2) the possibility of large UV contributions from the white dwarf and boundary layer, and (3) uncertainty in the effect of the Lyman discontinuity on the flux distribution. If very extensive wavelength coverage is available, a full fit of the spectrum to a disk model may be possible.

#### ii) Systems without Disks (AM Herculis Stars)

No practical technique of good accuracy is known. Until one is developed, the best solution is find the distance by detecting the secondary, or by any of the methods in (iii) above; add the observed fluxes to find the bolometric flux, convert to  $L_{\text{bol}}$ , and obtain  $\dot{M}$  from equation (15). Because all of these stars radiate most of their luminosity in an intense soft X-ray component which is still rising steeply as it enters the EUV (Tuohy *et al.* 1981), our ignorance of the EUV

domain makes estimates of  $L_{\text{bol}}$  very uncertain. Until better distance information is available, we will adopt the mean  $M_v$  of AM Her and VV Pup in their bright states ( $= 8.6$ ) as a "standard candle" for estimating the distance.

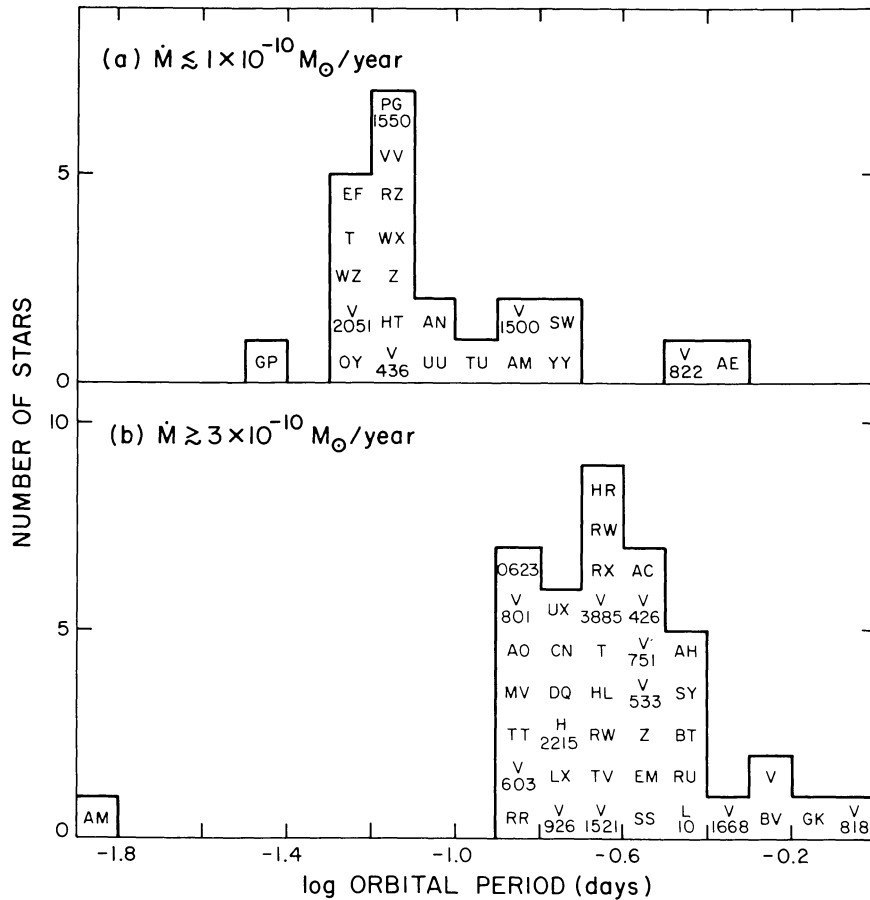
#### iii) X-Ray Binaries

For X-ray binaries, one can use the technique just cited for the AM Her stars. In practice, this works very well, because these stars radiate most of their luminosity in the accessible 2–20 keV band (Bradt and McClintock 1983). One can then obtain  $\dot{M}$  from equation (15), with  $M_*$ ,  $R_*$  chosen from neutron star models. If the distance cannot be otherwise estimated, the accretion disk "standard candle"  $M_v = +1.0$  (van Paradijs 1981) can be used.

#### d) $\dot{M}$ versus orbital Period, and Uncertainties

We have applied these techniques to estimate the average mass transfer rates in about two-thirds of all systems in Table 1, excluding those for which the data are too sparse. The results are shown in Figure 7. A fairly good correlation with orbital period is evident: a linear fit to the data yields the



FIG. 8.—Distribution of orbital periods for high- and low- $\dot{M}$  systems

empirical relation

$$\dot{M} = 5.1_{-2}^{+3} \times 10^{-10} P_4^{3.2 \pm 0.2} M_{\odot} \text{ yr}^{-1}. \quad (17)$$

Now that estimates of  $\dot{M}$  are available, we may return to Figure 1 and segregate stars by  $\dot{M}$  rather than by their eruption types. The natural threshold suggested by Figure 7 occurs at  $\dot{M} \approx 2 \times 10^{-10} M_{\odot} \text{ yr}^{-1}$ , which is also approximately the maximum  $\dot{M}$  possible in a system driven by gravitational radiation (RJW). If we use this threshold to divide these stars into high- and low- $\dot{M}$  systems, we find the distribution shown in Figure 8. This confirms the hypothesis suggested by Figure 1; with the lone exception of the pathological AM CVn,<sup>3</sup> all the high- $\dot{M}$  systems have  $P > 3.3$  hr, while the low- $\dot{M}$  systems are strongly concentrated toward shorter periods.

Since the correlation in Figure 7 is perhaps the most important observational result in this paper, and since there is widespread skepticism about the validity of the high accretion

<sup>3</sup>For this system, observations of orbital period change by Patterson *et al.* (1979) suggested a transfer rate of  $\sim 10^{-7} M_{\odot} \text{ yr}^{-1}$ . But since the period change has not been confirmed and since the interpretation is also open to doubt, we do not use this result. Instead we estimate the minimum transfer rate required to reproduce the absorption-line spectrum and the extremely blue continuum ( $F_{\lambda} \propto \lambda^{-2.2}$ ) extending from 1000 to 7000 Å.

rates we have derived (e.g., Paczyński 1983), this is probably a good time to point out that some very fundamental considerations more or less *compel* us to believe in high accretion rates ( $10^{-9}$ – $10^{-8} M_{\odot} \text{ yr}^{-1}$ ). We list three reasons why low rates (say,  $10^{-10} M_{\odot} \text{ yr}^{-1}$ ) can be ruled out for the intrinsically bright systems:

1. We must explain how the disks of many systems manage to be as bright as  $M_v \approx +4$ , with a luminosity  $L(1100\text{--}10000 \text{ Å}) \approx 10 L_{\odot}$ . If this luminosity is to come from accretion, we require  $\dot{M} > 5 \times 10^{-9} M_{\odot} \text{ yr}^{-1}$ , regardless of the details of the accretion model. This can be accomplished with a low accretion rate only if there exists some much more powerful energy source available. Only one such energy source is known: nuclear burning of the accreted hydrogen on the white dwarf. But theory and classical nova outbursts tell us that steady nuclear burning does not occur anywhere in this range of accretion rates, and observations have never shown signs of the strong UV flux, very blue colors, and large reflection effect which should be produced by a very hot white dwarf.

2. Both observation and theory tell us that classical nova shells have a mass  $\sim 5 \times 10^{-5} M_{\odot}$  (Gallagher and Starrfield 1978). The recurrence time for classical novae should therefore be  $\sim 5 \times 10^{-5} M_{\odot} / \dot{M}$ , which is  $5 \times 10^5 \text{ yr}$  if  $\dot{M} = 10^{-10} M_{\odot} \text{ yr}^{-1}$ . This means that if we count the number of classical novae we have observed to erupt in the last 100 yrs within

some specified volume, we must multiply by a factor of 5000 to obtain an accurate count of the local space density of classical novae. The result is  $10^{-4} \text{ pc}^{-3}$ , and this number is utterly excluded by observation, as discussed extensively in § V. Observations suggest a space density of  $\sim 4 \times 10^{-7} \text{ pc}^{-3}$ , implying roughly  $\langle \dot{M} \rangle \approx 2 \times 10^{-8} M_{\odot} \text{ yr}^{-1}$ .

3. Available data suggest that  $\sim 2\%$  of all white dwarfs are born in close binary systems that probably become CVs (§§ VII, VIII). But the present space density of CVs is only  $\sim 0.06\%$  of the space density of white dwarfs (§§ V, VIII). Therefore, most CVs must have short lifetimes ( $\sim 3\%$  of the galaxy's age), implying  $\langle \dot{M} \rangle \approx 4 \times 10^{-9} M_{\odot} \text{ yr}^{-1}$ .

One can fret endlessly over factors of 2 or so in the estimates, but these are very big problems and will not go away without major surgery on theory, observations, or both. While others may choose surgery, it seems a lot simpler to avoid all of these problems by supposing that the accretion rates *appear* high because they *are* high.

Even in a bloated paper such as this, we can only recoil in horror from the fearsome task of estimating uncertainties in distance and mass transfer rate for each of the  $\sim 75$  individual stars—except to make a few general comments. We have considered all of the available clues in estimating distance, assigning high weight to estimates based on nova shells and detection of the secondary, and lower weight to considerations of reddening, proper motion and parallax, the UV/optical continuum slope, position in the galaxy, the  $M_p$ -E.W.(H $\beta$ ) relation, “standard candle” arguments, and nondetections of the secondary. For each star in Tables 1 and 2, the information used for the distance estimate is identified in column (5) by a numerical code explained in the notes to Table 1. The  $\pm 1 \sigma$  uncertainties in (log distance) probably range from 0.1 to  $\sim 0.3$ . In other words, we would be surprised if more than a few distances were in error by more than a factor of 3.

The mass transfer rates are all obtained from models, and therefore have additional uncertainties—which are likely to be systematic, not random. For  $\dot{M} \geq 5 \times 10^{-10} M_{\odot} \text{ yr}^{-1}$ , the disks are optically thick, and there is no great sensitivity to the assumptions of the models. But for the low- $\dot{M}$ , optically thin disks, the models can, in principle, be sensitive to the value of the viscosity, the treatment of the boundary layer, and deviations from steady accretion flow. On the other hand, these worries are moderated by the fact that we are concerned with the *time-averaged*  $\dot{M}$ —and for most systems, an appreciable fraction of the light emerges during an optically thick state, i.e., during outburst.

Several other effects probably also introduce systematic errors in  $\dot{M}$ . Tylenda's disk models neglect any direct visual contribution from the boundary layer where the accretion disk grazes the white dwarf, and treat the absorption and subsequent reprocessing of high energy radiation into optical light by assuming that local viscous heating is the only source of pressure in the disk. Since the boundary layer must contribute *some* light, and since real disks are probably somewhat more “puffed up” than model disks, these assumptions are likely to cause overestimates of  $\dot{M}$ . On the other hand, two other effects may perturb the estimate in the opposite direction. *One*, the disk models assume a white dwarf mass of  $1.0 M_{\odot}$ , and the average observed mass seems to be  $\sim 0.6\text{--}0.8 M_{\odot}$  (see

§ VII below, and Shafer 1983*d*). *Two*, we have made the simplifying assumption that all of the matter “transferred” by the secondary is accreted by the primary. More precisely, we can distinguish between:  $\dot{M}_2$ , the rate of mass loss by the secondary;  $\dot{M}_{\text{disk}}$ , the rate of mass entering the disk; and  $\dot{M}_1$ , the rate of mass accretion onto the primary. In general, it should be true that

$$\dot{M}_2 > \dot{M}_{\text{disk}} > \dot{M}_1, \quad (18)$$

and what we have measured from consideration of  $M_p(\text{disk})$  is probably something intermediate between  $\dot{M}_1$  and  $\dot{M}_{\text{disk}}$ .

Each of these effects could be important in some disk models, but probably none are important in the “standard accretion model.” The boundary layer may be a strong UV or X-ray source, but is likely to be too hot to be a significant source of visual luminosity (Pringle 1977; Pringle and Savonije 1979). Pacharintanakul and Katz (1980) have shown that for a standard disk around a white dwarf, the gravitational energy released in situ is always greater, and is usually much greater, than the energy available from reprocessing. The possible error in mean white dwarf mass may cause underestimates of  $\sim 20\%$ – $50\%$ . The last effect is the most uncertain. It is difficult to constrain  $\dot{M}_2$  since it does not necessarily produce any radiation, and since there is at present no accepted theory for it. But we feel that over a sufficiently long time scale,  $\dot{M}_{\text{disk}}$  should not greatly exceed  $\dot{M}_1$ , since matter leaving the disk will in general carry away substantial angular momentum, which allows other matter to accrete. Because of this self-regulating property, it is very likely that  $\dot{M}_1 \approx (0.5\text{--}1.0) \dot{M}_{\text{disk}}$ , and we suspect that  $\dot{M}_1$  is really quite close to  $\dot{M}_{\text{disk}}$ .

With various reasonable perturbations to the standard accretion model (e.g., a bulge at the disk edge due to the impact of the stream, or a cavity at the center due to a magnetic field), these effects could individually be as important as a factor of 2 or so. The cumulative effect of such uncertainties could very well be important. But at present, there appears to be no reason not to proceed with using simple accretion disk models to make estimates of  $\dot{M}$ . When we better understand the complications that are present, we can improve the estimates. All of these points are worth worrying about in greater detail, but we heartily recommend that someone *else* should take up the task of worrying about them. *Tempus fugit*.

## V. CATAclySMIC VARIABLE DEMOGRAPHY

### a) Scale Height in the Galactic Disk

Knowledge of the distances allows us to convert the angular distribution of CVs in the sky to a spatial distribution in the Galaxy. We have calculated the height above and below the galactic plane for each star for which a distance estimate is available from Table 1. The results, shown in Figure 9, show that CVs approximately follow a Gaussian distribution with a scale height of  $190 \pm 30$  pc. Allowing for statistical error and selection effects, the true scale height could be anywhere from 100 to 250 pc. We shall adopt a value of 150 pc, since the

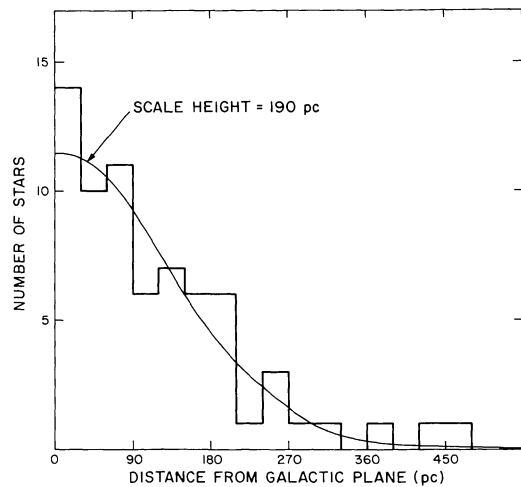


FIG. 9.—Distribution of heights above the galactic plane for systems with a distance cited in Table 1. A Gaussian distribution with a 190 pc scale height gives an approximate fit.

discovery of systems away from the galactic plane is probably somewhat favored.

#### b) Space Densities of Known Systems

We can obtain some idea of the space density of CVs by counting the number of known systems within some specified volume. We do this below, for the various subclasses.

##### i) AM Herculis Stars

Ten of these systems are known, and at least eight are strong soft X-ray sources. Because the entire soft X-ray sky has been surveyed to a flux limit below that of the observed systems, it is not likely that any large number of *nearby* AM Her stars remain to be discovered. The space density of known systems is  $\sim 3.5 \times 10^{-7} \text{ pc}^{-3}$ .

##### ii) Other Low- $\dot{M}$ Systems

We count 17 of these systems within  $\sim 200$  pc. Most are very faint in quiescence and spend  $\geq 90\%$  of their time in quiescence. These circumstances discriminate against discovery of these objects, and against finding their orbital periods. Hence, we expect that these systems have been significantly undercounted. The observed systems represent a space density of  $7 \times 10^{-7} \text{ pc}^{-3}$ .

##### iii) High- $\dot{M}$ Dwarf Novae

We count 19 of these systems within 500 pc, and seven within 200 pc. These systems are relatively bright, and most spend  $\geq 20\%$  of their time in eruption. Hence, no great undercount is likely; the known systems have  $D \approx 3 \times 10^{-7} \text{ pc}^{-3}$ .

##### iv) Low-Mass X-Ray Binaries

Most of these objects are so intrinsically luminous in X-rays as to be visible throughout the Galaxy. About 40 are known in the Galaxy, implying  $D \approx 5 \times 10^{-10} \text{ pc}^{-3}$ .

#### v) Classical Novae

Twelve old novae have been found within 1 kpc in  $\sim 70$  yr of observation (see Payne-Gaposchkin 1957; we count all nearby novae, not just those of known orbital period). This gives a density

$$D_{\text{CN}} \approx 1.7 \times 10^{-8} (T/100) \text{ pc}^{-3}, \quad (19)$$

where  $T$  is the recurrence period in years.

The classical nova space density depends critically on the recurrence period, which is poorly known. Let us assume that  $5 \times 10^{-5} M_{\odot}$  are ejected in a typical eruption (Gallagher and Starrfield 1978), and that  $0.5 M_{\odot}$  are available for mass transfer from the secondary. We shall assume that a fraction  $k_2$  of the mass lost by the secondary is accreted by the white dwarf, and that a fraction  $k_1$  of the accreted mass is expelled in the nova eruption. This allows for the possibilities that (1) some of the transferred mass is lost by means other than nova eruptions ( $k_2 < 1$ ); (2) some of the accreted mass is left behind in the eruption ( $k_1 < 1$ ); (3) some of the white dwarf mass is dredged up to supply the nova shell ( $k_1 > 1$ ). The number  $N$  of nova outbursts is then

$$N = \frac{\text{total mass ejected}}{\text{mass ejected in one eruption}} = 10^4 k_1 k_2. \quad (20)$$

What about the *lifetime* of the classical nova phase? We can obtain this by using the  $M(P)$  and  $\dot{M}(P)$  relations (eqs. [7] and [17]) to calculate the time required to go from a long period (say, 6–12 hr) to a 3.3 hr period. The result is  $\sim 4 \times 10^8$  yr. But a glance at Figure 7 reveals that the  $\dot{M}$  rates in classical novae are somewhat higher than given by equation (17). It is not clear if, or how, we should correct for this. Lacking any guidance from theory, we shall simply take the data at face value and assume that the correct  $\dot{M}(P)$  relation is a factor of 3 higher than given in equation (17). This reduces the lifetime to  $1.3 \times 10^8$  yr, from which we can infer a recurrence period

$$T = \frac{\text{nova lifetime}}{\text{number of outbursts}} = 1.3 \times 10^4 (k_1 k_2)^{-1} \text{ yr}. \quad (21)$$

What can we say about  $k_1$  and  $k_2$ ? Apparently  $k_1$  cannot be less than one by much: the matter left behind cannot be hydrogen (which would be promptly burned) and cannot be anything else either, since the total bolometric luminosity of the nova eruption indicates that only a few percent of the accreted hydrogen is actually burned (Gallagher and Starrfield 1978). It is also true that  $k_1$  cannot exceed one by much, because the nova shells predominantly consist of hydrogen. Hence,  $k_1 = 1$  seems to be a safe assumption. It is harder to constrain  $k_2$ , but we have earlier suggested the range 0.5–1.0. Thus, we obtain  $T = 1.3\text{--}2.6 \times 10^4$  yr, implying  $D_{\text{CN}} = 2.2\text{--}4.4 \times 10^{-6} \text{ pc}^{-3}$ .

This is  $\sim 30$  times less than the commonly quoted space density of  $10^{-4} \text{ pc}^{-3}$ , deduced from a different argument by Bath and Shaviv (1978). Those authors used the higher of two estimates for the observed  $D_{\text{CN}}$  given by Warner (1974), which is higher than given in equation (19) by a factor of 6. They



TABLE 3  
OTHER CONSTRAINTS ON NOVA SPACE DENSITY

FLUX LIMIT	PREDICTED NUMBER OF STARS <sup>a</sup>		OBSERVATION
	$D_{\text{CN}} = 10^{-4} \text{ pc}^{-3}$	$D_{\text{CN}} = 3 \times 10^{-6} \text{ pc}^{-3}$	
$m_v < 6.0$ (naked eye star)	5	0.15	none!
$m_v < 9.5$ (~ HD star)	400	13	1
$m_v < 11.0$ $F_x(2\text{--}10 \text{ keV}) > 3 \times 10^{-11}$ (ergs $\text{cm}^{-2} \text{ s}^{-1}$ ) (HEAO 1 limit)	2400 450	70 14	5 13 <sup>b</sup>
$F_x(0.1\text{--}4.0 \text{ keV}) > 6 \times 10^{-13}$ (ergs $\text{cm}^{-2} \text{ s}^{-1}$ ) (HEAO 2 IPC limit)	25,000, or 0.5 $\text{deg}^{-2}$ (all-sky)	750, or 0.016 $\text{deg}^{-2}$ (all-sky)	$\leq 0.02 \text{ deg}^{-2}$ (high latitude) $\leq 0.02 \text{ deg}^{-2}$ (low latitude)

<sup>a</sup>Assuming  $L_x(0.1\text{--}4.0 \text{ keV}) = 3 \times 10^{31} \text{ ergs s}^{-1}$ ,  $M_v = +4.2$ .

<sup>b</sup>Including all CVs other than AM Her stars, but not including the ~3–10 stars which are probably yet to be found among the ~100 unidentified HEAO 1 sources.

also made an assumption about what fraction of all white dwarfs are formed in close binaries that become classical novae; namely, that the fraction is the same in the solar neighborhood as it is in the nuclear bulge of M31. This assumption seems innocuous enough, but we estimate that it is wrong by a factor of ~3–10. Ford and Jacoby (1977) deduced that the white dwarf formation rate in the bulge of M31 was ~0.1  $\text{yr}^{-1}$ , compared to ~1  $\text{yr}^{-1}$  in our entire Galaxy. But the nova rate from the bulge of M31 is ~25  $\text{yr}^{-1}$ , comparable to the rate in our entire Galaxy. The reason for this is unknown, but it appears that classical novae are much more common in the bulge of M31. These two points are chiefly responsible for the factor of 30 discrepancy.

The space density in the solar neighborhood can also be constrained by comparing at various flux levels the number of stars predicted by the two estimates. For quiescent classical novae we shall adopt  $M_v = 4.2$  (Payne-Gaposchkin 1957; Duerbeck 1981) and  $L_x(0.1\text{--}4.0 \text{ keV}) = 3 \times 10^{31} \text{ ergs s}^{-1}$  (Becker and Marshall 1981). These predictions are shown in Table 3, together with available observational data. Examination of Table 3 shows that on every point of comparison, the higher estimate is in truly spectacular conflict with observation. While one ought to worry somewhat about the proper values of  $M_v$  and  $L_x$ ,<sup>4</sup> the conflict is so enormous that the lesson is reasonably clear: a space density of  $10^{-4} \text{ pc}^{-3}$  is much, much too high.

The X-ray data in Table 3 are in reasonable agreement with the lower estimate of space density, but the optical data are still discrepant by an order of magnitude. This is a well-known problem (discussed, e.g., by Bath and Shaviv 1978; Warner 1974), commonly attributed to the difficulty of discovering quiescent old novae, which typically lack the means (promi-

nent emission lines or eruptive activity) to call attention to themselves. Despite these difficulties, it does not seem easy to reconcile the five stars known having  $m_v < 11$  (TT Ari, RW Sex, QU Car, V3885 Sgr, and CPD -48°1577) with the 70 expected if  $D_{\text{CN}} = 3 \times 10^{-6} \text{ pc}^{-3}$ . We will subsequently find that sky surveys for faint blue stars suggest  $D_{\text{CN}} \ll 3 \times 10^{-6} \text{ pc}^{-3}$ , eliminating this discrepancy.

#### c) Space Densities from Unbiased Surveys at High Galactic Latitude

The space densities derived above for classes (ii) and (iii) are clearly lower limits, because they count only systems whose existence and orbital period are known.<sup>5</sup> Virtually all of these systems were first identified from their optical variability. This raises the worrisome possibility that many systems with only minor photometric variability may have been missed. Better space densities can be obtained from surveys which detect CVs with high efficiency and *without relying on variability*. In recent years there have been three such surveys of the high galactic latitude sky:

1. The Michigan-Tololo objective-prism survey of the south galactic pole for faint emission-line objects (e.g., MacAlpine and Williams 1981), covering 2000  $\text{deg}^2$ , with a limiting magnitude of 17–18 and a minimum equivalent width of ~30 Å. This should detect low- $\dot{M}$  CVs (which have strong emission lines) out to a distance of 300 pc, but misses high- $\dot{M}$  CVs.

2. The various surveys to identify serendipitous X-ray sources found by the *Einstein Observatory* IPC (Stocke *et al.* 1983; Mason *et al.* 1982; Margon, Chanan, and Downes 1982), covering a total of ~300  $\text{deg}^2$  to a flux limit  $F_x(0.1\text{--}4.0 \text{ keV}) \approx 3 \times 10^{-13} \text{ ergs cm}^{-2} \text{ s}^{-1}$ . Since the typical  $L_x$  for CVs

<sup>4</sup>Naturally, the conflict can be removed by adopting lower luminosities, e.g.,  $M_v \approx +9$ ,  $L_x \approx 10^{30} \text{ ergs s}^{-1}$ . But this is an *extremely undesirable* solution to the problem. It compels us to ignore the well-documented fact that  $M_v \approx +4$  both before and after eruption (Robinson 1975), and it floods the sky with faint blue emission-line stars, which ought to be easily detected by the Palomar-Green and Michigan-Tololo surveys (see below), and are not. The side effects of this medicine are much worse than the illness!

<sup>5</sup>The restriction to systems of known orbital period is not as serious as it might seem. The reason is that the space densities come primarily from the nearest, and therefore brightest, stars—and orbital periods are known for most of these. If we also include known CVs of unknown orbital period, and make crude distance estimates, we find that the space densities increase by a factor of ~1.3–2. We have not pursued this point further, since it is for most purposes superseded by the discussion of the unbiased surveys at high galactic latitude.

TABLE 4  
SPACE DENSITY CONSTRAINTS FROM HIGH-LATITUDE SURVEYS

QUANTITY	ALLOWED SPACE DENSITY ( $10^{-6} \text{ pc}^{-3}$ )		
	PG Survey	X-Ray Surveys	Michigan-Tololo Survey
$D_{\text{CN}}$ ..... (“classical novae,” $M_v \approx 4$ )	$< 3 h_{150}^{-3}$	$< 4 h_{150}^{-3}$	...
$D_{\text{HM}}$ ..... (high $\dot{M}$ , $M_v = 5-8$ )	$(0.8-1.6) h_{150}^{-3}$	$< 4 h_{150}^{-3}$	$< 4 h_{150}^{-3}$
$D_{\text{LM}}$ ..... (low $\dot{M}$ , $M_v = 8-11$ )	$(2.0-4.5) h_{150}^{-1}$	$(2-7) h_{150}^{-3}$	$(0.7-3) h_{150}^{-3} p^{-1}$
$D_{\text{CV}}$ ..... (total)	$(3-6) h_{150}^{-1}$	$(2-7) h_{150}^{-3}$	...

NOTE.—  $p$  = detection probability;  $h_{150}$  = density scale height in units of 150 pc.

is  $\sim 10^{31} \text{ ergs s}^{-1}$  (Cordova and Mason 1983), this should detect CVs out to 500 pc.

3. The Palomar-Green (PG) survey for faint blue objects ( $U - B \leq -0.4$ ), covering  $10,700 \text{ deg}^2$  with  $|b| > 30^\circ$  and an average limiting magnitude of 16.2 (Green *et al.* 1982). Essentially all CVs show sufficiently blue colors to be detected in this survey,<sup>6</sup> but the magnitude limit may exclude some of the most intrinsically faint stars.

The numbers of CVs detected in the surveys were 2, 2, and 35, respectively. In Table 4 we have used these numbers to estimate space densities, as follows. Because CVs range so widely in  $M_v$ , we have found it necessary to create three subclasses: “classical novae” (defined as CVs with  $M_v \approx +4$ ), “high- $\dot{M}$ ” objects ( $M_v = 5-8$ ), and “low- $\dot{M}$ ” objects ( $M_v = 8-11$ ). For each survey, the effective volume  $V$  was estimated from the number of square degrees and the distribution of galactic latitudes. A Gaussian space density law was assumed ( $D = D_0 \exp[-z/h]^2$ , where  $z$  is the height above the galactic plane and  $h$  is the density scale height). The results are expressed in terms of  $h_{150} = h/(150 \text{ pc})$ , and the volumes are formally proportional to  $h_{150}^3$ . The space density  $D_0$  (which we call  $D_{\text{CN}}$ ,  $D_{\text{HM}}$ , and  $D_{\text{LM}}$ , for the three cases) is then  $N/Vp$ , where  $N$  is the number of objects found (with an appropriate statistical uncertainty) and  $p$  is the detection efficiency. We feel that  $p$  should be nearly 1 for all classes in the X-ray surveys, and for high- $\dot{M}$  objects in the PG survey. For classical novae, it is possible that  $p$  is quite low in the Michigan-Tololo and PG surveys, in which the photographic exposure times were optimized for faint stars; consequently, only coarse limits are given. For low- $\dot{M}$  objects in the PG survey,  $p$  should be nearly 1 if  $h$  is as low as 100 pc, but is probably as low as 0.2 (based on properties of known low- $\dot{M}$  CVs) if  $h$  is 250 pc. We have tried to allow for this dependence in estimating  $D_{\text{LM}}$  from the PG survey. The Michigan-Tololo survey is sufficiently deep to reach essentially all CVs, suggesting  $p \approx 1$ , but

<sup>6</sup>High- $\dot{M}$  systems satisfy this criterion because of their high continuum color temperatures ( $\geq 12,000 \text{ K}$ ). Low- $\dot{M}$  systems have continuum colors indicative of much lower temperatures (say  $< 7000 \text{ K}$ ), but manage to sport an impressive  $U - B$  color anyway, chiefly due to a large Balmer jump in emission (e.g., see spectra in Williams 1983).

because the detection threshold is subjective and somewhat difficult to quantify, we have left the dependence on  $p$  in the result.

Somewhat weaker constraints on the space densities can be obtained as follows. The methods discussed in § IV enable us to estimate distance and height above the galactic plane for each of the 39 survey stars. From the distance estimates alone we obtain  $D_{\text{HM}} = 0.5-2 \times 10^{-6} \text{ pc}^{-3}$  and  $D_{\text{LM}} = 3-6 \times 10^{-6} \text{ pc}^{-3}$ , and from the heights we find  $h = 130-200 \text{ pc}$ . These constraints, derived from crude distances, are not as strong as the entries in Table 4, which do not depend sensitively on distance estimates. Finally, we can obtain a crude but model-independent estimate by multiplying the space density of previously known systems by the ratio of total to previously known systems among the 39 survey stars. The number of stars previously known is 11 (Ferguson 1982, private communication), of which six have known orbital periods. Thus, the ratio is 3.5 or 6.5, depending on whether we choose to require a known orbital period to certify a star as “previously known” (the point is debatable, and does not really matter). The space density of known systems in § Vb is  $1.4 \times 10^{-6} \text{ pc}^{-3}$ , yielding a total  $D_{\text{LM}} + D_{\text{HM}} = 4-9 \times 10^{-6} \text{ pc}^{-3}$ . The internal consistency of these various estimates provides some assurance that  $h$  is in fact probably close to 150 pc, and that our assumptions have probably not introduced any large systematic errors.

#### d) Space Densities of Classical Novae: Surveys at Low Galactic Latitude

From the high-latitude surveys we can derive only an upper limit to the space density of classical novae:  $D_{\text{CN}} \leq 3 \times 10^{-6} \text{ pc}^{-3}$ . Better constraints come from surveys at low galactic latitude, since these stars can be seen at distances much greater than their galactic scale height. We will discuss each of these in turn.

1. The photometric and spectroscopic survey of hot stars in the southern Milky Way by Garrison, Hiltner, and Schild (1977) was complete to 10th magnitude, covered  $3700 \text{ deg}^2$  of sky, and yielded precisely one cataclysmic variable (CPD  $-48^\circ 1577$ ; Garrison, Hiltner, and Schild 1982). This formally yields  $D_{\text{CN}} = 1 \times 10^{-6} \text{ cm}^{-3}$ , but the uncertainty is quite large

because (1) the errors are sensitive to the assumed mean and distribution of  $M_V$ ; (2) there are worries about incompleteness near any survey's detection limit, where most classical novae should be; and (3) with only one object found, the result is really only an upper limit. Considering these effects, we estimate that a more reliable constraint is something like  $D_{CN} \lesssim 3 \times 10^{-6} \text{ pc}^{-3}$ .

2. The *Einstein Observatory* X-ray survey of the galactic plane (Hertz and Grindlay 1984) covered  $275 \text{ deg}^2$  to a  $0.2\text{--}4.0 \text{ keV}$  flux limit of  $7 \times 10^{-13} \text{ ergs cm}^{-2} \text{ s}^{-1}$ . An estimated 17 sources were thought to be cataclysmic variables, although none of these have yet been confirmed by optical identification. Most of these sources have  $F_x/F_v$  ratios larger than those of known classical novae, and we estimate that at most five could be classical novae. With  $L_x = 3 \times 10^{31} \text{ ergs s}^{-1}$  (Becker 1981; Becker and Marshall 1981), classical novae should be detected in this survey out to  $\sim 500 \text{ pc}$ , yielding an effective volume of  $3 \times 10^6 \text{ pc}^3$ . We thus obtain  $D_{CN} \leq 2 \times 10^{-6} \text{ pc}^{-3}$ .

3. A continuing survey of the sky to identify optical counterparts of strong (*HEAO 1*) X-ray sources, from  $U-B$  colors on Schmidt plates, has covered  $\sim 300 \text{ deg}^2$  in the galactic plane to a magnitude limit of  $\sim 16$  (e.g., Patterson *et al.* 1983). We estimate that the threshold for detection is  $U-B \leq -0.45$ ; with average interstellar reddening, this limits detection to a radius of  $\sim 800 \text{ pc}$ . Six CVs have been found, of which probably 2–4 are accidental detections (since these are X-ray-selected fields, the CVs correctly identified with the X-ray sources should not be counted). This suggests  $D_{CN} \approx 2\text{--}4 \times 10^{-7} \text{ pc}^{-3}$ . This number is fairly sensitive to uncertainties in the treatment of reddening, and to small-number statistics. A more accurate estimate should emerge from the galactic plane survey of Downes (1984).

In summary, these surveys at low galactic latitude strongly suggest that  $D_{CN}$  is even less than we estimated from the simple theoretical argument given above in § Vb. Important uncertainties in that argument arise from (1) the statistical uncertainty implicit in the small number of objects used (12); (2) uncertainty in distance ("less than 1 kpc"); (3) uncertainty in mean accretion rate ( $4 \times 10^{-9} M_\odot \text{ yr}^{-1}$  assumed); (4) and uncertainty in the mean mass of a nova shell ( $5 \times 10^{-5} M_\odot$ ). We shall settle on a best estimate of  $4 \times 10^{-7} \text{ pc}^{-3}$ . This accounts for all known facts, including the one embarrassing feature of Table 3 (the excessive number of CN predicted with  $m_v < 11$ ). We suspect that the mean accretion rate should probably be boosted to  $\sim 10^{-8} M_\odot \text{ yr}^{-1}$ , which would account for half of the discrepancy with the theoretical argument. This value of  $D_{CN}$  drives the recurrence period  $T$  down to  $\sim 2000 \text{ yr}$ .

Again we emphasize that these arguments completely exclude values of  $D_{CN}$  near  $10^{-4} \text{ pc}^{-3}$ , unless we have a totally wrong idea of what an old nova is. *The only way to tolerate a very high space density of classical novae is to suppose that novae come primarily from objects which in quiescence do not resemble ANY of the stars we call "cataclysmic variables," and which can hide from all six unbiased surveys.* This is in contradiction to the observed facts that (1) quiescent old novae are photometrically and spectroscopically very similar to dwarf novae in eruption, and (2) historical light curves show that

preoutburst and postoutburst magnitudes of classical novae are essentially equal (Payne-Gaposchkin 1957; Robinson 1975). If the sky is really ablaze with huge numbers of undetected old novae, the stars must be very, very cleverly disguised.

#### e) Dependence of Space Density on Orbital Period

A very important constraint on CV evolution would be gained if we knew the space densities of systems of different orbital period. We can get a very crude idea by examining the data of Table 1 and Figure 1, but these are contaminated with strong selection effects which vary with orbital period (for many reasons, not the least of which is that  $\dot{M}$  depends strongly on orbital period). Nevertheless, this question is quite important, and even a rough estimate would be useful. We shall attempt to find a  $D(P_{\text{orb}})$  relation from consideration of the space densities of low- and high- $\dot{M}$  systems, assuming that our segregation by  $\dot{M}$  corresponds to a segregation by  $P_{\text{orb}}$ .

Of course, the best solution would be to find the orbital periods of the 39 systems found by the high latitude surveys. Lacking this information, we can still use the surveys in another way. Following the discussion of § IV, it is not difficult to coarsely distinguish low- $\dot{M}$  systems (faint, with strong emission features) from high- $\dot{M}$  systems (bright, with weak emission or absorption or both). By this criterion, the 39 stars divide as follows: 22 low- $\dot{M}$ , seven high- $\dot{M}$ , 10 undecided or intermediate cases (magnitudes and spectra are reported in the references cited above). Thus, the data suggest  $D(\text{low-}\dot{M})/D(\text{high-}\dot{M}) = 2\text{--}4$ . We shall assume that this is also the ratio  $D_S/D_L$  of the space density of short-period systems to that of long-period systems.

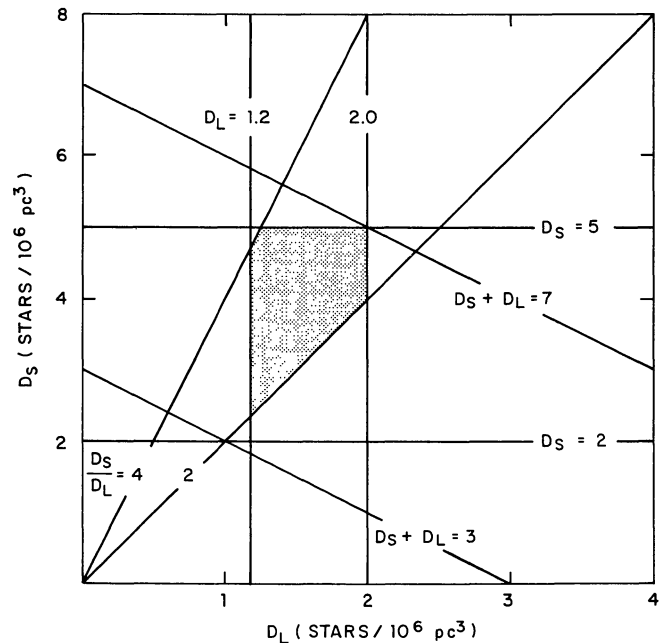


FIG. 10.—Constraints on the space density of short-period systems ( $D_S$ ) and long-period systems ( $D_L$ ). “Short” and “long” refer to orbital period intervals 1.3–2.2 and 3–10 hr, respectively. The shading represents the region consistent with all constraints.

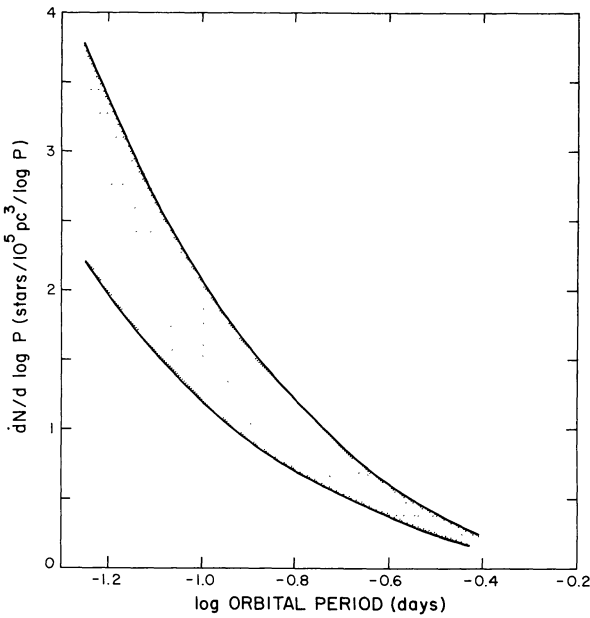


FIG. 11.—The shaded region encloses smooth and monotonic space density–orbital period relations which satisfy all the constraints of Fig. 10. Much different and more complex curves are also admissible, but all viable curves must rise steeply toward short periods (with a probable cutoff near  $\log P = -1.25$ ).

We can combine this constraint with the basic data in Table 4 and the discussion of §§ Vc, d. The resultant constraints on  $D_S$  and  $D_L$  are all shown in Figure 10, and are all satisfied within the shaded region.

Finally, we can construct  $D(P_{orb})$  relations which satisfy the constraints. Since the area under a curve does not determine the curve, there is an infinity of possible solutions. An infinite subset of this infinite set is shown in Figure 11. Here we show approximate bounds on smooth, monotonic curves that satisfy Figure 10. Since the empirical distribution of Figure 1 shows a pronounced gap near the peak of the curve, the assumption of “smooth and monotonic” is obviously a poor one. We show Figure 11 only to bring the support of a picture to an inescapable requirement: *the correct  $D(P_{orb})$  relation must rise very sharply toward short periods* (but should also yield approximately one-fourth of all systems in the long-period regime). Of course, theories of CV evolution should

be required to satisfy the constraints in Figure 10, not Figure 11.

Orbital period measurements for the 39 survey stars, when available, will render obsolete these indirect arguments.

f) *Absolute Magnitudes, Mass Transfer Rates, Lifetimes, and Space Densities*

In Table 5 we summarize the basic data on the following: (1) the absolute magnitudes and accretion rates of systems contained in Table 1, using the methods described in § IV; (2) the active lifetimes of these stars, obtained by integrating  $M_2/\dot{M}_2$  over a typical range in orbital period; and (3) the space densities of active systems, obtained by the methods discussed in this chapter (and including estimated corrections for selection effects, subject to the overall constraints on  $D_S$  and  $D_L$ ). In the category of “low- $\dot{M}$  dwarf novae” we include all of the low- $\dot{M}$  systems other than AM Her stars; and we have assumed that all high- $\dot{M}$  systems are either classical novae or “high- $\dot{M}$  dwarf novae.”

There is a potentially serious selection effect in the mean quiescent brightness of classical novae. Many novae fade below the limits of detectability, and hence their optical counterparts at quiescence are never studied. If quiescent old novae have a range in  $M_v$ , we will preferentially observe the ones which are intrinsically brighter, and hence deduce an excessive “typical” brightness. This selection effect must inevitably be present in lists of “well-studied” systems, but is probably weaker for the general population of novae. Duerbeck (1981) derived  $M_v$  for 35 quiescent old novae, selected by the availability of good data covering the nova outburst. This is essentially selection by *distance*, which avoids the problem just stated. We have taken Duerbeck’s data, removed the contributions of the mass-losing star where possible, corrected the brightness of the known eclipsing systems to an inclination of  $45^\circ$ , and present the resulting distribution of  $M_v$  in Figure 12. We find a mean  $M_v$  of +4.1, whereas we obtained +4.2 by blindly averaging the values for the best-studied systems, i.e., those in Table 1. The quality of the agreement is obviously accidental, but the basic lesson is that this selection effect is apparently (and somewhat surprisingly) not important.

g) *Which Stars Make Novae?*

Adopting a simple model wherein all CVs produce classical nova eruptions after accreting an envelope of  $10^{-4} M_\odot$ , we

TABLE 5  
CATAclysmic VARIABLE DEMOGRAPHY

CLASS	QUIESCENCE ( $M_v$ ) <sub>q</sub>	ERUPTION ( $M_v$ ) <sub>e</sub>	$\langle \dot{M} \rangle$ ( $M_\odot \text{ yr}^{-1}$ )	LIFETIME (yr)	SPACE DENSITY	
					Active ( $\text{pc}^{-3}$ )	Extinct ( $\text{pc}^{-3}$ )
Low- $\dot{M}$ dwarf novae .....	+9.2	+5.7	5 (-11)	1 (+10)	4 (-6)	...
High- $\dot{M}$ dwarf novae .....	+7.8	+4.3	1.5 (-9)	6 (+8)	8 (-7)	9 (-6)
AM Her stars.....	+10.7	+8.6	5 (-11)	1 (+10)	5 (-7)	...
Classical novae .....	+4.2	+4.2	1 (-8)	8 (+7)	4 (-7)	4 (-5)
Low-mass X-ray binaries ...	...	+1.2	3 (-9)	3 (+8)	5 (-10)	7 (-9)

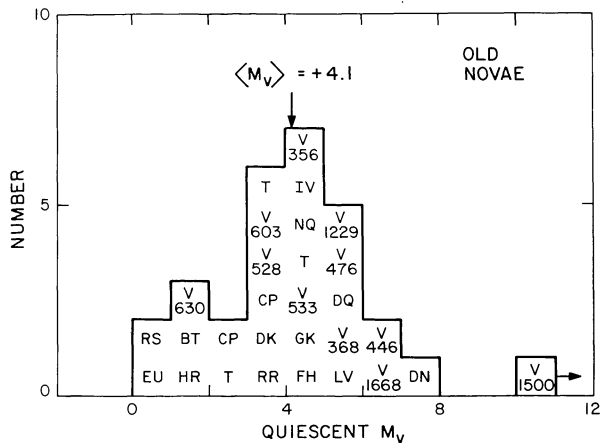


FIG. 12.—Distribution of  $M_v$  in quiescence for classical novae

can use the numbers in Table 5 to predict the nova rate from each class of object. The results are, in units of  $\text{pc}^{-3} \text{yr}^{-1}$ : low- $\dot{M}$  dwarf novae,  $2 \times 10^{-12}$ ; AM Her stars,  $3 \times 10^{-13}$ ; “old novae,”  $4 \times 10^{-11}$ ; and “high- $\dot{M}$  dwarf novae,”  $1 \times 10^{-11}$ . Since about half of the last-named class are not known to have true dwarf nova eruptions (but have an appropriate  $M_v$  and spectrum), the last number may be too high by a factor of 2. Thus,  $\sim 90\%$  of all classical novae should come from noneruptive high- $\dot{M}$  systems, and most of the remainder from eruptive high- $\dot{M}$  systems. This provides a very simple explanation for the well-known observational fact that all known classical novae are in long-period systems. Despite their relatively high space density, low- $\dot{M}$  systems do not appear to be an important producer of nova eruptions unless the critical envelope mass is vastly lowered for low accretion rates. In the nova models discussed by Nomoto (1982), a weak trend in the *opposite* direction is present (i.e., low- $\dot{M}$  systems require a slightly greater envelope mass for ignition).

The average  $\dot{M}$  attributed to classical novae in Table 5,  $10^{-8} M_{\odot} \text{yr}^{-1}$ , presents a problem, because current models of classical novae require a mean accretion rate  $\leq 10^{-10} M_{\odot} \text{yr}^{-1}$  (in order to guarantee that the hydrogen burning occurs under sufficiently degenerate conditions: Prialnik *et al.* 1982; Kutter and Sparks 1980; Fujimoto 1982). For the reasons stated above, we believe that the empirical accretion rates cannot be changed very much, especially in the downward direction. A shift to  $\langle \dot{M} \rangle = 10^{-9} M_{\odot} \text{yr}^{-1}$  could perhaps barely be tolerated, but would create very unpleasant problems with the space densities. The conflict is even more severe if we contemplate reducing the accretion rate of the *brightest* quiescent novae below  $10^{-10} M_{\odot} \text{yr}^{-1}$ . For HR Del, the observed 1100–10000 Å luminosity is  $\sim 2 \times 10^{35} \text{ergs}^{-1}$ , which demands  $\dot{M} > 10^{-8} M_{\odot} \text{yr}^{-1}$  if the energy source is accretion. Nuclear burning is  $\sim 50$  times more efficient, but, of course, that is what we are trying to avoid, in order to escape conflict with the nova models. It will not resolve the problem if the only way to prevent the white dwarfs from promptly burning their accreted hydrogen (theoretically) is to make them promptly burn their accreted hydrogen (observationally). In any case, we cannot tolerate steady nuclear

burning at a rate near the accretion rate, since it would produce a very hot white dwarf, a large reflection effect off the secondary, and (after outburst, which probably should not occur anyway) a nova shell greatly enriched in helium—all of which are contrary to observation. We conclude that the models must find a way to produce classical nova outbursts in systems accreting at rates of at least  $10^{-9} M_{\odot} \text{yr}^{-1}$ , and very likely  $10^{-8} M_{\odot} \text{yr}^{-1}$ .

#### h) Whither Cataclysmic Variables?

Finally, we wish to take note of the obvious: three of the five classes in Table 5 have accretion rates so high that they will soon exhaust their supply of matter to transfer. What happens to such systems? It seems inevitable that they become extinct, although one can imagine a variety of ways for this to happen. Assuming that CVs have been produced at a uniform rate throughout the age of the galactic disk (taken to be  $7 \times 10^9$  yr), we have estimated the present space density of such burned-out remnants in the last column of Table 5. The estimate for classical novae is quite large. We shall return to this fascinating subject of eschatology in §§ VII and VIII.

## VI. THE ORIGIN OF THE MASS TRANSFER

### a) Possible Mechanisms

The time has now come to compare the observed mass transfer rates with those predicted by existing models. Three models that are capable of yielding very large mass transfer rates are as follows:

- 1) Roche lobe overflow of the secondary due to dynamical instability;
- 2) Roche lobe overflow of the secondary due to nuclear evolution;
- 3) Accretion of matter from a wind emanating from the secondary.

While each of these mechanisms probably plays some role in CV evolution, none can be the principal driving mechanism presently at work in the observed systems. Model (1) must lead either to runaway mass loss on a very short time scale, or to a series of pulses of high  $\dot{M}$  separated by intervals of zero  $\dot{M}$  (e.g., Bath 1976). Both predictions are in conflict with observation. Models (2) and (3) predict transfer rates which are very low ( $\leq 10^{-12} M_{\odot} \text{yr}^{-1}$ ) for the entire main-sequence lifetime of the secondary (when the radius is nearly constant, and the surface gravity is too high to allow any significant stellar wind), and very high ( $\geq 10^{-8} M_{\odot} \text{yr}^{-1}$ ) when the secondary becomes a giant. A few stars with evolved secondaries (T CrB, HZ Her, etc.) are probably powered by such a mechanism, but in the majority of cases the derived  $\dot{M}$  rates and the identifications of main-sequence secondaries conflict fatally with the predictions.

As stressed in the introduction, the most promising mechanisms induce mass transfer by removing angular momentum from the binary, thus continually contracting the Roche lobe of the secondary. The most popular such mechanism is gravitational radiation (GR), which operates at a precisely predictable rate. The most recent calculations of its effect on CV

evolution (Taam, Flannery, and Faulkner 1980; RJW; Paczyński 1981; Paczyński and Sienkiewicz 1981) predict that systems generally evolve toward shorter periods, with mass transfer rates between  $10^{-11}$  and  $10^{-10} M_{\odot} \text{ yr}^{-1}$ , virtually independent of binary period. As shown in Figures 5 and 7, the observed mass transfer rates are in good accord with the GR prediction for systems with  $P \leq 3$  hr.

But for most systems with  $P > 3$  hr, it is clear that the mass transfer rates are much higher than can be produced by GR. Some more efficient mechanism for removing angular momentum is required. Since angular momentum in the *disk* must be transported outward to allow accretion to occur, it is tempting to suppose that this unknown transport mechanism manages to be so efficient that high angular momentum material is slung clear out of the disk, leaving the system altogether (e.g., Flannery and Ulrich 1977). But on closer inspection, this suggestion loses its appeal. First, tidal torques exerted by the secondary very quickly rob angular momentum from matter orbiting at large radii in the disk (Papaloizou and Pringle 1978); this allows accretion to occur but returns the angular momentum to the orbit, and hence does not accomplish the desired task. Second, this disk material is not *extremely* rich in angular momentum; even if *all* of the disk angular momentum magically disappears, the induced mass transfer rate only increases by a factor of 2 to 4 (Warner 1978; RJW; Kieboom and Verbunt 1981). This is largely because mass transfer from a low-mass to a high-mass star tends to widen the binary almost as fast as the angular momentum loss tends to contract it.

More drastic measures are required. In particular, we seek a mechanism that removes angular momentum whether or not accretion is occurring. This would eliminate the difficulty just mentioned, and also would permit "precataclysmic" secondaries to reach their Roche lobes in a reasonable time, without waiting the  $10^{10}$ – $10^{12}$  yr required for low-mass stars to expand significantly.

A mechanism satisfying this requirement is *magnetic braking in a stellar wind emanating from the secondary*. This remains the most popular mechanism for slowing the rotation of single stars (Weber and Davis 1967), and has been suggested as an important effect in binary stars as well (Huang 1966; Mestel 1975; Eggleton 1976). The secondary attempts to slow its rotation by ejecting a wind, which, like the proverbial spinning ice skater, maintains corotation as it streams outward along magnetic field lines. In this manner the wind may carry away very little mass but enormous amounts of angular momentum. But in a close binary with a lobe-filling secondary, tidal torques on the secondary are so efficient that angular momentum is rapidly (within  $10^4$  yr; see eq. [46] below) transferred from the orbit to keep the secondary in synchronism. Because of this continuous draining of orbital angular momentum, the two stars are forced together, and a high rate of mass transfer can be sustained. In what follows, we shall also refer to this mechanism as *rotational braking*, in order to emphasize that we do not *require* the presence of a magnetic field, except to take advantage of a known mechanism for slowing rotation; any other satisfactory method of slowing the secondary's rotation will stimulate mass transfer just as well.

Rotational braking can do the job as long as the angular momentum loss rate  $\dot{J}$  of the secondary is sufficiently high. In an important paper, Verbunt and Zwaan (1981; hereafter VZ) showed that if the usual formulation of the empirical slowdown rate of G stars is adopted ( $v_{\text{rot}} \propto t^{-1/2}$ ; Kraft 1967; Skumanich 1972), rates of mass transfer far in excess of  $10^{-10} M_{\odot} \text{ yr}^{-1}$  can be achieved. But this law is based solely on G stars with rotational velocities between 2 and 30  $\text{km s}^{-1}$ , whereas the secondaries in CVs are predominantly K and M stars rotating at  $\sim 130 \text{ km s}^{-1}$ . This leads us to ask how to estimate  $\dot{J}$  in cooler, more rapidly rotating stars.

## b) Estimating $\dot{J}$

### i) Single Stars

The rate of angular momentum loss from single main-sequence stars can be specified by the observed decline in rotational velocity with age. This is most reliably done by fitting spectral line profiles of G stars in a cluster, whose age is reasonably well determined by fitting the cluster color-magnitude diagram to the theory of stellar evolution. We show the most complete data set in Figure 13; the mean values for the Hyades, Pleiades, and UMa clusters are taken from Soderblom (1983), and the NGC 2264 data are from Vogel and Kuhi (1981). Because the latter authors observed T Tauri stars, whose radii and internal density distribution differ from those of main-sequence stars, we have attempted to correct the raw  $\langle v \sin i \rangle$  to a corresponding main-sequence value, by assuming that angular momentum is conserved in the final contraction to the main sequence. The many points at low velocity are also taken from Soderblom (1983), who determined ages from lithium abundances. All the measurements are of  $v \sin i$ , and have therefore been corrected for inclination by multiplying by  $4/\pi$ . Since a few nearly pole-on stars are probably present in Figure 13, and are not corrected by this procedure, we give low weight to the lithium-age points.

The straight-line fit in Figure 13 is the well-known  $v(t)$  law (or the "Skumanich relation"), discussed by Skumanich (1972), Smith (1979), and Soderblom (1983). All three observers agreed on a  $t^{-1/2}$  dependence, which led VZ and Taam (1983) to write the relation as

$$v_{\text{rot}} = f \times 10^{14} t^{-1/2} \text{ cm s}^{-1}, \quad (23)$$

where the value of  $f$  is empirically determined (Kraft and Skumanich, 0.7; Smith, 1.78; Soderblom, 0.94). We shall subsequently refer to this law with  $f=1$  as "the simplified braking law" or as "VZ." However, there is also observational uncertainty in the power of  $t$ , which becomes extremely important when the  $v(t)$  relation is extrapolated to ages and velocities beyond the range of observed values. Over the last decade, the " $t^{-1/2}$  law" has been invoked reverentially and often ("proof by successive publication"?), but it is still just an empirical relation, trustworthy only within fairly narrow limits.

If we attempt to make a linear fit to the data of Figure 13, i.e., fit a function of the form

$$v_{\text{rot}} = ft^{-n} \text{ cm s}^{-1}, \quad (24)$$

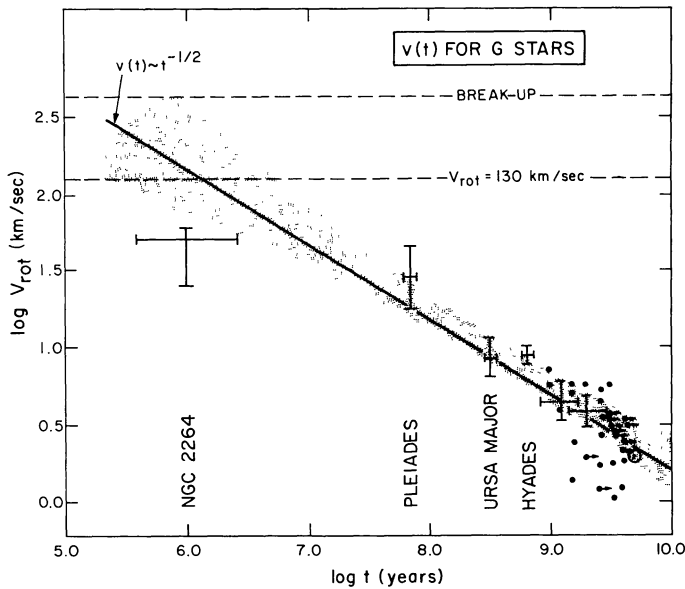


FIG. 13.—Empirical data on the mean rotation velocities ( $v_{\text{rot}}$ ) of G stars of various ages ( $t$ ). Most of the data are taken from Soderblom (1981), while the point for T Tauri stars in NGC 2264 is taken from Vogel and Kuhl (1981). The heavy line indicates the  $v(t)$  law most frequently cited (“Skumanich law”), but any straight-line fit within the shaded region is acceptable.

we find that essentially any straight line entirely within the shaded region of Figure 13 provides an acceptable fit. Because the data are quite heterogeneous, and observers may differ on the weights to assign to the various points, no precise formulation of confidence limits is possible here. But the permitted values of  $f$  and  $n$  are approximately given by the shaded region in Figure 14. While it is true that at  $n=0.5$  precisely,  $f$  is known to within a factor of  $\sim 2$ , the actual observational uncertainty in  $n$  introduces a very large uncertainty in  $f$ .

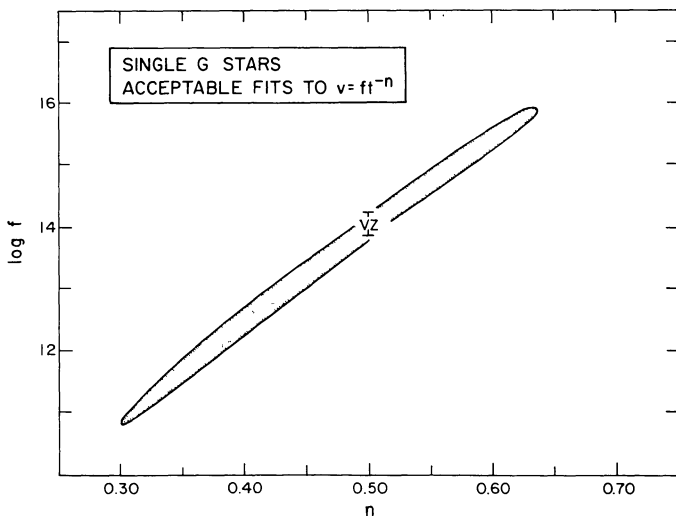


FIG. 14.—The shaded region shows acceptable values of  $f$  and  $n$  when the  $v(t)$  data are fitted to a function  $v = ft^{-n}$ . The model of Verbunt and Zwaan (1981) assumes that the  $(f, n)$ -values lie at the point labeled “VZ.”

We note with chagrin that the data cover only the range  $2\text{--}50 \text{ km s}^{-1}$ , and are well constrained only in the range  $3\text{--}25 \text{ km s}^{-1}$ . Alas, the secondaries in cataclysmic binaries are rotating much faster; combining equation (8) with  $v_{\text{rot}} = 2\pi R_2/P$ , we find that  $v_{\text{rot}}$  is virtually constant at  $130 \text{ km s}^{-1}$ :

$$v_{\text{rot}} = 130 \frac{\beta^{1.61}}{\alpha^{0.61}} P_4^{0.07} \text{ km s}^{-1}. \quad (25)$$

Thus, no data exist in the region of maximum interest, and such data will never exist for single stars, because single late-type stars with such a high  $v_{\text{rot}}$  do not exist. Further work on very young clusters may improve this situation, but for the present we are stymied. For help we turn to close binary systems, where late-type stars are maintained in rapid, synchronous rotation against their will, by the action of tidal torques.

#### ii) Eclipsing Binaries

In principle, it might be possible to estimate  $\dot{J}$  from observations of orbital period changes in close binaries. Very precise timings of minimum light can be obtained from the light curves of eclipsing systems, and the available baseline of 20–70 yr can reveal  $\dot{P}$  values as small as one part in  $10^{12}$ . But in general one must worry that the light curves may be contaminated by other perturbations of comparable size: e.g., effects of mass transfer, apsidal motion, third-body effects, star spots, and shifts in the light distribution across the eclipsed object. The ideal systems are detached main-sequence binaries, in which there is no mass transfer and no accretion disk. Unfortunately, these cool main-sequence binaries are extremely rare. Only four are known: ER Vul (G0+G5), UV Leo (G1+G1), YY Gem (M1+M1), and CM Dra (M5+M5). Two other detached systems, V471 Tau (K2+wd) and GK Vir (M+wd), are also very suitable for this purpose; in these systems, the “clean” geometry of the eclipse of a bare white dwarf enables one to specify the moment of dynamical conjunction to within a few seconds. Finally, we can add another 15 stars if we are willing to consider *semi*detached binaries, all of which are in CVs. These are desirable to include since they contain main-sequence secondaries, are all rotating at the same high velocity, and are plentiful. On the other hand, the mass transfer presents additional complications, and CVs are known to show erratic period changes which are transient and possibly spurious (see, e.g., Pringle 1975; Eason *et al.* 1983).

Since there is no obvious observational distinction between a “spurious” and a “real” period change, we can do no better than to simply fit the eclipse timing data impartially for each of the 22 stars. This procedure is discussed in detail by Patterson (1984), and is illustrated in Figure 15 for the four “classical” main-sequence binaries. For each star, any deviation of the points from a straight line in the “O–C diagram” indicates the existence of a period change. At least two of the four stars in Figure 15 show a significant period decrease. The same procedure was employed for all 22 stars, except that for the CVs, the uncertainty attached to each timing was taken to be either the dispersion of timings in a single season, or 0.007 cycles, whichever is greater. The reason for this is that the

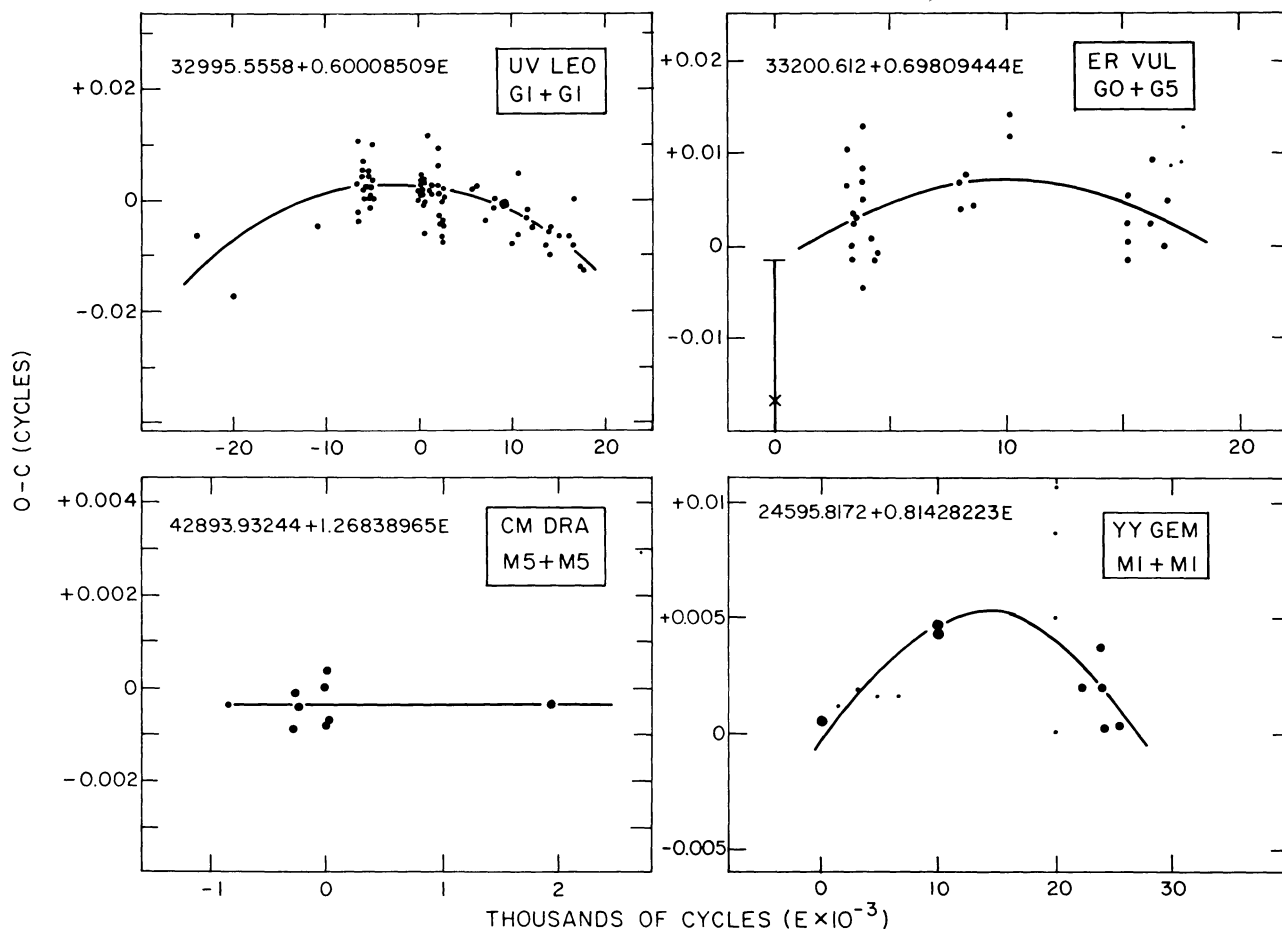


FIG. 15.— $O - C$  diagrams for the four “classical” main-sequence binaries. Test ephemerides are shown in the individual frames, and the size of the circles indicates the assigned weight. The best parabolic or linear fit to the residuals is also shown.

best-studied systems (UX UMa, U Gem, DQ Her, RW Tri) show erratic phase wanderings of about this size.

The resultant values of  $\dot{P}/P$  are shown in Figure 16, plotted versus the observed or estimated mass of the secondary. The CVs are shown in the circles, and the detached binaries are shown in diamonds. Error bars indicate estimated  $\pm 1 \sigma$  limits, but are suppressed when they are smaller than the symbols. As Figure 16 illustrates, there is a definite preference for decreasing periods, but it appears to be limited to long-period systems, i.e., those with more massive secondaries.

At this point, the reader should meditate briefly (see, e.g., Kruszewski 1966) on the difficulty of producing large secular period decreases in these systems. (In draft versions of this paper, problems arose from insufficient reader meditation here.) Conservative mass transfer from a low-mass to a high-mass star produces a period *increase*, as does mass loss from the system. The only known method of producing a secular period decrease, especially a *large* secular period decrease, is *angular momentum loss*. We shall therefore assume that angular momentum loss is responsible, although, of course, we cannot exclude the possibility that we have seriously underestimated the erratic phase wandering, which by coincidence (and misfortune!) has produced the systematic effect seen in

Figure 16. If the total system angular momentum is taken to be the orbital angular momentum (the rotational component contributes  $\leq 10\%$  in CV binaries), then a swift application of Kepler’s third law and equation (7) yields

$$\dot{J} = 2.7 \times 10^{36} \frac{M_1^{2/3}}{(1+q)^{1/3}} \frac{\beta^{1.83}}{\alpha} P_4^{1.55} \left( \frac{\dot{P}}{P} \right)_{-7} \text{ ergs}, \quad (26)$$

where we have used the notation of § III, with  $(\dot{P}/P)_{-7} = \dot{P}/P$  in units of  $10^{-7} \text{ yr}^{-1}$ . With the binary system parameters from Table 1 and from Popper (1980), we may estimate  $\dot{J}$  and  $v_{\text{rot}}$  for each star, using equation (26). The five CV systems with secondaries earlier than M3 show  $\dot{J} \approx 3 \times 10^{36}$  ergs, while those with cooler secondaries show  $\dot{J} \lesssim 4 \times 10^{35}$  ergs.

### iii) A $\dot{J}(v)$ Relation for G Stars

The machinery is now nearly in place for deriving a  $\dot{J}(v)$  relation for G stars. The single-star data are in the form  $v = ft^{-n}$ , where acceptable values of  $f$  and  $n$  are given by Figure 14. Since the binary-star data are in the form  $\dot{J}(v)$ , we must transform the  $v(t)$  data to the  $\dot{J}(v)$ -plane, and easily



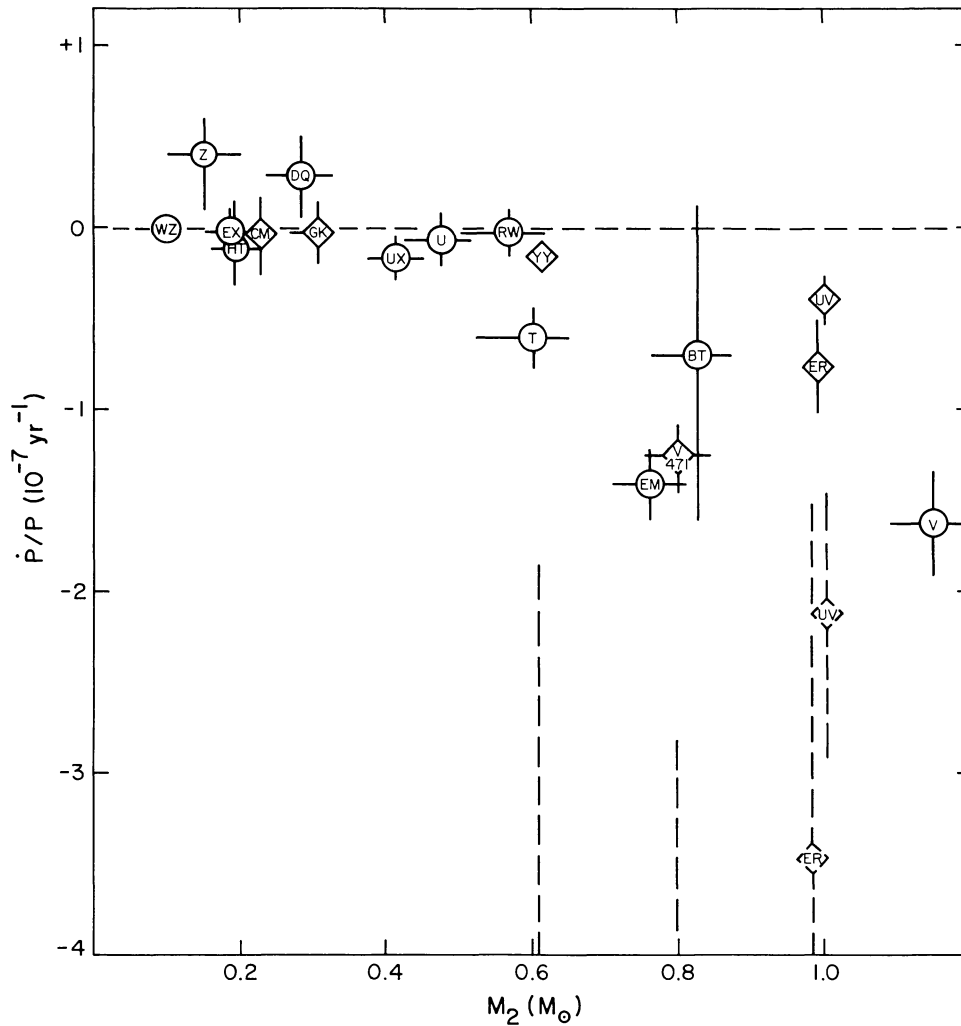


FIG. 16.—Empirical data on  $\dot{P}/P$  for all rapidly rotating stars in close binaries. CVs are shown in circles, others in diamonds. Dashed symbols represent the  $\dot{P}/P$  values corrected to  $v = 130 \text{ km s}^{-1}$  (the value appropriate for CVs), using the scaling of eq. (29).

obtain

$$\dot{J} = -nf^{1/n}v \left( \frac{n+1}{n} \right) k^2 MR, \quad (27)$$

where the star's moment of inertia is  $k^2 MR^2$ . We assume, here and throughout this work, that the stars are in rigid-body rotation—although it may eventually be necessary to abandon this assumption. Integration of the density profile in model low-mass main-sequence stars (e.g., Schwarzschild 1958) shows that  $k^2 \approx 0.07$  in the range  $0.3\text{--}1.5 M_\odot$ . As long as we restrict our discussion to G stars, we can write  $M = 1 M_\odot$ ,  $R = 1 R_\odot$ , and thus obtain

$$\dot{J} = -9.7 \times 10^{42} n f^{-1/n} v \left( \frac{n+1}{n} \right) \text{ ergs.} \quad (28)$$

Using this equation, the constraints on  $f$  and  $n$  in Figure 14 can be converted to the  $\dot{J}(v)$ -plane, and the results are shown in Figure 17. The region permitted by the  $v(t)$  data is shaded,

and the locations of the important calibrating points are marked by arrows. Since we can measure  $\dot{J}$  directly in the solar wind, we show at the lower left an error bar representing the extreme range of empirical estimates of  $\dot{J}_\odot$  (which rely on various models for the variation of wind with solar latitude; see the discussion of Soderblom 1983). At the upper right are the important constraints provided by the bona fide G stars ER Vul and UV Leo, another point representing V471 Tau (K2), and—just for comparison—average values for CVs with “hot” and “cool” secondaries. The fact that the independent binary star data are located in or near the shaded region gives welcome assurance that our choice of a power-law fitting function (i.e., linear in the log-log plane) does not lead to obvious inconsistencies.

We show the fits in a more useful way in Figure 18. Here are shown the loci of solutions for  $\dot{J}(v)$ , using: (1) only the data of Figure 13 (*solid contour*); (2) the data of Figures 13 and 17 (*dashed contour*). Depending on how much weight the reader is inclined to give the points at high velocity (which are all obtained from  $\dot{P}$  studies, and are therefore not immune to

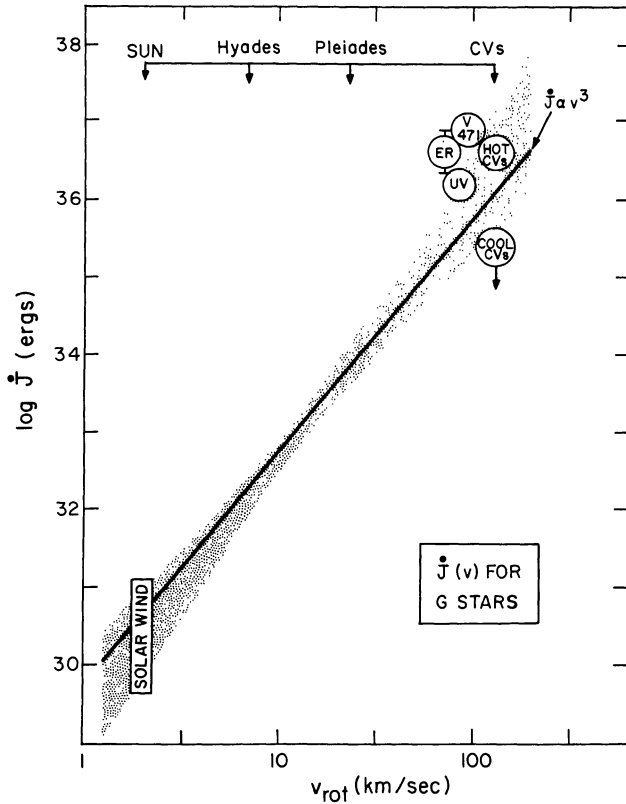


FIG. 17.—Dependence of the angular momentum loss rate  $\dot{J}$  on the rotational velocity  $v$ . Straight lines lying within the shaded region satisfy the  $v(t)$  data of Fig. 13. Also shown are the observed  $\dot{J}$ -values for three rapidly rotating detached main-sequence stars (UV Leo [G1], ER Vul [ $\sim$ G3], and V471 Tau [K2]), and the range of estimates for  $\dot{J}$  in the solar wind.

spurious phase wandering), everyone can find a contour to his or her own liking. We also point out the location assumed by VZ.

Finally we are in a position to derive a  $\dot{J}(v)$  law for G stars. The overlap of contours suggests that within a factor of 2,

$$\dot{J}(v) = 8 \times 10^{36} (v/130 \text{ km s}^{-1})^{3.75 \pm 0.35} \text{ ergs.} \quad (29)$$

iv) Wanted: A  $\dot{J}(M)$  Relation

Now we encounter another apparent setback. Equation (29) gives the slowdown rate of a G star, but since CV secondaries never change their rotational velocities (being frozen at 130 km s<sup>-1</sup>) but vary in mass, we are much more interested in the dependence of  $\dot{J}$  on the mass  $M$  of the secondary. How can we find the right  $\dot{J}(M, v)$  relation? One possibility is to find  $v(t)$  relations for lower mass stars and transform  $v(t)$  to  $\dot{J}(v)$  for, say, four different classes of stars (e.g., G, K, early M, late M). We could then interpolate to find a general  $\dot{J}(M, v)$ .

VZ and Taam (1983) surmounted this problem by assuming that the particular  $v(t)$  relation which they adopted for G dwarfs holds exactly for all late-type dwarfs. Rotational velocity data for single K and M dwarfs are extremely scarce, but are in general not compatible with this very strong assumption. In particular: (1) in the field and in the Hyades, K stars are typically rotating more slowly than G stars (Baliunas *et al.* 1983); and (2) in the Pleiades, the reverse may be true (van Leeuwen and Alphenaar 1982). Such data are now being rapidly acquired through the increased use of digital techniques in high-resolution spectroscopy, but we are still a few years away from being able to state empirical  $v(t)$  relations for K and M stars.

v) Found: A  $\dot{J}(M)$  Relation at  $v = 130$  Kilometers per Second

In the meantime, what can we do? It turns out that the  $\dot{P}$  data for CVs provide a means of bypassing the need for  $v(t)$  relations. If we compare the  $\dot{J}$  values observed in CVs to each other, we can isolate the dependence on mass since all the secondaries are rotating at nearly the same velocity. Thus, in principle we can determine  $\dot{J}(M)$  directly, for the one value of  $v_{\text{rot}}$  that we really care about.

This is shown in Figure 19, taken from the  $\dot{P}$  study of Patterson (1984). We feel safe in including an extra point at  $1 M_{\odot}$ , obtained from Figures 17 and 18 (this requires only a small extrapolation in  $v_{\text{rot}}$ ). For comparison we have superposed the prediction of the simplified braking law for G stars (heavily extrapolated in both mass and velocity). The VZ line bears some resemblance to the data, but apparently underestimates  $\dot{J}$  losses for stars above  $\sim 0.5 M_{\odot}$ . If we fit a function of the form

$$\dot{J} = C(M/M_{\odot})^a \quad (30)$$

to the data, we find acceptable fits for a range of values shown in Figure 20 with contours of confidence limits. Values of  $a$  up to 6.3 are permitted at the 95% confidence level, but in practice, we know that low-mass stars do not lose angular momentum at the low rates required by, say,  $a > 5$ . This is

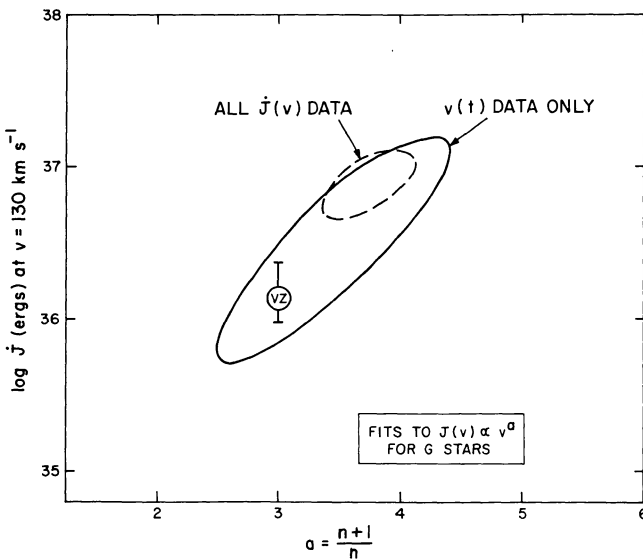


FIG. 18.—Locus of solutions for  $\dot{J}$  ( $v = 130 \text{ km s}^{-1}$ ), using (1) only data from Fig. 13 (solid contour), and (2) data from Figs. 13 and 17 (dashed contour). The confidence level of the contours is not known, but is thought to be  $\sim 90\%$ .

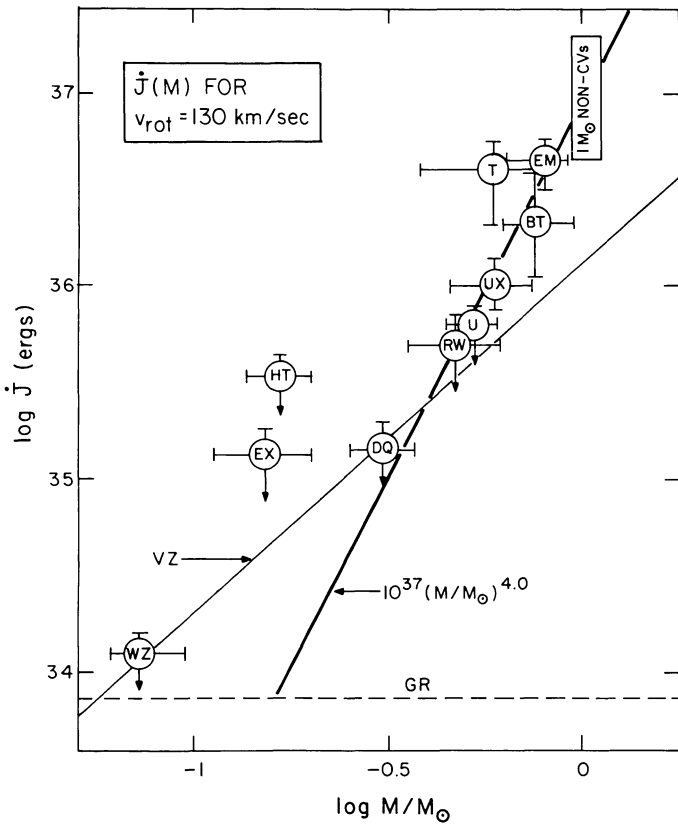


FIG. 19.—Dependence of  $\dot{J}$  on mass  $M$ , for stars rotating at 130  $\text{km s}^{-1}$  (CVs, plus a point for  $1 M_{\odot}$  “non-CVs” obtained from Fig. 18). The heavy straight line is the best fit to the data, while lighter line is the relation implicitly assumed by VZ.

shown by the high  $\dot{J}$  seen in YY Gem, the fact that the properties of CVs do not depend *drastically* on the mass of the secondary, and, perhaps most importantly, the fact that single, rapidly rotating, low-mass stars do not exist. We shall quantify this limit by noting that DQ Her, at  $M = 0.3 M_{\odot}$ , possesses a disk far too bright to be explained by GR. Adopting the requirement that  $\dot{J} \geq 6 \times \dot{J}_{GR}$  at  $M = 0.3 M_{\odot}$ , we find that all points to the right of the heavy line in Figure 20 are excluded. Consequently, the allowed solutions are all quite near the relation

$$\dot{J}(v = 130 \text{ km s}^{-1}) = 10^{37} (M/M_{\odot})^{4 \pm 1} \text{ ergs.} \quad (31)$$

By comparison, the implicit prediction of VZ is  $\dot{J} = 1.5 \times 10^{36} \text{ ergs } (M/M_{\odot})^{1.88}$ , shown by the little circle at the lower left of Figure 20.

vi) Overall Results

Finally, these results deserve a quick summary. We have sought the best possible prescription for  $\dot{J}$ . The simplified braking law adopted by VZ and Taam (1983) suffers from three fatal flaws:

1. It assumes that the slope of the  $v(t)$  relation for G stars is precisely known, while the true observational uncertainty can affect  $\dot{J}$  by several orders of magnitude.
2. A very large extrapolation in rotation velocity is required.
3. It assumes that the  $v(t)$  relation for G stars also holds *exactly* for K and M stars, and the available data more or less rule out this assumption.

We have attempted to fix the first two problems by finding the range of  $v(t)$  or  $\dot{J}(v)$  laws allowed by the data, and adding a few calibration points at high rotation velocity. The third problem is more severe, and much new observational data are required. But in the  $\dot{P}$  data for rapidly rotating main-sequence

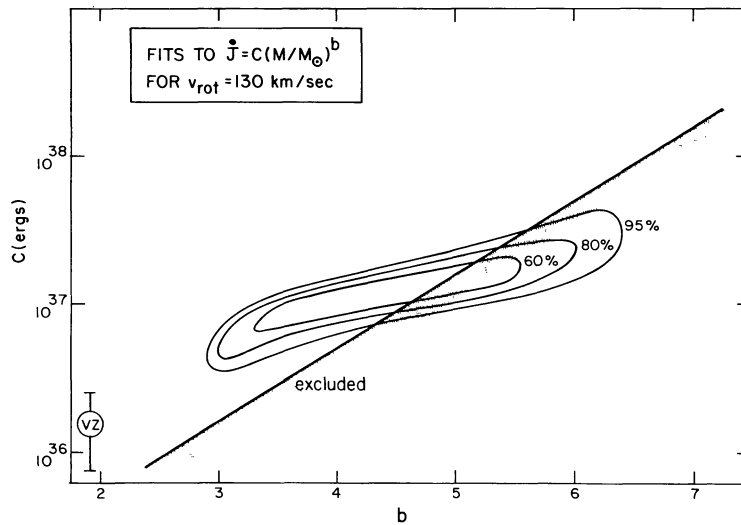


FIG. 20.—Detailed results of fitting the  $\dot{J}$  data of Fig. 17 to a function of the form  $\dot{J} = C(M/M_{\odot})^b$ . The contours indicate parameter values which fit the data within 60%, 80%, and 95% confidence limits. Points to the right of the heavy line are excluded by the requirement that  $\dot{J}$  exceed  $5 \times 10^{34} \text{ ergs}$  at  $M = 0.3 M_{\odot}$ . The point labeled “VZ” at lower left is the prediction when the simplified  $v(t)$  law is assumed to hold exactly for all late-type stars.

stars in eclipsing binaries (most of which are in CV systems), we have a constraint on  $\dot{J}(M)$  at one particular rotation velocity, namely,  $v_{\text{rot}} = 130 \text{ km s}^{-1}$ . Since this is the velocity of interest, this  $\dot{J}(M)$  relation is precisely what we need. We will adopt equation (31) as our working relation.

It should not escape attention that we have also given in equation (29) a  $\dot{J}(v)$  relation for G stars. We have chosen not to use this relation, since it is based only on 1  $M_{\odot}$  stars—too massive for our purposes. As for a general  $\dot{J}(M, v)$  relation, the best guess at this point is something like

$$\dot{J} = 10^{37} (v/130 \text{ km s}^{-1})^{3.7} (M/M_{\odot})^{4.0} \text{ ergs}, \quad (32)$$

but this can be greatly improved when the rotation velocity data for single K and M stars improve significantly.

### c) Producing $\dot{M}$ from $\dot{J}$

Having found a prescription for  $\dot{J}$ , we now need a theory to predict the resultant induced mass transfer rates  $\dot{M}$ . A reasonable first-order theory assumes the following:

- 1) The wind carrying away the angular momentum transports a negligible amount of mass;
- 2) As the orbital separation decreases, all of the mass peeled away from the lobe-filling secondary goes into accretion, with none lost.

We will adopt these assumptions because they are reasonably plausible, and provide a basis for calculating  $\dot{M}$ . In § VI d(ii) below, we will investigate the effects of relaxing them.

Let us consider a main-sequence secondary of mass  $M_2$  which fills its Roche lobe in a close binary system. At  $v = 130 \text{ km s}^{-1}$ , the angular momentum loss due to rotational braking is

$$\dot{J}_2 = 10^{37} (M_2/M_{\odot})^4 \text{ ergs}. \quad (33)$$

The other angular momentum loss mechanism is GR, which, according to the well-known dipole formula, yields

$$\dot{J}_{\text{GR}} = 3.46 \times 10^{-67} \frac{(M_1 M_2)^2}{M^{2/3}} P^{-7/3} \text{ ergs}. \quad (34)$$

With our usual notation and  $m_2 = M_2/M_{\odot}$ ,  $m_1 = M_1/M_{\odot}$ , this reduces to

$$\dot{J}_{\text{GR}} = 9.95 \times 10^{33} \left(\frac{\beta}{\alpha}\right)^{3.67} m_1^2 P_4^{0.07} m^{-2/3} \text{ ergs}. \quad (35)$$

Now if the total mass of the system is constant, it can be shown from equations (4) and (5), and Kepler's third law that

$$\dot{J}_{\text{orb}} = 1.14 \times 10^{52} \left(\frac{\alpha}{\beta}\right)^{1/2} \frac{m_2^{0.27}}{m^{0.33}} (m - 1.79m_2) \dot{m}_2 \text{ ergs}. \quad (36)$$

If rotational braking dominates and tidal torques always drain the orbital angular momentum to replenish that lost by the

secondary, then

$$\dot{J}_{\text{orb}} = \dot{J}_2, \quad (37)$$

and a little arithmetic yields

$$\dot{M}_2 = 7.5 \times 10^{-10} \left(\frac{\beta}{\alpha}\right)^{7.33} \frac{m^{0.33} P_4^{4.55}}{(m - 1.79m_2)} M_{\odot} \text{ yr}^{-1}. \quad (38)$$

This is the master equation of binary evolution driven by rotational braking. If the evolution is driven by GR alone, then we have

$$\dot{J}_{\text{orb}} = \dot{J}_{\text{GR}}, \quad (39)$$

and

$$\dot{M}_2 = 3.57 \times 10^{-11} \left(\frac{\beta}{\alpha}\right)^{3.67} \frac{m_1^2 P_4^{-0.26}}{m^{1/3} (m - 1.79m_2)} M_{\odot} \text{ yr}^{-1}. \quad (40)$$

### d) Confrontation with Data

#### i) Mass Transfer Rates

We can now compare these predictions to the observed mass transfer rates in CVs. It is convenient to do so in terms of orbital period, since that quantity is observable and determines  $\alpha$ ,  $\beta$ , and  $m_2$ , at least approximately, through equations (4)–(7). In Figure 21 we show the predicted mass transfer rates, for three assumed values of the mass of the compact star. Since  $\dot{M} \propto \dot{J}$ , it suffices to simply add the mass transfer rates induced by GR and RB. From RB alone, we would expect  $\dot{M} \propto P^{4.5}$ , but the dominance of GR (which produces  $\dot{M} \approx 7 \times 10^{-11} M_{\odot} \text{ yr}^{-1}$ , nearly independent of binary period) at short periods flattens the theoretical dependence on  $P$  out to  $\sim P^3$ , in good agreement with the observed dependence.

Thus, our rotational braking theory (assuming  $\alpha = \beta = 1$ , and ZAMS secondaries in thermal equilibrium) produces a quite good fit to the observations, with the predicted transfer rates generally about a factor of 2–10 too high.

Just in case (perish the thought!) there are readers who do not accept any of the  $\dot{J}$  evidence from eclipsing binaries, but believe that the simplified braking law from slowly rotating G stars represents the best guess for stars of any velocity and spectral type, we have calculated the  $\dot{M}(P)$  relation under the exact assumptions made by VZ and Taam (1983). The results are shown in Figure 22, which should be compared to Figure 21. The general behavior of the curve is very similar to that of Figure 21. We still obtain approximately  $\dot{M} \propto P^3$ , with the predicted rates still about a factor of 3–10 too high. Some differences between the figures can be seen at the shortest and longest periods.

The lesson of this is that for the purpose of predicting  $\dot{M}(P)$ , there is no great sensitivity to exactly which braking law is adopted. The important point is that the observed  $\dot{J}$  rates in K and early M stars are  $\sim 1\text{--}10 \times 10^{36}$  ergs, and this should induce an  $\dot{M} \approx 1\text{--}10 \times 10^{-9} M_{\odot} \text{ yr}^{-1}$ . Referring to

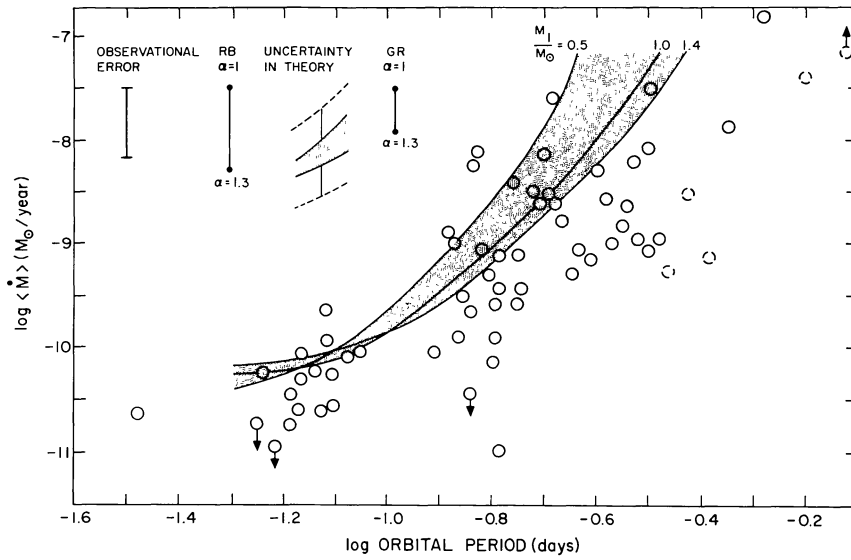


FIG. 21.—Theoretical mass transfer rate vs. orbital period, with the observational data from Fig. 7 superposed. The three curved lines show the transfer rates expected from RB+GR, for three values of the mass of the compact star. The rate expected from GR alone is a nearly horizontal line at  $\log \langle \dot{M} \rangle \approx -10.2$ . Effects of varying  $\alpha$  and allowing for uncertainties in the braking law are shown at the upper left.

Figure 19, any straight line between the heavy line that we favor and the light line adopted by VZ will simply produce an  $\dot{M}(P)$  relation intermediate between the shaded regions of Figures 21 and 22. However, the assumptions we have made play a very important role, and it is time to reexamine them.

ii) Perturbing Effects

1. Effects of mass loss.—What we have calculated is, strictly speaking, the secondary's mass loss rate  $\dot{M}_2$ . The  $\dot{J}$  losses

grind the binary dimensions down at a certain rate, and if the secondary remains on the main sequence, this implies an  $\dot{M}_2$ . But if some of the mass lost by the secondary does not fall on the compact star, then the accretion rate  $\dot{M} < \dot{M}_2$ . There are at least three plausible scenarios for systemic mass loss in CVs; mass loss (1) in the braking wind itself, (2) in classical nova eruptions, and (3) in the accretion process itself (e.g., through high velocity winds from the compact star, or through ejection at the disk's outer edge). Each of these mechanisms could be

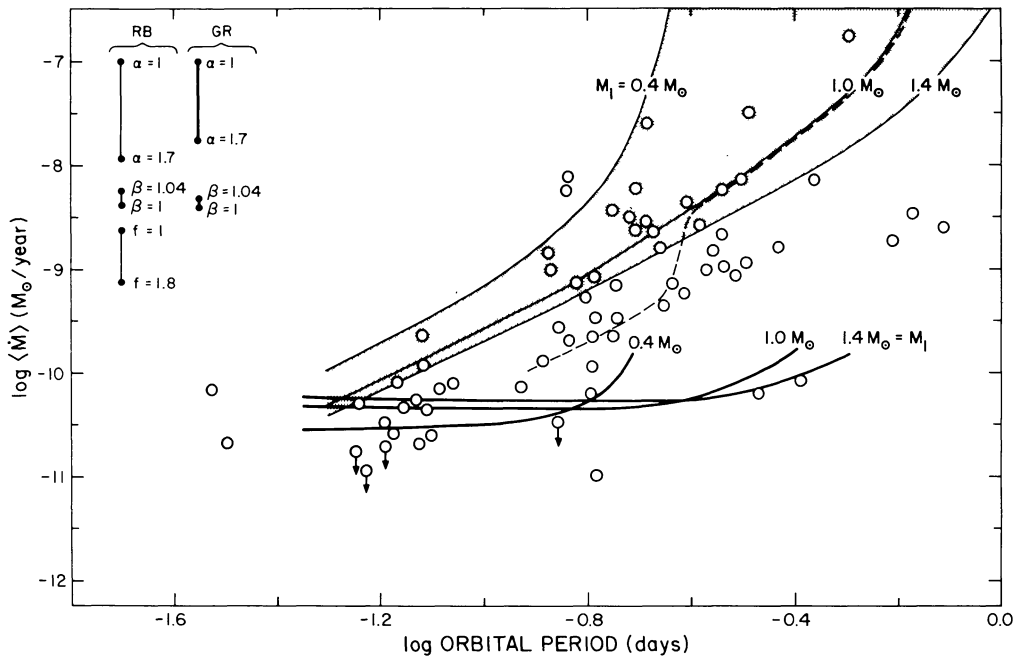


FIG. 22.—Another version of Fig. 21, with our favored braking law replaced by the simplified braking law of VZ. Here the induced transfer rates from RB and GR are shown separately.

quite important. The first will certainly act to slow evolution<sup>7</sup> and lower  $\dot{M}$ , and the second appears to have had the same effect in the one system for which data are available (BT Mon; Schaefer and Patterson 1983). We know of no way to place interesting constraints on the third mechanism, which might retard or accelerate evolution, depending on the prescription for the  $J/M$  ratio of the lost matter. Subject to this important caveat, we may say that these perturbing effects act to reduce the expected accretion rate.

2. *Departure from the ZAMS.*—Although the data reviewed in § III showed that CV secondaries are approximately on the ZAMS, it would be quite surprising if this were *exactly and universally* true. Since all CV secondaries have been whittled down from stars of higher mass, it would not be surprising to find a few slightly evolved from the ZAMS. In equation (4) we have invented the parameter  $\alpha$  to represent the actual mass-radius ratio for each star, which may differ from 1 because of an error in the adopted ZAMS mass-radius law, or because the star's radius is greater than the true (unknown) ZAMS radius. The first effect can vary  $\alpha$  in range  $0.9 < \alpha < 1.1$ , but the second can only *increase*  $\alpha$ , and by rather large amounts: according to the definition of Iben (1967), "main-sequence" stars can have  $\alpha$  anywhere in the range 1.0–1.7. As can be seen at the upper left of Figure 21 and in equation (38), a small increase in  $\alpha$  can decrease the expected value of  $\dot{M}$  very substantially. The reason for this is that  $\alpha > 1$  produces a lower mass secondary at a given orbital period, and in our scheme  $\dot{J}$  is strongly dependent on mass.<sup>8</sup>

3. *Loss of thermal equilibrium.*—Another perturbing effect that is probably important arises from the loss of thermal equilibrium in the secondary, which is forced by  $\dot{J}$  and the constricting Roche lobe to lose matter at high rates. We have four relations which define time scales: the empirical time scale for mass transfer, defined by  $M_2/\dot{M}_2$  and equation (17); the two theoretical time scales, according to our braking law ("P") and the VZ braking law; and the thermal time scale of the secondary, defined by

$$\tau_{\text{KH}} = 3 \times 10^7 \frac{(M_2/M_\odot)^2}{(R_2/R_\odot)(L_2/L_\odot)} \text{ yr.} \quad (41)$$

In order to facilitate comparisons, we will make power-law approximations to the three mass transfer time scales, and parameterize in terms of the mass of the secondary (assumed

<sup>7</sup>It is interesting to note that if the stellar magnetic field  $B$  is estimated by scaling up from solar values with  $B$  assumed proportional to the rotation frequency (see discussion in Mochnecki 1981), then application of the Weber-Davis wind model (Weber and Davis 1967) shows that the mass-loss rate in the wind is not negligible, but comparable to the induced mass transfer rate. This would slightly decrease the predicted mass transfer rates, and significantly decrease the predicted lifetimes. We do not correct for this effect, since we wish to avoid reliance on specific, detailed assumptions about the magnetic field and the wind—preferring instead to rely on an *empirical* prescription for  $\dot{J}$ .

<sup>8</sup>But this is true only in our scheme of reckoning, not necessarily in nature. A slightly evolved star may have more vigorous surface convection, which may increase  $\dot{J}$  more significantly than the smaller mass decreases it.

to be a ZAMS star). We obtain

$$\tau_{\dot{M}_2} = \begin{cases} 1.6 \times 10^8 m_2^{-1.6} \text{ yr} & \text{(empirical)} \\ 5 \times 10^7 m_2^{-1.7} \text{ yr} & \text{(P law)} \\ 1.2 \times 10^8 m_2^{-1.1} \text{ yr} & \text{(VZ law)} \end{cases} \quad (42)$$

To evaluate  $\tau_{\text{KH}}$ , we require a mass-luminosity relation. For the lower main sequence, the data of Veeder (1974) and Lacy (1977a) are consistent with a relation

$$L_2/L_\odot = \begin{cases} m_2^{4.8} & 0.6 < m_2 < 1.0 \\ 0.31 m_2^{2.65} & 0.13 < m_2 < 0.6 \end{cases} \quad (43a)$$

$$(43b)$$

We can now express  $\tau_{\dot{M}_2}/\tau_{\text{KH}}$  purely as a function of  $m_2$ , and we show the results in Figure 23. Throughout the interval  $0.13 < m_2 < 0.9$ , the theoretical time scales and the thermal time scale are seen to be equal within a factor of  $\sim 2$ . The empirical time scale is somewhat longer, although, as we have previously noted, this would be shortened if some of the mass lost by the secondary does not accrete onto the white dwarf. Of course, no significance should be attached to the detailed shape of any curve in Figure 23. We have adopted approximations for  $\tau_{\dot{M}_2}$ ,  $\tau_{\text{KH}}$ , and the  $M$ - $R$ - $L$  calibrations of Veeder (1974), Lacy (1977a), and this paper. Small systematic errors in the approximations and in the data may easily account for the shape of the curves. Figure 23 really conveys only one message, but it is a remarkable one: although the mass transfer rate varies by nearly three orders of magnitude, the mass transfer proceeds on a thermal time scale to within a factor of 2 or 3.

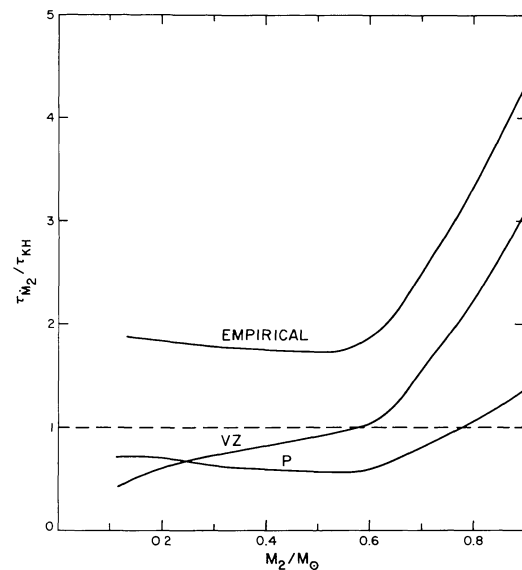


FIG. 23.—Comparison of the mass-transfer time scale  $\tau_{\dot{M}_2}$  to the secondary's Kelvin-Helmholtz time scale  $\tau_{\text{K-H}}$ , for various secondary masses. The time scale  $\tau_{\text{K-H}}$  is given by eq. (41), and  $\tau_{\dot{M}_2}$  is deduced from the empirical accretion rates, from our favored braking law, and from the simplified braking law of VZ.

This coincidence of time scales suggests the possibility that angular momentum loss from magnetic braking in CVs may be *saturated*, i.e., that  $\dot{J}(v)$  reaches a maximum value for some  $v < 130 \text{ km s}^{-1}$  (possibly when the condition  $\tau_j \equiv J/\dot{J} \approx \tau_{\text{KH}}$  is reached)—and does not increase, or increases weakly, for higher  $v$ . Some evidence for this can be found in the  $\dot{J}$  rates of Figure 16, and in the observed dependence of coronal X-ray luminosity on rotation velocity (Walter 1982; Cruddace and Dupree 1983). This is a fascinating and important possibility, but will have to wait for some future work to explore properly.

The more critical point for this study is that the ZAMS secondaries in CVs appear to be always on the verge of losing thermal equilibrium. When driven out of thermal equilibrium, the star fails to contract sufficiently fast as it loses mass. The radius increases relative to the ZAMS radius, and perhaps also absolutely. Because  $\dot{M} \propto \alpha^{-7.33}$  in our scheme, a significant drop in  $\dot{M}$  may occur. Our procedure cannot predict the behavior of stars under such circumstances, but Taam (1983) and Rappaport, Verbunt, and Joss (1983) have calculated the response of the secondary with the VZ braking law (but allowing for some deviations). Interpolating between Taam's  $f = 0.7$  and  $f = 1.78$  models, we find that for  $f = 1$  the star departs from thermal equilibrium for  $P \leq 6$  hr. The resultant decline in the predicted  $\dot{M}_2$  for a model with  $M_1 = 1.0 M_\odot$  is shown as the dashed curve in Figure 22. Uncertainties in the braking law and in the models prevent any detailed comparison of such curves, but the basic point is clear enough: departures from thermal equilibrium tend to diminish the expected  $\dot{M}$  (see Taam 1983; Spruit and Ritter 1983; Rappaport, Verbunt, and Joss 1983 for additional discussion on this point).

4. *Turning off the wind.*—We have used a braking law based on a power law fitted to the data in the  $(M, \dot{J})$ -plane. But it should be noted that the data in Figure 16 do not strongly constrain the  $\dot{J}(M)$  dependence for  $M \leq 0.3 M_\odot$ . For small  $M$ , the function  $\dot{J}(M)$  must fall *at least* as sharply as given by the VZ braking law, but probably falls much more sharply. In fact, the data are consistent with an *abrupt* transition to  $\dot{J}_{\text{GR}}$  for any  $M \leq 0.25 M_\odot$ . This is of interest because such a transition can produce an orbital period “gap” (see § VII), and because there is observational evidence that the coolest stars lack a mechanism for shedding angular momentum. For single M stars in the field, Joy and Abt (1974) found that the percentage of stars showing emission lines increased smoothly from  $\sim 5\%$  at a spectral type of M0 to  $\sim 100\%$  at M5.5 and later. If, as is widely believed, emission is a signature of rapid rotation, then the coolest stars may as a class be rotating more rapidly. (Unfortunately, there do not exist sufficient radial velocity data to confirm or deny this.) But we know of no reason why late M stars should be systematically *younger* than early M stars. Therefore, it seems that the coolest stars have not been able to shed angular momentum as quickly as their warmer cousins.

A likely correlative of angular momentum loss, in the sense that both originate from stellar “activity”, is X-ray luminosity. Golub (1983) reports that late-type stars show a rapid decline in X-ray luminosity near a spectral type of M5. According to Popper (1980), a spectral type of M5 corresponds to a mass of  $\sim 0.25 M_\odot$ .

There is also theoretical evidence that the dynamo process, thought to be responsible for magnetic activity in late-type stars, operates at the interface between the outer convective zone and the radiative core (Spruit and van Ballegoijen 1982). If this is so, then we would expect the braking wind to die abruptly when the secondary's radiative core disappears, which occurs at  $M \approx 0.3 M_\odot$  in the models of Grossman, Hays, and Graboske (1974).

Thus, rapid extinction of a braking wind in very low mass stars is thoroughly consistent with what we know about late M stars. This appears to be a very promising way to obtain a period gap in the range 2–3 hr.

#### e) Time Scale for Synchronization

We have assumed above that synchronous rotation of the lobe-filling secondary is always guaranteed. Since this assumption is absolutely vital, and since many CVs must go through phases in which the Roche lobe is not filled, it is worth a brief digression to make a quantitative estimate of the synchronization time and its dependence on the fraction of the Roche lobe that is filled.

From the work of Zahn (1966*a, b*) and Alexander (1973), DeCampli and Baliunas (1979) estimated the synchronization time scale  $\tau_{\text{sync}}$  in stars with convective envelopes as

$$\tau_{\text{sync}} \approx 0.047 \left( \frac{R_2}{a} \right)^{-6} q^2 \frac{M_2}{R_2 \langle \mu \rangle}, \quad (44)$$

where  $M_2$  and  $R_2$  are the mass and radius of the star,  $a$  is the binary separation, and  $\langle \mu \rangle$  is the mean convective viscosity. We adopt equation (5) as usual, and replace equation (4) with

$$\frac{R_2}{a} = 0.462 \left( \frac{q}{1+q} \right)^{1/3} \beta k, \quad (45)$$

where  $k$  is the fraction of the Roche lobe radius that is filled. Following the discussion of DeCampli and Baliunas, we can make only a crude estimate of the mean convective viscosity, namely,  $\langle \mu \rangle \approx 10^{12} \text{ g cm}^{-1} \text{ s}^{-1}$ . In this case, equation (44) transforms to

$$\tau_{\text{sync}} \approx 5 \times 10^3 \text{ yr} \frac{(1+q)^2 m_2^{0.12}}{\alpha \beta^6 k^6 \langle \mu \rangle_{12}} \quad (46)$$

in our standard notation, with  $\langle \mu \rangle_{12} = \langle \mu \rangle / 10^{12} \text{ g cm}^{-1} \text{ s}^{-1}$ .

The only strong dependence in this relation arises from the factor  $k^{-6}$ , which comes from the usual  $r^{-6}$  dependence of tidal forces (e.g., Newton 1687). For lobe-filling systems,  $k = 1$ , and therefore  $\tau_{\text{sync}} \approx 5000 \text{ yr}$ —shorter than all other time scales of evolutionary significance. Thus, synchronous rotation of a lobe-filling secondary is a very good assumption indeed. For a very detached system we might have  $k \approx 0.1$ , which lengthens  $\tau_{\text{sync}}$  to  $5 \times 10^9 \text{ yr}$ . Since this is approximately the age of the galactic disk, synchronism is then no longer a good assumption.

No comprehensive observational study of synchronism in close binaries has yet been done, but the available data suggest that equation (46) cannot be too far wrong. Levato (1976)

studied a sample of stars near a spectral type of F5, and found that the transition to nonsynchronism occurred at  $k \approx 0.1$ . We are more concerned with spectral types of K and M, where the data are more sparse. The secondaries in Algol systems are thought to be synchronously rotating; they are typically K subgiants, with  $k$  in the range 0.3–1.0 (usually =1.0). And there are two very well-determined systems consisting of twin M dwarfs, namely, YY Gem and CM Dra; these systems have  $k = 0.4$  and 0.2, respectively, and their orbital light curves indicate that they are synchronously rotating (Leung and Schneider 1978; Lacy 1977b). We know of no firm counterexample to an assumed transition at  $k = 0.1$  for *all* secondaries with convective envelopes. These facts are roughly consistent with equation (46), which we will therefore adopt until something better comes along.

### f) Summary

In summary, we have used empirical data on rotation and period changes to estimate quantitatively the effect of magnetic braking on cataclysmic variables. Data on the rotational braking of single stars are useful, but do not extend to the interesting regimes of high rotation velocity ( $\geq 100 \text{ km s}^{-1}$ ) and late spectral type (K,M). However, we can obtain constraints on  $\dot{J}$  in these regimes by using measurements of  $\dot{P}$  in eclipsing binaries. Although one cannot rule out the possibility of a spurious value of  $\dot{P}$  in any particular binary, we note that all 22 systems are consistent with a simple braking law, which is, in turn, consistent with an extrapolation (although not with *any* extrapolation) of the single-star braking law to the high velocities present in the binaries. Looking at Figures 17–19, it seems quite plausible that the observed values of  $\dot{P}$  may be indicative of the long-term  $\dot{J}$  losses. But this important point certainly needs further study, as there is still no way to guarantee that we have not been misled by phase wanderings unrelated to long-term evolution.

If the overall trend in the  $\dot{P}$  data is accepted at face value, we can derive a  $\dot{J}(M, v)$  law, which is particularly well-constrained at  $v = 130 \text{ km s}^{-1}$ , the velocity of interest. We then calculate the mass-loss rate inflicted on the secondary by  $\dot{J}$  and the constricting Roche lobe. These rates vary approximately as  $P^3$ , in agreement with the data, but are, in general, about a factor of 2–10 too high. Most or all of the perturbing effects act to reduce the expected rates, and hence to reduce the discrepancy between theory and observation. For the shortest periods, it appears likely that magnetic braking gives way to GR as the principal mechanism driving the evolution.

## VII. THE PERIOD GAP

We can now return to Figures 1, 7, and 8 and discuss the significance of the “orbital period gap” between 2.1 and 2.8 hr. We begin by reviewing previous suggestions for how this gap is created and preserved.

### a) Previous Attempts

#### i) Webbink's Hypothesis

Several authors (Webbink 1979; Whyte and Eggleton 1980) have pointed out that a dichotomy in orbital periods could be

created very early in CV evolution, during the red-giant phase of the primary. If the initial orbital period is fairly small ( $\leq 2$  yr), then the expanding primary will reach its confining Roche lobe during the first ascent of the red-giant branch (“case B”), and will overflow and lose its envelope, thus becoming a white dwarf immediately and short-circuiting further nuclear evolution. If the orbital period is longer, the primary fails to reach its Roche lobe, undergoes helium flash, and contracts to start a new life on the horizontal branch. Eventually the star climbs the red giant branch a second time (“case C”), and will reach its Roche lobe if the orbital period is in the range 2–100 yr (Paczynski 1971). Even with a smooth distribution of initial orbital periods, Nature will ruthlessly divide systems into those that have a nearly full lifetime on the horizontal branch, or none at all. This dichotomy might then be preserved in subsequent evolution, although none of these authors studied this in detail.

Although the horizontal-branch lifetime is short, the core luminosity is so high that the mass of the degenerate core grows significantly during this time. Thus, systems which have undergone case B mass transfer should possess low-mass ( $\leq 0.45 M_{\odot}$ ) helium white dwarfs, while case C should yield predominantly high-mass ( $\geq 0.55 M_{\odot}$ ) carbon-oxygen white dwarfs (Webbink 1979). Therefore, if the model is correct, white dwarf masses on either side of the period gap should be systematically different.

We confront this prediction with observation in Figure 24. While the data are somewhat sparse, it appears that the predicted segregation of masses is not supported; the mean white dwarf mass is  $\sim 0.8 M_{\odot}$  on both sides of the gap.

#### ii) The Onset of Complete Convection

If we adopt the assumption that the secondaries are ZAMS stars, then a system with  $P_{\text{orb}} = 3$  hr contains a secondary of mass  $0.3 M_{\odot}$ . This is approximately the mass at which the convective envelope, which progressively deepens as the spectral type gets progressively later, finally reaches the hydrogen-burning core (Schwarzschild 1958). This will cause sudden mixing of envelope material into the nuclear-burning regions,

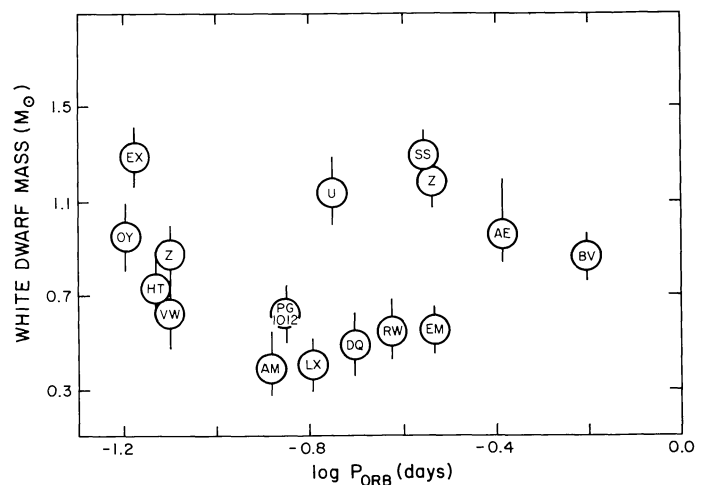


FIG. 24.—Distribution of white dwarf masses with orbital period



with unpredictable consequences. D'Antona and Mazzitelli (1982) suggest that the supply of fresh  $\text{He}^3$  (available in large quantity as a product of previous nuclear burning via the not quite completed  $p$ - $p$  cycle) into the core will cause a sudden increase of the stellar radius, leading to a phase of dynamic mass transfer. This might cause systems to travel through the period gap very rapidly, giving a low probability of observing them.

This approach has promise, but problems remain. The models of D'Antona and Mazzitelli display a great diversity of behavior, depending on initial conditions. The models assume a constant rate of mass loss from the secondary, and it is not at all clear what will happen with a self-consistent prescription for the mass loss. In addition, their Figure 10 suggests that the resultant changes in radius are  $\leq 10\%$ , whereas we will find below that radius changes of at least 30% are apparently required to explain the observed period gap. More extensive and more self-consistent models (e.g., Joss and Rappaport 1983) are required, hopefully including the response of the system during and after the phase of dynamic mass transfer.

### iii) Cessation of Mass Transfer

Robinson *et al.* (1981) have suggested that stars travel through the period gap in a state of little or no mass transfer, thus extinguishing the cataclysmic activity that enables these systems to be discovered. As evidence of this, they cite the observed tendency of stars with orbital periods near the gap to reach states of very low mass transfer—as if the secondaries were verging on the total cessation of mass transfer. If true, this would be an important clue to the period gap.

Let us see if the empirical data support this suggestion. We may construe a "state of low mass transfer" to be signified by (a) a low mass transfer rate when faintest, (b) a low *mean* mass transfer rate, or (c) a large brightness change between quiescence and eruption. Arguments could be advanced for each one of these interpretations. In Figure 25 we show the distribution of stars qualifying under each one of these criteria in (a), (b), and (c), and the distribution of all stars in (d). The question is, are the distributions in (a), (b), or (c) more strongly clumped near  $\log P = -1.0$  than the distribution in (d)?

The answer is no. This is more or less obvious from inspection of Figure 25, and is confirmed by a simple test. The rms deviation about  $\log P = -1.0$  is found to be 3.7, 3.5, and 3.7 (in units of  $|\Delta \log P| = 0.1$ ) for (a), (b), and (c), compared with 3.9 for the entire collection of stars. Thus, with any of these definitions, the low- $\dot{M}$  stars do not preferentially cluster near the period gap. (Of course, low- $\dot{M}$  stars do preferentially have short periods, as shown above; this is presumably why the three tests are faintly positive.) Nor do the stars near the gap show any particular proclivity for low  $\dot{M}$ : the two stars defining the edge of the gap, YZ Cnc and TU Men, are normal dwarf novae, and the 10 stars straddling the gap include only three stars (AM Her, TT Ari, and MV Lyr) which qualify as low- $\dot{M}$  systems according to any of the three criteria above. We conclude that an appraisal of all the observational evidence does not support this suggestion.

This does not imply that no definition can be found which yields a significant clustering near the period gap. Shafter

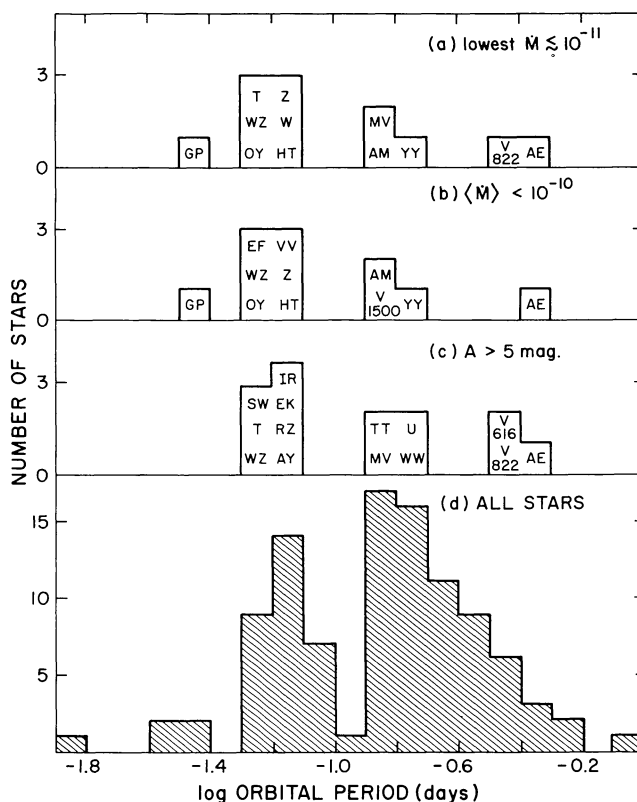


FIG. 25.—(a)–(c) Distribution of orbital periods for systems of “low mass transfer rate,” identified by three different criteria. (d) Distribution for all stars.

(1983d) points out that a clustering at the long-period side of the period gap is a property of the “VY Sculptoris” class of cataclysmic variable, which he defines as follows: stars which show rare, deep minima in their long-term light curves, and which are not AM Her stars. This is true, but we are uncomfortable with this extremely specific *a posteriori* definition, motivated not by physical considerations but by a desire to have a homogeneous group which clusters near  $p = 3$  hr. (Different definitions were used by Bond 1981, who invented the class, and by Robinson *et al.* 1981.) It is hard to understand why the cessation of mass transfer should be signified by rare minima; at first thought, rare maxima, or no maxima, would seem to be more physically reasonable. We are also worried about selection effects. In long-period systems, the secondary’s light is competitive with that of the disk; hence, excursions to a low- $\dot{M}$  state will produce only rather weak minima—making these stars ineligible for VY Scl membership, and also harder to discover. Very short period CVs have low accretion rates, which may make deep minima unfeasible since  $\dot{M}$  may never be able to fall below the rate set by gravitational radiation. In short, we are not persuaded that the VY Scl stars represent anything other than ordinary UX UMa (or Z Cam) stars of short orbital period. Even if there *are* new physical effects associated with these stars, it seems likely that they carry information about variability time scales in the secondary (approximately months to decades)—not about secular evolution, which proceeds on much longer time scales.

### b) Interpretation of the Gap

From the above work it is clear that the “period gap” is a misleading term because it suggests that there is a hole in the period distribution of a single class of object. In fact, the segregation of systems by an  $\dot{M}$  criterion (Fig. 8) shows that there are really *two* distributions, and *the period gap is created by superposing these two distinct distributions.*

If the two distributions never mix in the course of evolution, then the period gap can be understood directly. The short  $P$  systems, driven by GR, reach a minimum period of  $\sim 1.3$  hr and begin to evolve toward longer period, when the secondaries are driven out of thermal equilibrium (Paczynski 1981; RJW). Because it requires  $\sim 3\text{--}7 \times 10^9$  yr for the period to evolve from 2 to 1.3 to 2 hr (RJW), few systems in this period regime can leave it in the lifetime of the Galaxy. The long-period systems, driven by rotational braking, probably reach a period of  $\sim 3\text{--}6$  hr when their secondaries are driven out of thermal equilibrium. What happens then depends on the exact prescription for angular momentum losses.

#### i) Constant $\dot{J}$

Paczynski (1981) assumed a constant  $\dot{J}$  and showed that the system “bounces” at a period given by

$$P_{\min} = 1.45 m_1^{0.23} (\dot{J}/\dot{J}_{\text{GR}})^{0.34} \text{ hr.} \quad (47)$$

For example,  $\dot{J}/\dot{J}_{\text{GR}} = 10$  implies  $P_{\min} = 3.2$  hr. The system subsequently evolves toward longer periods, until the secondary is evaporated. Thus, long-period systems never enter, or even approach, the short-period regime at all. Since the Galaxy may not be sufficiently old for short-period systems to wander back to long periods, this can produce a period gap.

#### ii) Smoothly Decreasing $\dot{J}$

However, this success is rather artificial since we assumed a sharp dichotomy in  $\dot{J}$  to begin with. All of the viable magnetic braking models predict that  $\dot{J}$  should depend strongly on  $M_2$ , at least for  $M_2 \leq 0.6 M_{\odot}$ . With  $\dot{J}$  smoothly decreasing as  $M_2$  does, it is by no means clear that any “period bounce” will occur, and detailed calculations with the VZ braking law (Taam 1983; Rappaport, Verbunt, and Joss 1983) revealed no such bounce (until the GR bounce at 1.3 hr). Taam’s calculations showed that the secondaries departed somewhat from thermal equilibrium (as might be expected from Fig. 23), but never so drastically as to cause a period bounce. Thus, all systems will invade the short-period regime, and there will be no period gap.

#### iii) Turning off the Wind

To produce a period gap, we need to postulate a sharper decline of  $\dot{J}$  with  $M_2$ , for systems with  $P \approx 3$  hr. In § VI we have cited evidence—from single stars, and from theoretical arguments—that angular momentum losses are probably very low in stars of  $M_2 \leq 0.2\text{--}0.3 M_{\odot}$  (see also Spruit and Ritter 1983; Rappaport, Verbunt, and Joss 1983). This has, or could have, fascinating consequences. Suppose, for example, that rotational braking follows our braking law until  $M_2 = 0.2 M_{\odot}$ ,

when it abruptly vanishes. According to Taam’s Figure 2,<sup>9</sup> the secondary is at this point distended by a factor of 1.32 over its ZAMS radius. From equation (8) this implies  $P = 3.5$  hr. The remaining  $\dot{J}$  mechanism is GR, so the orbit now shrinks on a time scale  $\tau_{\text{GR}}$ , which in our notation is

$$\tau_{\text{GR}} = \frac{J}{\dot{J}} = 8.1 \times 10^9 \left( \frac{\alpha}{\beta} \right)^{1.83} P_4^{1.44} \frac{m^{0.33}}{m_1} \text{ yr.} \quad (48)$$

Meanwhile, the star itself shrinks on a time scale  $\tau_{\text{KH}}$ , which is much shorter than  $\tau_{\text{GR}}$ . From equations (41), (43), and (48) we deduce

$$\frac{\tau_{\text{GR}}}{\tau_{\text{KH}}} = \begin{cases} 8.1 \beta^{4.9} \alpha^{-3.9} P_4^{5.9} m^{0.3} m_1^{-1.0} & 0.6 < m_2 < 1.0 \\ 18.4 \beta^{1.0} \alpha^{0.0} P_4^{3.3} m^{0.3} m_1^{-1.0} & 0.13 < m_2 < 0.6 \end{cases} \quad (49a)$$

$$(49b)$$

For  $M_1 = 1 M_{\odot}$  and a secondary near the main sequence, this ratio does not approach unity until  $P \approx 1.5$  hr. So the star detaches itself from its Roche lobe and shrinks until reaching its main-sequence radius, in the case  $0.24 R_{\odot}$ . A billion or so years later, the ongoing action of GR shrinks the Roche lobe down to the surface of the secondary, and shortens the orbital period to 2.3 hr. Now mass transfer can begin again; the system is reawakened as a low- $\dot{M}$ , short-period CV.

This scenario is rather attractive. The period gap is a natural consequence of the secondary’s departure from thermal equilibrium and the turnoff of magnetic winds for spectral types later than  $\sim M4$ . A period bounce near 3 hr is not required, although it is permitted. More detailed calculations of this effect, including the location and width of the resultant period gap, have been made by Spruit and Ritter (1983).

#### c) Hiding the Dead Novae

But there may be another difficulty with the period gap beyond its mere *existence*. The time required for a system driven by GR to traverse the gap is

$$\Delta t \approx 10^7 \text{ yr} \frac{m^{1/3}}{m_1 m_2} \left[ (P_i/\text{hr})^{8/3} - (P_f/\text{hr})^{8/3} \right], \quad (50)$$

where  $P_i$  and  $P_f$  are, respectively, the initial and final periods. For the case we have considered above, this gives  $\Delta t = 1 \times 10^9$  yr. This is short compared to the age of the Galaxy, and therefore we expect that most long-period systems should have traversed the gap to become low- $\dot{M}$ , short-period systems. Assuming that we live at a representative moment in the Galaxy’s life, we can calculate the expected space densities of long- and short-period systems. From Table 5 we have  $D_{\text{CN}} \approx 4 \times 10^{-7} \text{ pc}^{-3}$ ,  $\tau_{\text{CN}} \approx 8 \times 10^7 \text{ yr}$ ,  $\tau_{\text{SP}} \approx \tau_{\text{GAL}}$ , from which we expect a space density  $D_{\text{SP}}$  of short-period systems given by

$$D_{\text{SP}} = D_{\text{CN}} \times \frac{\tau_{\text{SP}}}{\tau_{\text{CN}}} \approx 4 \times 10^{-5} \text{ pc}^{-3}. \quad (51)$$

<sup>9</sup>Taam actually used the VZ braking law, but the differences are small in this period regime.

This exceeds our estimate for  $D_{SP}$  (Table 4) by a factor of  $\sim 10$ . There is a basic problem of conservation here: where have all the dead novae gone?

Let us inspect the argument more carefully for uncertainties. We estimate that the uncertainties in the empirical numbers are approximately as follows:  $D_{CN} = 2-8 \times 10^{-7} \text{ pc}^{-3}$ ,  $D_{SP} = 2-6 \times 10^{-6} \text{ pc}^{-3}$ ,  $\tau_{CN} = 0.5-2.0 \times 10^8 \text{ yr}$ ,  $\tau_{SP} = 0.5- > 1.0 \tau_{GAL}$ . (Of course,  $\tau_{SP}$  is to be replaced with  $\tau_{GAL}$  if  $\tau_{SP} > \tau_{GAL}$ ). Hence, if we were to adopt low values of  $D_{CN}$  and  $\tau_{SP}$ , and high values of  $D_{SP}$  and  $\tau_{CN}$ , the discrepancy would vanish. So we shall state the point more precisely: *the number of short-period systems we observe is uncomfortably small, if all of the long-period systems evolve fairly promptly into short-period systems*. This difficulty can be overcome as follows:

1. Adopt extreme values for the four critical quantities, with each error pushing the estimate in the same direction. But this is an unlikely solution, because we shall find in § VIIIe that this conservation problem can also be deduced from considerations of the birthrate and death rate of CVs—*independent of the above argument*.

2. Prolong the duration of the detached state to  $\geq 5 \times 10^9 \text{ yr}$ . This could happen, for example, if  $\dot{J}$  were considerably greater than we have estimated—which could drive the system to much longer periods before becoming detached. Since the secondaries we observe in CVs are near the main sequence, this possibility is somewhat disfavored.

3. Find a means of *destroying* the secondary in classical novae—perhaps by continuing to inflict a high  $\dot{J}$  on the system *sine fine*, invoking an instability of the sort considered by Ruderman and Shaham (1983), or both.

#### d) Summary

In summary, the period gap can be reasonably understood as the result of a rapid extinction of the braking wind from a star which has been driven slightly out of thermal equilibrium. Using our favored braking law, we find from Figure 6 of Spruit and Ritter (1983) that a period gap in the range 2.0–2.7 hr is expected. The happy concordance with observation suggests that this may well be the right idea, and furthermore that the extinction of the wind probably does coincide with the transition to a completely convective state at  $M_2 \approx 0.2-0.3 M_\odot$ . But if long-period systems actually evolve across the gap and become short-period systems, we have difficulty in understanding the observed low space density of short-period systems. The resolution of this problem is not yet known, but at present it seems most probable that there exists a mechanism which destroys CVs (and low-mass X-ray binaries) on a time scale short compared to the age of the Galaxy. This mechanism could operate on *either* side of the period gap.

### VIII. THE BIG PICTURE

This work has been primarily a study of mass transfer rates and mechanisms during the active lifetimes of CVs. We believe that we have identified the most important mechanisms: angular momentum loss via magnetic braking for the high- $\dot{M}$  systems and via GR for the low- $\dot{M}$  systems. Now we turn to the prior evolution of these systems, and make a few remarks about birthrates and death rates.

#### a) The Formation of a Close Binary

As has been pointed out by many authors (e.g., Ritter 1976; Webbink 1979), CVs must originate from very wide binaries, with initial orbital periods  $\geq 1 \text{ yr}$ . This is because the observed white dwarf masses are generally quite high, implying that the ancestor stars lived for a long time as red giants before reaching their Roche lobes. When the Roche lobe is finally reached, an episode of very rapid mass transfer must ensue, both because nuclear evolution continues to force expansion, and because the mass ratio makes the system unstable. According to Webbink (1979), the mass transfer rate during this phase may reach  $0.1 M_\odot \text{ yr}^{-1}$ . The secondary cannot assimilate the accreted matter, and itself bloats up into a red giant-like object which fills its Roche lobe (Kippenhahn and Meyer-Hofmeister 1977). Even this does not appease the rampaging primary. It is widely assumed that the system now wraps itself in a single “common envelope” (Paczynski 1976; Taam, Bodenheimer, and Ostriker 1978; Meyer and Meyer-Hofmeister 1979). The common-envelope phase is spectacular but brief; the primary’s envelope is driven off in  $\sim 10^4 \text{ yr}$ , and carries with it a huge fraction of the system’s orbital angular momentum. Thus, it is thought, do close binaries emerge from systems that were initially very wide.

At the termination of the common-envelope phase, the decline in accretion allows the secondary to contract to an equilibrium radius appropriate to its mass; i.e., it resumes life as a main-sequence star. Hence, the system is now a close, detached binary containing a main-sequence star and a hot, freshly formed white dwarf.

#### b) The V471 Tauri Stars: Precataclysmic Binaries

These systems are faint and nonruptive, and consequently very difficult to discover. Seven are known with orbital periods less than 1 day, and another four between 1 and 20 days (the “V471 Tau” stars; see Tables 1 and 2). Five of them are actually surrounded by planetary nebulae (Bond, Liller, and Mannery 1978; Bond 1983). Because planetary nebulae only survive for  $\sim 10^4 \text{ yr}$  and are almost certainly produced by red giants, and because the systems are at present much too compact to accommodate a red giant, it seems likely that these five systems have undergone common-envelope–binary evolution in the last  $10^4 \text{ yr}$ .

Each V471 Tau star will become a bona fide CV as soon as the secondary reaches its Roche lobe. In a few cases the secondary may be sufficiently massive to accomplish this by expanding as a result of its own nuclear evolution. But for secondaries  $\leq 1 M_\odot$ , this process is too slow, and a way must be found to contract the Roche lobe to meet the star’s surface.

The natural solution is angular momentum loss, via GR or any other available mechanism. GR will decrease the orbital period on a time scale of  $\sim 10^{10} (P/4 \text{ hr})^{1.44} \text{ yr}$ , and hence will produce CVs only very slowly. Of the 11 known V471 Tau stars, only one (the central star of Abell 41) could begin mass transfer in the next  $3 \times 10^9 \text{ yr}$ , if GR dominates.

Since mass transfer has not yet started, the various mechanisms available to the accretion disk are not yet feasible. The only efficient known mechanism that is available at this point

is magnetic braking. We have seen above that this will operate on a time scale of  $\sim 10^{7-8}$  yr for G and K secondaries, and probably on a somewhat longer time scale for early M secondaries. Rotational velocity data for field stars (see below) show that A and early F stars do not experience magnetic braking, and therefore such secondaries must wait a very long time for nuclear evolution to initiate their (very short lived) mass transfer phase. This implies that A and F spectral types should be very rare or absent among CVs.

### c) *Where Are the Early-Type Secondaries?*

In Figure 26 we show all available data on the spectral types of CV secondaries, drawn from Tables 1 and 2. The circles indicate "later than," used for stars whose secondaries are not visible in the spectrum. We include a few stars with unknown orbital periods, because they possess visible secondaries; these are TU Leo, EY Cyg, and CH UMa. We exclude all stars with giant or subgiant secondaries. In the left half of the figure, we show observed mean rotational velocities for single main-sequence stars as a function of spectral type (Allen 1973). Also shown are the rotational velocities at breakup, given by  $v = (GM/R)^{1/2}$ . Note that the breakup velocity of A–M stars is approximately constant at  $\sim 400$  km s $^{-1}$ , while the observed rotation velocities show a strong dependence on spectral type. Of course, this sharp transition between slow and fast rotators has been known for decades (e.g., Struve 1930; Kraft 1967). Without exception, the CV secondaries are G, K, and M stars—precisely those stars which are known to have an efficient means for shedding angular momentum. This is readily explained if, in the precataclysmic phase, systems may have secondaries of any spectral type, but only the G–M stars succeed in shedding angular momentum sufficiently fast to reach their Roche lobes in a reasonable time.

It is possible that the restriction of CV secondaries to late spectral types is a selection effect, since it might be difficult to identify a CV against the background light of an early-type companion. This is probably true for the dwarf novae, which reach only  $M_v \approx +4$  at maximum. But it seems unlikely for the classical novae, which reach  $M_v = -5$  to  $-11$  at maximum. As a nova fades from maximum light, identification of its remnant with an early-type star would be straightforward. Indeed, such systems should be preferentially observed since early-type stars can be seen to greater distances.

Another possibility is that mass transfer from early-type secondaries may be unstable, since the mass-losing star may be considerably more massive than the white dwarf. If this is so, an A or F star reaching its Roche lobe could quickly lose most of its mass and become a G or K star, from which we would expect stable mass transfer. Or it could be that A and F main-sequence secondaries exist but do not reach their Roche lobes, because they do not experience magnetic braking. Thus, it is not exactly clear what Figure 26 is telling us about the prior evolution. But it offers very suggestive evidence that the same mechanism which slows the rotation of single stars is responsible for the feeding of cataclysmic variables, and perhaps also for their *creation*.

### d) *Magnetic Braking in Cool Stars*

We favor a magnetic braking mechanism not only because it produces a good fit to the observational data, but also because it seems to be a universal characteristic of stars with convective envelopes. For single main-sequence stars, we have already noted its probable role in producing the transition between slow and fast rotators at a spectral type of  $\sim F5$ –G0. Brecher and Channugam (1978) argued that magnetic braking may also operate effectively in single red giants, on the grounds that the ancestors of red giants (B and A stars) are fast rotators, while their descendants (neutron stars and white dwarfs) rotate with speeds many orders of magnitude smaller than their breakup speeds.

Moving into the realm of close binaries, we find the same story. Cool stars are found in every kind of system: detached (RS CVn stars, BY Dra stars, V471 Tauri stars), semidetached (Algols, cataclysmic variables), and contact (W UMa stars). They are all forced by tidal torques to rotate synchronously with the orbit, if they fill more than  $\sim 1/10$  of their Roche lobes (see eq. [46]). Hence, they are all likely to take on the characteristics of "active" stars—chromospheric emission lines, star spots, and coronal X-ray emission. Each of these classes (except CVs) does, in fact, show all of these characteristics, and it has now been abundantly demonstrated that the degree of activity is determined by the rotation rate (e.g., Walter 1981; Dupree 1981). In the case of CVs, the observational proof is difficult since accretion onto the compact primary also produces very substantial emission lines, light variations, and X-rays. But since every other kind of cool star participates in the "rotation-activity" connection, it seems rather likely that CV secondaries do. Thus, it is likely that they possess fairly strong surface magnetic fields, as proposed for all rapidly rotating cool stars (e.g., Mullan 1974).

For a star of fixed mass and radius, dynamo theories produce poloidal fields  $B_p$  proportional to the rotation frequency (e.g., Malkus 1959). Scaling up from the Sun, we expect  $B_p \approx 60$ –600 gauss for CV secondaries. Mochnacki (1981) showed that for a stellar wind of  $10^{-12} M_\odot$  yr $^{-1}$ , a surface field of  $\sim 20$ –100 gauss is sufficient to insure that the wind will corotate to at least a few stellar radii, producing efficient magnetic braking. Hence, we do not require exotic values for the two critical parameters—magnetic field and mass loss rate in the wind—on which observation has failed thus far to set interesting limits.

Finally, it is noteworthy that the theory described above makes no reference to the compact star, which passively accretes matter transferred from the tortured secondary. In fact, why not replace the compact star with a normal main-sequence star? Synchronization will still occur, and  $\dot{J}$  losses in a braking wind will be just as large (or larger, since two stars are now contributing). If braking losses reduce the lifetimes of CV systems to  $\sim 10^8$  yr, should they not do the same to short-period *detached* binaries with cool main-sequence components? We should then expect to see rather few of these systems in catalogs of close binaries.

We have tested this by extracting the data for detached main-sequence binaries from Batten's *Seventh Catalog of Spectroscopic Binaries* (Battin, Fletcher, and Mann 1978). All of

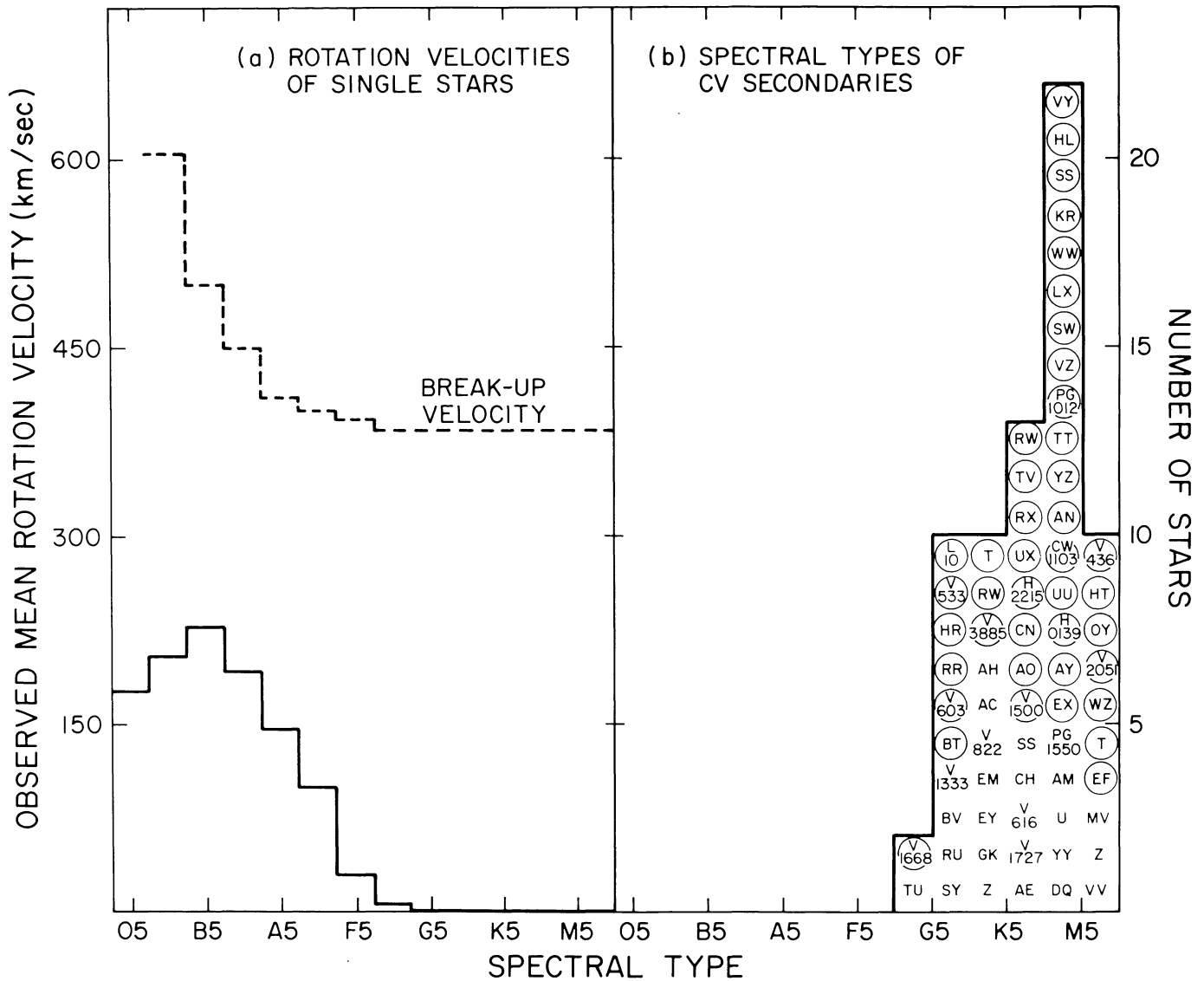


FIG. 26.—(a) *Solid curve*, observed mean rotation velocity of single main-sequence stars in the field; *dashed curve*, rotation velocities of these stars at breakup. (b) Distribution of spectral types in CV secondaries, taken from Table 1. Circles mean “later than.” It is apparent that all CV secondaries are stars which, if left to themselves, would like to brake their rotation.

these systems have known periods and at least approximately known spectral types. Therefore, it is possible to estimate, within an uncertainty of  $\lesssim 50\%$ , the fraction of the Roche lobe that is filled. In Figures 27a, 27b we show the distribution of observed systems with  $R_*/R_{\text{lobe}}$  (or with orbital period, which is given by the inset scale) for hot and cool dwarfs, respectively. It is obvious from inspection that the hot stars (median period  $\approx 7^d$ ) tend to be in closer binaries than the cool stars (median period  $\approx 35^d$ ).

*Interpretation* of this difference is certainly a hazardous enterprise, given the selection effects which must plague the catalog. One severe and obvious selection effect is that long-period systems are less likely to be discovered, because their radial velocity variations are smaller. But we have not been able to think of any plausible and strong selection effect which depends on spectral type and can produce the result in Figure

27. Therefore, we have considered the possibility that short-period binaries with GK dwarfs are relatively rare because some mechanism reduces their lifetimes far below the nuclear lifetimes of the individual stars. In Figure 27c, we show how the statistics might be used to evaluate this hypothesis. Let us suppose (not for any deep reason, just for simplicity of illustration) that star formation produces binaries with a distribution in  $R_*/R_L$  which does not depend on spectral type. Presumably that distribution is something like the one shown by BA dwarfs, which are not subject to braking processes. How severely must we deplete this distribution to obtain the one seen in Figure 27b? Well, if we normalize the two distributions to yield the same number of stars for  $\log R_*/R_L < -1.4$  (where even the GK dwarfs will not synchronize, and therefore will not be strongly braked), then we obtain Figure 27c. Some depletion is evident around  $\log R_*/R_L = -1$ , and it

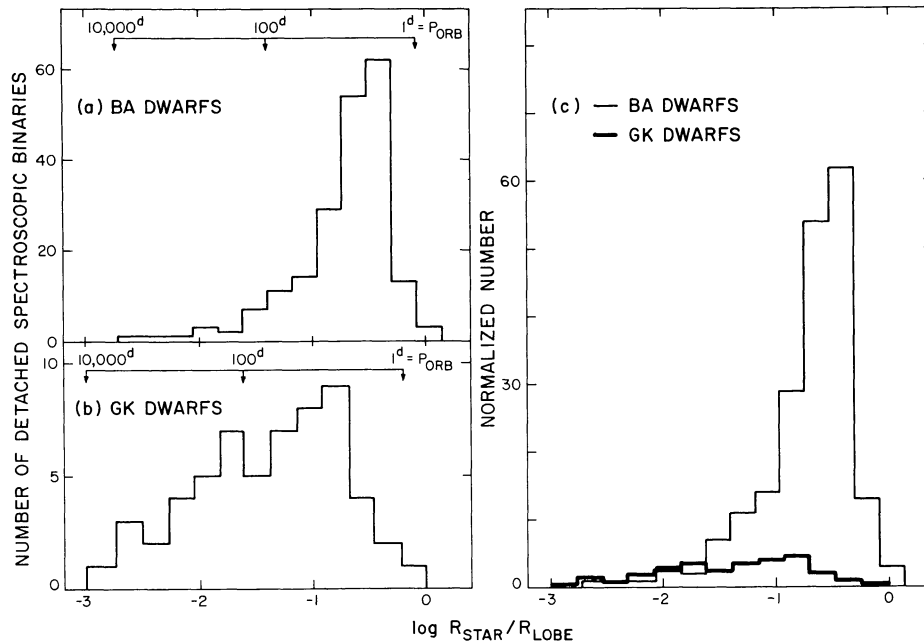


FIG. 27.—Distribution of known main-sequence spectroscopic binaries with  $R_*/R_L$  (or with orbital period, given by the inset scale). (a) Systems with B and A dwarfs. (b) Systems with G and K dwarfs. (c) BA and GK dwarfs plotted on a scale with the same number of stars present with  $\log R_*/R_L < -1.4$ . The difference in distributions could be due to a depletion of binaries with GK dwarfs and  $\log R_*/R_L > -1.4$ .

gets really serious for  $\log R_*/R_L > -0.7$ . It is certainly premature to claim that this is the correct interpretation, but I find it difficult to look at Figure 27c without thinking of depletion mechanisms.

We can also examine the population of *eclipsing* binaries for signs of depletion; these are all very close binaries, as expected since they show eclipses. We would like to know the number of cool and hot dwarfs among the population of eclipsing main-sequence binaries, compared to the numbers of cool and hot dwarfs in a magnitude-limited star catalog such as the Michigan HD catalog (containing spectral types and luminosity classes for 25,000 dwarfs, and thought to be complete for  $m_v < 9.0$ ; Houk and Cowley 1975 et seq.). Popper (1980) presents a complete list of eclipsing binaries which can be reasonably certified as consisting of main-sequence stars. We have taken the stars in Popper's list, and discarded those fainter than the HD magnitude limit, in order to compare with the HD catalog. We present the distribution of the remaining 44 stars with spectral type in Figure 28, together with the distribution of all main-sequence stars in the HD catalog. It is clear that the two distributions are different, in the sense that cool stars are underrepresented among the eclipsing binaries. In fact, there is only *one* binary consisting of G, K, or M dwarfs, and its membership is quite marginal (UV Leo;  $m_v \approx 9.0$ , spectral class G1 + G1).

Thus, we have three independent lines of evidence which suggest a short lifetime for close binaries with GKM dwarfs: the period distribution of spectroscopic binaries, the spectral type distribution of main-sequence eclipsing binaries, and the observed period decreases seen in Figures 15 and 16. One simple way to understand all of these facts is to suppose that there really is a mechanism which removes angular momen-

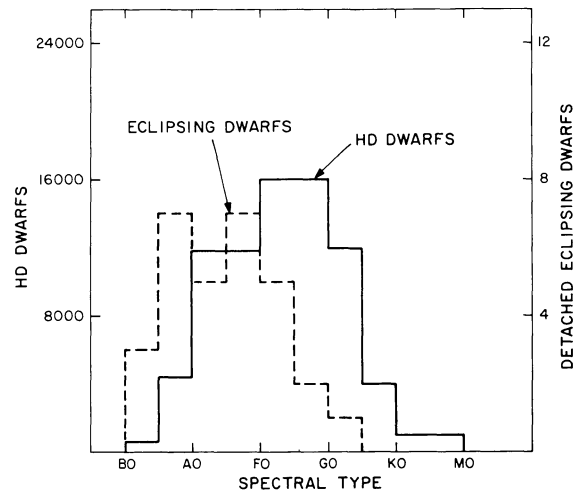


FIG. 28.—Distribution of bright ( $m_v < 9.0$ ) known main-sequence eclipsing binaries (*heavy line*), and of stars in the Michigan HD catalog (*light line*), with spectral type. The differences in distributions could be due to a depletion of close binaries with cool main-sequence components.

tum and destroys all of these binaries on a time scale of  $\sim 10^8$  yr.

### e) Birthrate and Death Rate of Cataclysmic Variables

#### i) Birthrate

Despite their relatively low space densities, it seems incapable that the CV birthrate is very high, up to a few percent of the total rate of white dwarf formation. Let  $\psi$  be the

fraction of white dwarfs formed in CV systems. We can find  $\psi$  directly by comparing the space densities of classical novae and white dwarfs, but we must allow for the short lifetimes of novae:

$$\psi = \frac{D_{\text{CN}} \tau_{\text{GAL}}}{D_{\text{WD}} \tau_{\text{CN}}}, \quad (52)$$

with the notation of § VIII. We use  $D_{\text{CN}} = 4 \times 10^{-7} \text{ pc}^{-3}$ ,  $D_{\text{WD}} = 10^{-2} \text{ pc}^{-3}$  (Liebert 1980),  $\tau_{\text{GAL}} = 7 \times 10^9 \text{ yr}$ , and  $\tau_{\text{CN}} = 8 \times 10^7 \text{ yr}$ . Thus, we obtain  $\psi \approx 0.004$ .

A second estimate can be made from the frequencies of planetary nebulae and novae, assuming that each planetary nebula signals the birth of a white dwarf. The data from our own Galaxy are riddled with selection effects, but Ford and Jacoby (1978) and Ford (1978) presented a set of data which appeared to detect all planetaries and novae in a portion of the nuclear bulge of M31. Bath and Shaviv (1978) extended Ford's argument to show that

$$\frac{160}{\psi} < \frac{\tau_{\text{CN}}}{T} < \frac{660}{\psi}, \quad (53)$$

where  $T$  is the recurrence time between nova outbursts. Assuming that our estimates for  $\tau_{\text{CN}}$  and  $T$  also hold for novae in the bulge of M31, we find  $\psi$  in the range 0.004–0.017.

A third and very direct estimate comes from the observed incidence of precataclysmic binaries in central stars of planetary nebulae. From an ongoing survey, Bond (1983) estimates an incidence of  $\sim 0.03$ – $0.05$ .

Thus, three independent estimates agree that  $\sim 1$ – $3\%$  of all white dwarfs are formed in systems that become cataclysmic variables (most of which are classical novae). The white dwarf birthrate in our Galaxy is estimated to be  $\sim 1 \text{ yr}^{-1}$ , implying a CV birthrate of  $\sim 0.02 \text{ yr}^{-1}$ .

#### ii) Death Rate

Since many of the white dwarfs in CVs are fairly massive and are (at least temporarily) gaining mass from their companions, it is possible that some may eventually reach the Chandrasekhar limit of  $1.4 M_{\odot}$  and collapse to form a neutron star. It has therefore been frequently proposed that these systems are responsible for Type I supernovae (e.g., Starrfield, Truran, and Sparks 1981). If every CV produces a supernova, then we could account for a supernova rate of  $0.02 \text{ yr}^{-1}$ . In practice, the production rate must be considerably lower, because many systems are not sufficiently massive to reach the Chandrasekhar limit, and many (at least the classical novae) are known to have an efficient means of expelling a fraction—and perhaps all—of the accreted matter. For the reasons stated earlier (§ V), it is somewhat difficult to understand how the white dwarfs can grow in mass, without generating a lot of luminosity which is not seen (because it appears that only a few percent of the accreted hydrogen is actually burned). An occasional deviant might wander over the Chandrasekhar limit; e.g., the white dwarf in SS Cyg is near  $1.4 M_{\odot}$  at present, and presumably has many years of accretion ahead of it. But the estimated rate of Type I supernovae in the Galaxy is  $0.008 \text{ yr}^{-1}$  (Tammann 1974; Dallaporta

1974), and it seems impossible that 40% of CVs could encounter this fate.

The majority of CVs, or perhaps all of them, must be wiped off the books in some other way. They must be destroyed before reaching the enormous space density that their birthrate and apparent longevity (as short-period systems) would require. This is the problem we encountered at the end of § VII, but now we see that if the birthrate argument is accepted, the problem does not depend sensitively on our estimates of space densities and lifetimes. If the formation rate is 2% of the white dwarf formation rate, then the space density should be  $\sim 2\%$  of the white dwarf space density—unless there is an intervening time scale which is very long, or there is destruction. Since the total space density of CVs is fairly well determined to be  $\sim 0.06\%$  of the white dwarf space density, and since we have not found any time scales sufficiently long to hide most systems in an inactive state, we suspect that some destruction mechanism is at work.

#### f) Cookbook for Evolution

We shall conclude with our favorite scenario for the evolution of CVs. Following the arguments of Paczyński (1976) and Webbink (1979), we assume that most CVs reach short orbital periods through a common-envelope–binary phase, occurring when the more massive member of the binary (the primary) becomes a red giant. When this phase terminates, we are left with a white dwarf and a main-sequence secondary which in general underfills its Roche lobe—i.e., a V471 Tauri star. Presumably all periods and nearly all spectral types are possible; the 11 known V471 Tau stars range in period from 2.7 hr to 16 days, with spectral types from A to late M. Secondaries with convective envelopes will be brought into synchronous rotation very rapidly, if the binary is not too detached.

a) If the secondary is earlier than  $\sim G0$ , then it must wait for its own nuclear evolution to begin mass transfer. This will take a very long time, but will eventually occur, and produce a very short-lived phase of mass transfer. Such objects should be extremely rare, and none are known to exist (although V Sge is a reasonable candidate, and T CrB and FF Aqr could be well on the way).

b) If the secondary is later than  $\sim M4$ , then neither nuclear evolution nor stellar winds can begin mass transfer within the age of the Galaxy. If the orbital period is less than 0.5 days, then GR can do the job in  $\leq 10^{10} \text{ yr}$ . It seems likely that GK Vir and the central star of Abell 41 are destined to come alive as short-period CVs in  $\leq 10^{10} \text{ yr}$ . The subsequent evolution should be dominated by GR as described by Paczyński and Sienkiewicz (1981) and RJW.

c) If the secondary spectral type is in the range G0–M3, then the secondary attempts to slow its rotation by ejecting a wind. But tidal torques maintain the star in synchronous rotation, and therefore the effect is to drain angular momentum from the orbit and to bring the Roche lobe down to the star's surface in  $10^7$ – $10^8 \text{ yr}$ . The system becomes a bona fide CV, transferring mass at a rate given approximately by

$$\dot{M} = 1.3 \times 10^{-9} \left[ \frac{M_2}{0.4 M_{\odot}} \right]^{2.1} M_{\odot} \text{ yr}^{-1} \quad (54)$$

if the accreting star is of  $1 M_{\odot}$ . After  $10^8$ – $10^9$  yr, the secondary is whittled down to  $\sim 0.3 M_{\odot}$ . The subsequent evolution is unclear, and is sensitive to the precise assumptions made about the braking wind. The wind may die, possibly because the secondary loses its radiative core. In this case the system is likely to traverse the period gap in a detached state, and to be reawakened in  $\sim 10^9$  yr as a low- $\dot{M}$  system. But if braking losses remain high, it is possible that systems enter a phase of *increasing* period, and the secondary could be devoured completely. The second of these alternatives would also produce a period gap, and would enable us to understand just what has happened to all those classical novae which presumably have been lighting up the night sky for the last  $7 \times 10^9$  yr.

#### IX. SUMMARY AND CONCLUSIONS

1. We perform a service to humanity by compiling the observational data for the 124 cataclysmic and low-mass X-ray binaries of known orbital period. We include all data judged to be relevant for questions of evolution. A strong correlation of eruption type with orbital period is noted.

2. We study the available data on single stars and stars in wide binaries to establish an empirical mass-radius relation for low-mass ZAMS stars:  $R/R_{\odot} = (M/M_{\odot})^{0.88}$ .

3. We compare observations of CV secondaries to the predictions of both the theoretical and the empirical ZAMS. The theoretical relation fails everywhere. The empirical relation fits the data almost perfectly for secondaries in systems with  $P \leq 9$  hr, but systems of longer period contain secondaries that are slightly evolved.

4. We discuss various ways of learning the mass transfer rate  $\dot{M}$ . The most generally useful method yields  $\dot{M}$  by comparing the time-averaged absolute visual magnitude  $\langle M_v \rangle$  to theoretical models of accretion disks. Use of an empirical correlation between  $M_v$  and the equivalent width of H $\beta$  emission approximately doubles the number of systems for which reasonable estimates of  $\langle M_v \rangle$  are possible. The resultant values of  $\dot{M}$  show a strong correlation with orbital period:  $\dot{M} \propto P^{3.2}$ .

5. We use our tables of  $\dot{M}$  and distance, along with the results of recent sky surveys, to deduce the scale height, space densities, and lifetimes of CVs. The scale height appears to be in the range 130–200 pc. The total space density is  $6 \times 10^{-6}$  pc $^{-3}$ , and is dominated by low- $\dot{M}$  systems. Classical novae are  $\sim 10$  times less abundant, but because they survive for only  $\sim 1\%$  of the Galaxy's age, a large population of dead classical novae ought to exist.

6. Because the secondaries are cool and rapidly rotating ( $\sim 130$  km s $^{-1}$ ), it is natural to expect that they have the typical characteristics of such stars: magnetic fields, active coronae, and possibly a significant stellar wind. Such a wind can rob the secondary of enormous amounts of rotational angular momentum with very little mass loss, but the existence of tidal torques guarantees that the secondary will maintain synchronism by draining the orbital angular momentum. Thus, the dimensions of the binary will shrink, and a high rate of mass transfer can be sustained. We collect all available data on angular momentum loss rates, and find that for main-sequence stars, a good power-law scaling relation is  $\dot{J} \propto$

$M^{4.0} v^{3.7}$ . We calculate the theoretical values of  $\dot{M}$  for two models of magnetic braking, and find good agreement with the observations. But it is apparent that gravitational radiation—hopelessly inadequate for systems with  $P \geq 3$  hr—dominates the evolution for the stars of shortest orbital period.

7. At  $P \approx 3$  hr, the secondaries have a mass  $\sim 0.3 M_{\odot}$ , and the braking theory becomes more uncertain. The star is now fully convective, the rate of kinetic energy loss in the wind is now comparable to the nuclear luminosity, and the Kelvin-Helmholtz time scale is now too long to maintain thermal equilibrium. What happens is unclear, but is probably related to the absence of observed systems with orbital periods in the range 2.1–2.8 hr. Even within a magnetic braking theory, the behavior of stars approaching  $M = 0.3 M_{\odot}$  appears to be very sensitive to the precise assumptions made about the braking wind. The various possibilities are discussed in §§ VII and VIII.

8. We note that all secondaries in CVs are of spectral types later than G0, which among field stars separates the slow and the fast rotators. This further emphasizes the likelihood that magnetic braking is presently at work, and suggests that it is also responsible for the *creation* of CVs.

9. We cite several arguments which lead us to believe that  $\sim 1\%$ – $3\%$  of all white dwarfs are born in systems that become cataclysmic variables, most of which are classical novae. It is quite difficult to understand where all these systems are today, since the present space density of CVs is only 0.06% of the white dwarf space density. This is the problem of the *dead novae*. We believe that the most likely solution is that the compact stars completely devour their companions, although one cannot rule out a very large population of detached systems with periods between 2 and 6 hr. This difficulty is not beyond the possibility of dispute, but can only be eliminated by adopting extreme values for the space densities and lifetimes, and rejecting altogether the evidence of a high CV birthrate.

10. Finally, we note that the theory described above should apply to essentially *all binary stars with cool components*, i.e. (swallow hard!), *most of the stars in the Galaxy*. The observed statistics of main-sequence binaries do in fact suggest that there exists some mechanism which reduces the lifetime of close, detached binaries containing GKM dwarfs. If we are correct in identifying this with magnetic braking, it creates the exciting prospect that by the improvement of braking laws such as that of equation (32), we can develop theories of binary star evolution which can be confronted with the menagerie of observational data, at a level of sophistication comparable to that which we have come to expect from theories of single-star evolution.

I am grateful to Bohdan Paczyński for igniting my interest in this subject during a fateful lunch at W. 81st and Columbus, and for helpful discussions; and to many who communicated results in advance of publication—especially Allen Shafter, Paula Szkody, Don Ferguson, Glen Williams, and Ron Taam. At least a half-dozen people contributed significantly to the typing of this oft-revised manuscript, none more cheerfully and ably than Donna Irwin. This research was supported in part by NASA contract NAS8-30453.



## REFERENCES

- Agrawal, P. C., Riegler, G. R., and Rao, A. R. 1983, *Nature*, **301**, 318.  
 Alexander, M. E. 1973, *Ap. Space Sci.*, **23**, 495.  
 Allen, C. W. 1973, *Astrophysical Quantities* (London: Athlone).  
 Bahcall, J. N., and Chester, T. J. 1977, *Ap. J.*, **215**, 121.  
 Bailey, J. 1979, *M.N.R.A.S.*, **188**, 681.  
 ———. 1981, *M.N.R.A.S.*, **197**, 31.  
 Bailey, J. A., Axon, D. J., Hough, J. H., Watts, D. J., Giles, A. B., and Greenhill, J. G. 1983, *M.N.R.A.S.*, **205**, 1P.  
 Baliunas, S. L., et al. 1983, *Ap. J.*, **275**, 752.  
 Barwig, H., Hunger, K., Kudritzki, R. P., and Vogt, N. 1982, *Astr. Ap.*, **114**, L11.  
 Barwig, H., and Schoembs, R. 1981, *Inf. Bull. Var. Stars*, No. 2031.  
 Bath, G. T. 1976, in *IAU Symposium 73, The Structure and Evolution of Close Binaries*, ed. P. Eggleton, S. Mitton, and J. Whelan (Dordrecht: Reidel), p. 173.  
 Bath, G. T., and Pringle, J. E. 1981, *M.N.R.A.S.*, **194**, 967.  
 Bath, G. T., Pringle, J. E., and Whelan, J. A. J. 1980, *M.N.R.A.S.*, **190**, 185.  
 Bath, G. T., and Shaviv, G. 1978, *M.N.R.A.S.*, **183**, 515.  
 Batten, A. H., Fletcher, J. M., and Mann, P. J. 1978, *7th Catalog of Orbital Elements of Spectroscopic Binary Systems* (Pub. Dom. Ap. Obs. Victoria, **15**, No. 5).  
 Becker, R. H. 1981, *Ap. J.*, **251**, 626.  
 Becker, R. H., and Marshall, F. E. 1981, *Ap. J. (Letters)*, **244**, L93.  
 Berriman, G. 1983, Ph.D. thesis, California Institute of Technology.  
 Bianchini, A. 1980, *M.N.R.A.S.*, **192**, 127.  
 Bianchini, A., Sabbadin, F., and Hamazoglu, E. 1982, *Astr. Ap.*, **106**, 176.  
 Biermann, P., Kuehr, H., Liebert, J., Stockman, H. S., Strittmatter, P., and Tapia, S. 1982, *IAU Circ.*, No. 3680.  
 Blair, W. P., Raymond, J. C., Dupree, A. K., Wu, C.-C., Holm, A. V., and Swank, J. H. 1984, *Ap. J.*, **278**, 290.  
 Bond, H. E. 1981, unpublished.  
 ———. 1983, in *Cataclysmic Variables and Low-Mass X-Ray Binaries*, ed. D. Q. Lamb and J. Patterson (Dordrecht: Reidel), in press.  
 Bond, H. E., Kemper, E., and Mattei, J. 1982, *Ap. J. (Letters)*, **260**, L79.  
 Bond, H. E., Liller, W., and Mannery, E. J. 1978, *Ap. J.*, **233**, 252.  
 Bradt, H. V., and McClintock, J. E. 1983, *Ann. Rev. Astr. Ap.*, in press.  
 Branduardi-Raymont, G., Corbet, R. H. D., Mason, K. D., Parmar, A. N., Murdin, P. G., and White, N. E. 1983, *M.N.R.A.S.*, **205**, 403.  
 Brecher, K., and Chanmugam, G. 1978, *Ap. J.*, **221**, 969.  
 Bruch, A. 1982, unpublished.  
 Brunt, C. 1982, unpublished.  
 Campolongo, F., Gilmozzi, R., Guidoni, U., Messi, R., Natali, G., and Wells, J. 1980, *Astr. Ap.*, **104**, 24.  
 Charles, P. A., Thorstensen, J. R., Bowyer, S., and Middleditch, J. 1979, *Ap. J. (Letters)*, **231**, L131.  
 Chevalier, C., and Ilovaisky, S. A. 1982, *Astr. Ap.*, **112**, 68.  
 Chincarini, G., and Walker, M. F. 1981, *Astr. Ap.*, **104**, 24.  
 Chlebowski, T., Halpern, J. P., and Steiner, J. E. 1981, *Ap. J. (Letters)*, **247**, L35.  
 Cominsky, L. R. and Wood, K. S. 1983, *IAU Circular* No. 3822.  
 Copeland, H., Jensen, J. O., and Jorgensen, H. E. 1970, *Astr. Ap.*, **5**, 12.  
 Cordova, F. A., and Mason, K. O. 1983, in *Accretion Driven Stellar X-Ray Sources*, ed. W. H. G. Lewin and E. P. J. van den Heuvel (Cambridge: Cambridge University Press), in press.  
 Cowley, A. P., and Crampton, D. 1975, *Ap. J. (Letters)*, **201**, L65.  
 Cowley, A. P., Crampton, D., and Hesser, J. E. 1977a, *Ap. J.*, **214**, 471.  
 ———. 1977b, *Pub. A.S.P.*, **89**, 716.  
 Cowley, A. P., Crampton, D., and Hutchings, J. B. 1979, *Ap. J.*, **231**, 539.  
 ———. 1980, *Ap. J.*, **241**, 269.  
 ———. 1982a, *Ap. J.*, **259**, 730.  
 ———. 1982b, *Ap. J.*, **255**, 596.  
 ———. 1982c, *Ap. J.*, **256**, 605.  
 Cowley, A. P., Crampton, D., Hutchings, J. B., and Marborough, J. M. 1975, *Ap. J.*, **195**, 421.  
 Cowley, A. P., Hutchings, J. B., and Crampton, D. 1981, *Ap. J.*, **246**, 489.  
 Crampton, D., and Cowley, A. P. 1980, *Pub. A.S.P.*, **92**, 147.  
 Cruddace, R. G., and Dupree, A. K. 1984, *Ap. J.*, **277**, 263.  
 Dallaporta, N. 1974, in *Supernovae and Supernova Remnants*, ed. C. B. Cosmovici (Dordrecht: Reidel), p. 122.  
 D'Antona, F., and Mazzitelli, I. 1982, *Ap. J.*, **260**, 722.  
 DeCampli, W. M., and Baliunas, S. L. 1979, *Ap. J.*, **230**, 815.  
 Deinzer, W., and Stix, M. 1971, *Astr. Ap.*, **12**, 111.  
 Demarque, P. 1972, in *Stellar Evolution*, ed. H. Y. Chiu and A. Muriel (Cambridge: MIT Press), p. 107.  
 Downes, R. 1984, Ph.D. thesis, University of California at Los Angeles.  
 Duerbeck, H. W. 1981, *Pub. A.S.P.*, **93**, 165.  
 Dupree, A. K. 1981, *Solar Phenomena in Stars and Stellar Systems*, ed. R. M. Bonnet and A. K. Dupree (Dordrecht: Reidel), p. 407.  
 Eason, E. L. E., Africano, J. L., Klinke, A., Quigley, R. J., Rogers, W., and Worden, S. P. 1983, *Pub. A.S.P.*, **95**, 58.  
 Echevarria, J., Jones, D. H. P., and Costero, R. 1982, *M.N.R.A.S.*, **200**, 23P.  
 Eggleton, P. 1976, in *IAU Symposium 73, The Structure and Evolution of Close Binaries*, ed. P. Eggleton, S. Mitton, and J. Whelan (Dordrecht: Reidel), p. 209.  
 Etzel, P. B., Lanning, H. H., Patenaude, D. J., and Dworetzky, M. M. 1977, *Pub. A.S.P.*, **89**, 616.  
 Faulkner, J. 1971, *Ap. J. (Letters)*, **170**, L99.  
 Faulkner, J. 1976, in *IAU Symposium 73, The Structure and Evolution of Close Binaries*, ed. P. Eggleton, S. Mitton, and J. Whelan (Dordrecht: Reidel), p. 193.  
 Faulkner, J., Flannery, B., and Warner, B. 1972, *Ap. J. (Letters)*, **175**, L79.  
 Ferguson, D. H., Liebert, J., Green, R. F., McGraw, J. T., and Spinrad, H. 1981, *Ap. J.*, **251**, 205.  
 Ferland, G. J., Lambert, D. L., McCall, M. J., Shields, G. A., and Slovak, M. H. 1982, *Ap. J.*, **260**, 794.  
 Flannery, B., and Ulrich, R. 1977, *Ap. J.*, **212**, 533.  
 Ford, H. C. 1978, *Ap. J.*, **219**, 595.  
 Ford, H. C., and Jacoby, G. H. 1978, *Ap. J.*, **219**, 437.  
 Frank, J., and King, A. R. 1981, *M.N.R.A.S.*, **195**, 227.  
 Frank, J., King, A. R., Sherrington, M. R., Jameson, R. F., and Axon, D. J. 1981, *M.N.R.A.S.*, **195**, 505.  
 Fujimoto, M. Y. 1982, *Ap. J.*, **257**, 752.  
 Gallagher, J. S., and Starrfield, S. G. 1978, *Ann. Rev. Astr. Ap.*, **16**, 171.  
 Garrison, P. F., Hiltner, W. A., and Schild, R. E. 1977, *Ap. J. Suppl.*, **35**, 111.  
 ———. 1982, *IAU Circ.* No. 3730.  
 Ghosh, P., Elsner, R. F., Weisskopf, M. C., and Sutherland, P. G. 1981, *Ap. J.*, **251**, 230.  
 Gilliland, R. L. 1982a, *Ap. J.*, **254**, 563.  
 ———. 1982b, *Ap. J.*, **258**, 576.  
 ———. 1982c, *Ap. J.*, **263**, 302.  
 Gilliland, R. L., and Phillips, M. M. 1982, *Ap. J.*, **261**, 617.  
 Golub, L. 1983, in *IAU Colloquium 71, Activity in Red-Dwarf Stars*, ed. S. Catalano and M. Rodono (Dordrecht: Reidel), in press.  
 Gottlieb, E. W., Wright, E. L., and Liller, W. 1975, *Ap. J. (Letters)*, **195**, L33.  
 Grauer, A. D., and Bond, H. E. 1981, *Pub. A.S.P.*, **93**, 388.  
 ———. 1982, *IAU Circ.*, No. 3714.  
 Green, R. F., Ferguson, D. H., Liebert, J., and Schmidt, M. 1982, *Pub. A.S.P.*, **94**, 560.  
 Green, R. F., Richstone, D. O., and Schmidt, M. 1978, *Ap. J.*, **224**, 892.  
 Gregory, P. C., and Fahlman, G. G. 1981, *Nature*, **287**, 805.  
 Grossman, A. S., Hays, D., and Graboske, H. C. 1974, *Astr. Ap.*, **30**, 95.  
 Haefner, R. 1981, *Inf. Bull. Var. Stars*, No. 2045.  
 Hammerschlag-Hensberge, G., McClintock, J. E., and van Paradijs, J. 1982, *Ap. J. (Letters)*, **254**, L1.  
 Hassall, B. J. M., Pringle, J. E., Ward, M. J., Whelan, J. A. J., Mayo, S. K., Echevarria, J., Jones, D. H. P., and Wallis, R. E. 1981, *M.N.R.A.S.*, **197**, 275.  
 Herbig, G. H., Preston, G. W., Smak, J., and Paczyński, B. 1965, *Ap. J.*, **141**, 167.  
 Hertz, P., and Grindlay, J. E. 1984, *Ap. J.*, **278**, 137.  
 Horne, K. 1980, *Ap. J. (Letters)*, **242**, L167.  
 Horne, K. 1983, private communication.  
 Horne, K., Lanning, H. H., and Gomer, R. H. 1982, *Ap. J.*, **252**, 681.  
 Horne, K., Szkody, P., Shaffer, A., and Wade, R. A. 1983, in preparation.  
 Hoshi, R. 1979, *Progr. Theor. Phys.*, **61**, 1307.  
 Houk, N., and Cowley, A. P. 1975, *Michigan Spectral Catalogue* (University of Michigan: Ann Arbor).  
 Hoxie, D. T. 1973, *Astr. Ap.*, **26**, 437.  
 Huang, S. S. 1966, *Ann. d'Ap.*, **29**, 331.  
 Hutchings, J. B. 1979, *Ap. J.*, **232**, 176.  
 Hutchings, J. B., Cowley, A. P., Crampton, D., Fisher, W. A., and Liller, M. H. 1982, *Ap. J.*, **252**, 690.  
 Hutchings, J. B., Cowley, A. P., Crampton, D., and Williams, G. 1981, *Pub. A.S.P.*, **93**, 741.  
 Hutchings, J. B., Crampton, D., and Cowley, A. P. 1979, *Ap. J.*, **232**, 500.  
 ———. 1981, *Ap. J.*, **247**, 195.  
 Hutchings, J. B., Crampton, D., Cowley, A. P., Thorstensen, J. R., and Charles, P. A. 1981, *Ap. J.*, **249**, 680.  
 Hutchings, J. B., and Thomas, B. 1982, *Pub. A.S.P.*, **94**, 102.  
 Iben, I. 1967, *Ann. Rev. Astr. Ap.*, **5**, 571.  
 Jameson, R. F., King, A. R., and Sherrington, M. R. 1981, *M.N.R.A.S.*, **195**, 235.  
 Joss, P. C., and Rappaport, S. 1983, *Ap. J.*, **270**, L73.

- Joy, A. H., and Abt, H. A. 1974, *Ap. J. Suppl.*, **28**, 1.
- Kaitchuk, R., Honeycutt, R. K., and Schlegel, E. M. 1983, *Ap. J.*, **267**, 239.
- Kaluźniński, L. J., Holt, S. S., and Swank, J. H. 1980, *Ap. J.*, **241**, 779.
- Kemper, E. 1982, private communication.
- Kieboom, K., and Verbunt, F. 1981, *Astr. Ap.*, **95**, L11.
- Kilkenny, D., Hill, P. W., and Penfold, J. E. 1981, *M.N.R.A.S.*, **194**, 429.
- Kiplinger, A. L. 1979, *Ap. J.*, **234**, 997.
- \_\_\_\_\_. 1980, *Ap. J.*, **236**, 839.
- Kippenhahn, R., and Meyer-Hofmeister, E. 1977, *Astr. Ap.*, **54**, 539.
- Kraft, R. P. 1963, *Ap. J.*, **135**, 408.
- \_\_\_\_\_. 1967, *Ap. J.*, **150**, 551.
- Kraft, R. P., Krzemiński, W., and Mumford, G. S. 1969, *Ap. J.*, **158**, 589.
- Kraft, R. P., and Luyten, W. J. 1965, *Ap. J.*, **142**, 1041.
- Krautter, J., Klare, G., Wolf, B., Duerbeck, H. W., Rahe, J., Vogt, N., and Wargau, W. 1981, *Astr. Ap.*, **102**, 337.
- Kruszewski, A. 1966, *Adv. Astr. Ap.*, **4**, 233.
- Krzemiński, W., and Smak, J. I. 1971, *Acta Astr.*, **21**, 133.
- Kurochkin, N. E., and Shugarov, S. Yu. 1980, *Astr. Tsirk.*, No. 1114.
- Kutter, G. S., and Sparks, W. M. 1980, *Ap. J.*, **239**, 988.
- Lacy, C. 1977a, *Ap. J. Suppl.*, **34**, 479.
- \_\_\_\_\_. 1977b, *Ap. J.*, **218**, 444.
- \_\_\_\_\_. 1983, preprint.
- Lamb, D. Q. 1974, *Ap. J. (Letters)*, **192**, L129.
- Lamb, D. Q., and Patterson, J. 1984, in *Cataclysmic Variables and Related Objects*, ed. M. Livio and G. Shaviv (Dordrecht: Reidel), in press.
- Lanning, H. H. 1982, *Ap. J.*, **253**, 752.
- Lanning, H. H., and Pesch, P. 1981, *Ap. J.*, **244**, 280.
- Latham, D. W., Liebert, J., and Steiner, J. 1981, *Ap. J.*, **246**, 919.
- Leung, K.-C., and Schneider, D. P. 1978, *Ap. J.*, **83**, 618.
- Levato, H. 1976, *Ap. J.*, **293**, 680.
- Liebert, J. 1980, *Ann. Rev. Astr. Ap.*, **18**, 363.
- Liebert, J., Stockman, H. S., Angel, J. R. P., Woolf, N. J., Hege, K., and Margon, B. 1978, *Ap. J.*, **225**, 201.
- Liebert, J., Tapia, S., Bond, H. E., and Grauer, A. D. 1982a, *Ap. J.*, **254**, 232.
- Liebert, J., Williams, R. E., Tapia, S., Green, R. F., Rautenkranz, D., Ferguson, D. H., and Szkody, P. 1982b, *Ap. J.*, **256**, 594.
- Lynden-Bell, D., and Pringle, J. B. 1974, *M.N.R.A.S.*, **168**, 603.
- MacAlpine, G. M., and Williams, G. A. 1981, *Ap. J. Suppl.*, **45**, 113.
- Malkus, W. V. R. 1959, *Ap. J.*, **130**, 259.
- Mardirossian, F., Mezzetti, M., Pucillo, M., Santin, P., Sedmak, G., and Giurcin, G. 1980, *Astr. Ap.*, **85**, 29.
- Margon, B., Chanan, G., and Downes, R. 1982, *Ap. J. (Letters)*, **253**, L7.
- Marsh, T. R., Wade, R. A., and Oke, J. 1983, *M.N.R.A.S.*, submitted.
- Marshall, N., and Millit, J. M. 1981, *Nature*, **293**, 379.
- Mason, K. O., and Cordova, F. A. 1982, *Ap. J.*, **262**, 253.
- Mason, K. O., Cordova, F. A., Middleditch, J., Reichert, G., Bowyer, S., Murdin, P. G., and Clark, D. 1983b, *Pub. A.S.P.*, **95**, 370.
- Mason, K. O., Middleditch, J., Cordova, F. A., Jensen, K. A., Reichert, G., Murdin, P. G., Clark, D., and Bowyer, S. 1983a, *Ap. J.*, **264**, 575.
- Mason, K. O., Reichert, G., Bowyer, S., and Thorstensen, J. 1982, *Pub. A.S.P.*, **94**, 521.
- Mayo, S. K., Wickramasinghe, D. T., and Whelan, J. A. J. 1980, *M.N.R.A.S.*, **193**, 793.
- McClintock, J. E., London, R. A., Bond, H. E., and Grauer, A. D. 1982, *Ap. J.*, **258**, 245.
- McClintock, J. E., Petro, L. D., Remillard, R. A., and Ricker, G. R. 1983, preprint.
- McClintock, J. E., Remillard, R. A., and Margon, B. 1981, *Ap. J.*, **243**, 900.
- McHardy, I. M., Pye, J. P., Fairall, A. P., Warner, B., Allen, S., Cropper, M., and Ward, M. J. 1982, *IAU Circ.*, No. 3687.
- Mestel, L. 1975, *Mém. Soc. Roy. Sci. du Liège*, **8**, 79.
- Meyer, F., and Meyer-Hofmeister, E. 1979, *Astr. Ap.*, **78**, 167.
- Middleditch, J., and Fahlman, G. G. 1982, *IAU Circ.*, No. 3745.
- Middleditch, J., Mason, K. O., Nelson, J. E., and White, N. E. 1981, *Ap. J.*, **244**, 1001.
- Middleditch, J., and Nelson, J. E. 1976, *Ap. J.*, **208**, 567.
- Mochnecki, S. 1981, *Ap. J.*, **245**, 650.
- Motch, C. 1981, *Astr. Ap.*, **100**, 277.
- Mullan, D. 1974, *Ap. J.*, **192**, 149.
- Murdin, P., Allen, D. A., Morton, D. C., Whelan, J. A. J., and Thomas, R. M. 1980, *M.N.R.A.S.*, **192**, 709.
- Nather, R. E., Robinson, E. L., and Stover, R. J. 1981, *Ap. J.*, **244**, 269.
- Nelson, B., and Young, A. 1970, *Pub. A.S.P.*, **82**, 699.
- Newton, I. 1687, *Philosophiae Naturalis Principia Mathematica* (English transl. A. Motte [1729] and F. Cajori [1934]) (Berkeley: University of California Press).
- Nomoto, K. 1982, *Ap. J.*, **253**, 798.
- Noskova, R. I. 1982, *Astr. Tsirk.*, No. 1128.
- Nousek, J., Luppino, G., Gajar, S., Bond, H. E., and Graver, A. D. 1982, *IAU Circ.*, No. 3733.
- Oke, J. B., and Wade, R. A. 1982, *A.J.*, **87**, 670.
- Osaki, Y. 1974, *Pub. Astr. Soc. Japan*, **26**, 429.
- Pacharintanakul, P., and Katz, J. I. 1980, *Ap. J.*, **238**, 985.
- Paczyński, B. 1965, *Acta Astr.*, **15**, 197.
- \_\_\_\_\_. 1967, *Acta Astr.*, **17**, 287.
- \_\_\_\_\_. 1971, *Ann. Rev. Astr. Ap.*, **9**, 183.
- \_\_\_\_\_. 1976, in *IAU Symposium 73, The Structure and Evolution of Close Binaries*, ed. P. Eggleton, S. Mitton, and J. Whelan (Dordrecht: Reidel), p. 75.
- \_\_\_\_\_. 1981, *Acta Astr.*, **31**, 1.
- \_\_\_\_\_. 1983, in *Cataclysmic Variables and Low-Mass X-Ray Binaries* ed. D. Q. Lamb and J. Patterson (Dordrecht: Reidel), in press.
- Paczyński, B., and Schwarzenberg-Czerny, A. 1980, *Acta Astr.*, **30**, 126.
- Paczyński, B., and Sienkiewicz, R. 1981, *Ap. J. (Letters)*, **248**, L27.
- \_\_\_\_\_. 1983, *Ap. J.*, **268**, 825.
- Papaloizou, J., and Pringle, J. E. 1978, *M.N.R.A.S.*, **182**, 423.
- Patterson, J. 1979a, *Ap. J.*, **231**, 789.
- \_\_\_\_\_. 1979b, *A.J.*, **84**, 804.
- \_\_\_\_\_. 1979c, *Ap. J.*, **234**, 978.
- \_\_\_\_\_. 1981, *Ap. J. Suppl.*, **45**, 517.
- \_\_\_\_\_. 1982, unpublished.
- \_\_\_\_\_. 1984, in preparation.
- Patterson, J., and Price, C. 1981, *Ap. J. (Letters)*, **243**, L83.
- Patterson, J., Roberts, W., Schwartz, D. A., Remillard, R., Morgan, E., and Bradt, H. 1983, *Bull. AAS*, **15**, 636.
- Patterson, J., Robinson, E. L., Nather, R. E., and Handler, F. 1979, *Ap. J.*, **232**, 819.
- Patterson, J., Schwartz, D. A., Williams, G., Fesen, R. A., and Szkody, P. 1984, in preparation.
- Patterson, J., and Steiner, J. E. 1983, *Ap. J.*, **142**, 1041.
- Payne-Gaposchkin, C. 1957, *The Galactic Novae* (New York: Dover).
- Pederson, H., van Paradijs, J., and Lewin, W. H. G. 1981, *Nature*, **294**, 725.
- Petro, L. 1982, private communication.
- Plavec, M. 1968, *Adv. Astr. Ap.*, **6**, 201.
- Popper, D. M. 1980, *Ann. Rev. Astr. Ap.*, **18**, 115.
- Popper, D. M., Jorgenson, H., Morton, D., and Leckrone, D. 1970, *Ap. J. (Letters)*, **161**, L57.
- Prialnik, D., Livio, M., Shaviv, G., and Kovetz, A. 1982, *Ap. J.*, **257**, 312.
- Pringle, J. E. 1975, *M.N.R.A.S.*, **170**, 633.
- \_\_\_\_\_. 1977, *M.N.R.A.S.*, **178**, 195.
- Pringle, J. E., and Savonije, G. J. 1979, *M.N.R.A.S.*, **187**, 777.
- Rappaport, S., Joss, P. C., and Webbink, R. F. 1982, *Ap. J.*, **254**, 616 (RJW).
- Rappaport, S., Verbunt, F., and Joss, P. C. 1983, *Ap. J.*, **275**, 713.
- Rayne, M. W., and Whelan, J. A. J. 1981, *M.N.R.A.S.*, **196**, 73.
- Ritter, H. 1976, *M.N.R.A.S.*, **175**, 279.
- \_\_\_\_\_. 1981, *ESO Messenger*, **21**, 16.
- \_\_\_\_\_. 1982, unpublished.
- Robinson, E. L. 1975, *A.J.*, **80**, 515.
- \_\_\_\_\_. 1976, *Ann. Rev. Astr. Ap.*, **14**, 119.
- Robinson, E. L., Barker, E. S., Cochran, A. L., Cochran, W. D., and Nather, R. E. 1981, *Ap. J.*, **251**, 611.
- Robinson, E. L., and Faulkner, J. 1975, *Ap. J. (Letters)*, **200**, L23.
- Robinson, E. L., Nather, R. E., and Kepler, S. O. 1982, *Ap. J.*, **24**, 337.
- Ruderman, M., and Shaham, J. 1983, *Nature*, **304**, 425.
- Schaefer, B., and Patterson, J. 1983, *Ap. J.*, **268**, 710.
- Schatzman, E. 1962, *Ann. d'Ap.*, **25**, 18.
- Schmidt, G. D., Stockman, H. S., and Grandi, S. A. 1983, *Ap. J.*, **271**, 735.
- Schmidt, G. D., Stockman, H. S., and Margon, B. 1981, *Ap. J. (Letters)*, **243**, L157.
- Schneider, D. P., Young, P., and Schectman, S. A. 1981, *Ap. J.*, **245**, 644.
- Schoembs, R. 1982, *Astr. Ap.*, **115**, 196.
- Schoembs, R., and Stolz, B. 1981, *Inf. Bull. Var. Stars*, No. 1986.
- Schoembs, R., and Vogt, N. 1981, *Astr. Ap.*, **97**, 185.
- Schwarzschild, M. 1958, *The Structure and Evolution of the Stars* (New York: Dover).
- Shafter, A. W. 1983a, *Ap. J.*, **267**, 222.
- \_\_\_\_\_. 1983b, *Inf. Bull. Var. Stars*, No. 2354.
- \_\_\_\_\_. 1983c, *Inf. Bull. Var. Stars*, No. 2377.
- \_\_\_\_\_. 1983d, Ph.D. thesis, University of California at Los Angeles.
- Shafter, A. W., and Szkody, P. 1984, *Ap. J.*, **276**, 305.
- Shafter, A. W., Szkody, P., Liebert, J., Bond, H. E., and Grauer, A. D. 1984, in preparation.
- Shafter, A. W., and Ulrich, R. K. 1982, *Bull. AAS*, **14**, 880.
- Shakura, N. I., and Sunyaev, R. A. 1973, *Astr. Ap.*, **24**, 337.
- Shara, M. 1983, private communication.
- Shara, M., and Moffat, A. F. J. 1983, *Ap. J.*, **264**, 560.

- Sherrington, M. R., Lawson, P. A., King, A. R., and Jameson, R. F. 1980, *M.N.R.A.S.*, **191**, 185.
- Skumanich, A. 1972, *Ap. J.*, **171**, 565.
- Smak, J. I. 1971, *Acta Astr.*, **21**, 15.
- \_\_\_\_\_. 1975, *Acta Astr.*, **25**, 371.
- \_\_\_\_\_. 1983, preprint.
- Smith, M. A. 1979, *Pub. A.S.P.*, **91**, 737.
- Soderblom, D. 1983, *Ap. J. Suppl.*, **53**, 1.
- Spruit, H. C., and Ritter, H. 1983, preprint.
- Spruit, H. C., and van Balleogooijen, A. A. 1982, *Astr. Ap.*, **113**, 350.
- Starrfield, S., Truran, J. W., and Sparks, W. M. 1981, *Ap. J. (Letters)*, **243**, L27.
- Steiner, J. E., Schwartz, D. A., Jablonski, F. J., Busko, I. C., Watson, M. G., Pye, J. P., and McHardy, I. M. 1981, *Ap. J. (Letters)*, **249**, L21.
- Stocke, J., et al. 1983, *Ap. J.*, **273**, 458.
- Stockman, H. S., Foltz, C., Tapia, S., and Schmidt, G. 1982, *IAU Circ.*, No. 3696.
- Stolz, B. 1981, *ESO Messenger*, **26**, 16.
- Stover, R. J. 1981a, *Ap. J.*, **248**, 684.
- \_\_\_\_\_. 1981b, *Ap. J.*, **249**, 673.
- \_\_\_\_\_. 1984, in *Cataclysmic Variables and Low-Mass X-Ray Binaries*, ed. D. Q. Lamb and J. Patterson (Dordrecht: Reidel), in press.
- Stover, R. J., Robinson, E. L., and Nather, R. E. 1981, *Ap. J.*, **248**, 696.
- Stover, R. J., Robinson, E. L., Nather, R. E., and Montmayor, T. J. 1980, *Ap. J.*, **240**, 597.
- Struve, O. 1930, *Ap. J.*, **72**, 1.
- Szkody, P. 1982, private communication.
- Szkody, P., and Crosa, L. 1981, *Ap. J.*, **251**, 620.
- Szkody, P., Shafter, A. W., and Cowley, A. P. 1984, *Ap. J.*, in press.
- Szkody, P., and Wade, R. A. 1981, *Ap. J.*, **251**, 201.
- Taam, R. 1983, *Ap. J.*, **268**, 361.
- Taam, R., Bodenheimer, P., and Ostriker, J. P. 1978, *Ap. J.*, **222**, 269.
- Taam, R., Flannery, B., and Faulkner, J. 1980, *Ap. J.*, **239**, 1017.
- Tammann, G. A. 1974, in *Supernovae and Supernova Remnants*, ed. C. B. Cosmovici (Dordrecht: Reidel), p. 155.
- Thorstensen, J. 1983, private communication.
- Thorstensen, J. R., and Charles, P. A. 1982, *Ap. J.*, **253**, 756.
- Thorstensen, J., Charles, P. A., and Bowyer, S. 1978, *Ap. J. (Letters)*, **220**, L131.
- Thorstensen, J., Charles, P. A., Margon, B., and Bowyer, S. 1978, *Ap. J.*, **223**, 260.
- Tuohy, I. R., Mason, K. O., Garmire, G. P., and Lamb, F. K. 1981, *Ap. J.*, **245**, 183.
- Tutukov, A. V., and Yungelson, L. R. 1979, *Acta Astr.*, **29**, 665.
- Tylenda, R. 1981, *Acta Astr.*, **31**, 127.
- van der Klis, M., and Bonnet-Bidaud, J. M. 1982, *Astr. Ap. Suppl.*, **50**, 129.
- van Leeuwen, F., and Alphenaar, P. 1982, *ESO Messenger*, **28**, 15.
- van Paradijs, J. 1981, *Astr. Ap.*, **103**, 140.
- Veeder, G. 1974, Ph.D. thesis, California Institute of Technology.
- Verbunt, F., and Zwaan, C. 1981, *Astr. Ap.*, **100**, L7 (VZ).
- Visvanathan, N., Hillier, J., and Pickles, A. 1982, *IAU Circ.*, No. 3658.
- Visvanathan, N., and Wickramasinghe, D. T. 1981, *M.N.R.A.S.*, **196**, 275.
- Vogt, N. 1975, *Astr. Ap.*, **41**, 15.
- \_\_\_\_\_. 1981, unpublished.
- \_\_\_\_\_. 1982, *Ap. J.*, **252**, 653.
- Vogt, N., and Breysacher, J. 1980, *Ap. J.*, **235**, 945.
- Vogt, N., Schoembs, R., Krzemiński, W., and Pederson, H. 1981, *Astr. Ap.*, **94**, L29.
- Vogt, N., and Semeniuk, I. 1980, *Astr. Ap.*, **89**, 223.
- Vogel, S. N., and Kuhl, L. V. 1981, *Ap. J.*, **245**, 960.
- Wade, R. A. 1979, *A. J.*, **84**, 562.
- \_\_\_\_\_. 1981, *Ap. J.*, **246**, 215.
- \_\_\_\_\_. 1982, unpublished.
- Wade, R. A., and Oke, J. B. 1982, *Bull. AAS*, **14**, 880.
- Walker, M. F. 1963, *Ap. J.*, **138**, 313.
- \_\_\_\_\_. 1981, *Ap. J.*, **245**, 677.
- \_\_\_\_\_. 1982, *Ap. J.*, **253**, 745.
- Walter, F. M., Bowyer, S., Mason, K. O., Clarke, J. T., Henry, J. P., Halpern, J., and Grindlay, J. 1982, *Ap. J. (Letters)*, **253**, L67.
- Wargau, W., Drechsel, H., Rahe, J., and Bruch, A. 1983, *M.N.R.A.S.*, **204**, 35p.
- Warner, B. 1974, *M.N.A.S. So. Africa*, **33**, 21.
- \_\_\_\_\_. 1976, in *IAU Symposium 73, The Structure and Evolution of Close Binaries*, ed. P. Eggleton, S. Mitton, and J. Whelan (Dordrecht: Reidel), p. 85.
- \_\_\_\_\_. 1978, *Acta Astr.*, **28**, 303.
- Warner, B., and Nather, R. E. 1971, *M.N.R.A.S.*, **152**, 219.
- Warner, B., and Thackeray, A. D. 1975, *M.N.R.A.S.*, **172**, 433.
- Webbink, R. F. 1979, in *IAU Colloquium 53, White Dwarfs and Variable Degenerate Stars*, ed. H. M. Van Horn and V. Weidemann (University of Rochester: New York), p. 426.
- Weber, E. J., and Davis, L. D. 1967, *Ap. J.*, **148**, 217.
- White, N., and Holt, S. S. 1982, *Ap. J.*, **257**, 318.
- White, N. E., Parmar, A. N., and Mason, K. O. 1983, *IAU Circ.*, No. 3882.
- White, N. E., and Swank, J. 1982, *Ap. J. (Letters)*, **253**, L61.
- Whyte, C. A., and Eggleton, P. 1980, *M.N.R.A.S.*, **190**, 801.
- Williams, R. 1980, *Ap. J.*, **235**, 939.
- Williams, R. E., and Ferguson, D. H. 1982, *Ap. J.*, **257**, 672.
- Williams, G. 1983, *Ap. J. Suppl.*, **53**, 523.
- Williams, G., and Patterson, J. 1983, in preparation.
- Young, A., and Capps, R. W. 1971, *Ap. J. (Letters)*, **166**, L81.
- Young, A., and Nelson, B. 1972, *Ap. J.*, **174**, 27.
- Young, A., Nelson, B., and Mielbrecht, R. 1972, *Ap. J.*, **174**, 27.
- Young, P., and Schneider, D. P. 1979, *Ap. J.*, **230**, 502.
- \_\_\_\_\_. 1980, *Ap. J.*, **238**, 955.
- \_\_\_\_\_. 1981, *Ap. J.*, **247**, 960.
- Young, P., Schneider, D. P., and Schectman, S. A. 1981a, *Ap. J.*, **245**, 1035.
- \_\_\_\_\_. 1981b, *Ap. J.*, **245**, 1043.
- \_\_\_\_\_. 1981c, *Ap. J.*, **244**, 259.
- Young, P., Schneider, D. P., Sargent, W. L. W., and Boksenberg, A. 1982, *Ap. J.*, **252**, 269.
- Young, A., and Wentworth, S. T. 1982, *Pub. A.S.P.*, **94**, 815.
- Zahn, J. P. 1966a, *Astr. Ap.*, **57**, 383.
- \_\_\_\_\_. 1966b, *Astr. Ap.*, **67**, 162.

JOSEPH PATTERSON: Department of Astronomy, Columbia University, New York, NY 10027